

3.9 Adsorption on oxide surfaces

3.9.1 Introduction

The interaction of gases with oxide surfaces is important for many all-day processes like corrosion as well as for large-scale industrial fabrication of chemicals with catalytic processes. In order to understand the microscopic processes occurring when gases contact oxide surfaces, two different approaches may be followed. One approach is to study real world systems with their full complexity. Due to this complexity, hard-to-interpret experimental results are to be expected. If the systems are to be investigated in-situ under working pressures which may be in the bar range or higher, a number of powerful techniques like electron spectroscopy which works only under high or ultra-high vacuum conditions can not be applied.

Another approach is to study idealized systems ("model systems") under high or ultra-high vacuum conditions. These systems are usually well ordered and their composition is not too complex. This permits to apply many powerful surface science techniques and it is often possible to understand in detail the microscopic processes occurring during gas-substrate contact. However, the systems are simpler than the real world systems and the pressure is usually lower than the pressure of gases interacting with real systems. This means that it is not sure that the processes occurring during gas-surface interaction are the same as the ones occurring in the non-idealized real systems under working pressure conditions. Nevertheless, this approach has generated a number of important results and ideas concerning gas-surface interactions which are surely also important for processes occurring in "real" systems. In the context of a discussion of these two approaches key phrases like "material gap", "complexity gap", or "pressure gap" may be heard. These phrases refer to differences between the two approaches concerning the degree of realism. One of the topics of current surface science research is to increase the degree of realism by going towards increasingly complex systems and by a development of more powerful experimental techniques which extend the usable pressure regime. This chapter tries to give an overview of results obtained for one type of idealized systems, i.e. molecular adsorbates on ordered oxide surfaces which may be single crystal surfaces or the surfaces of thin ordered oxide films.

3.9.2 Abbreviations used in the text

$\Delta\phi$	workfunction change measurements
AES	Auger electron spectroscopy
AFM	atomic force microscopy
AM1	Austin Model 1 (semi-empirical theoretical method)
ARUPS	angular resolved ultra-violet photoelectron spectroscopy
B3LYP	a density functional method due to Lee, Yang and Parr which incorporates a 3-parameter functional due to Axel Becke
BEG	Blume-Emery-Griffiths (theoretical model)
CARS	coherent anti-Stokes Raman spectroscopy
CFS	constant final state (spectroscopy)
DFT	density functional theory
DV-X α	discrete variational X α (theoretical method)
ELS	energy loss spectroscopy
ESD	electron stimulated desorption (spectroscopy)
ESDIAD	electron stimulated desorption ion angular distribution (spectroscopy)
ESR	electron spin resonance (spectroscopy)
EXAFS	extended X-ray absorption fine structure (spectroscopy)
FLAPW	full potential linearized augmented plane wave (theoretical method)
FTIR	Fourier transform infrared (spectroscopy)
GC	gas chromatography
HAS	helium atom scattering (spectroscopy)

HF	Hartree-Fock (theoretical method)
HREELS	high resolution electron energy loss spectroscopy
IMPT	inter-molecular perturbation theory
INDO	semi-empirical theoretical method
IR	infrared (spectroscopy)
IRAS	infrared absorption spectroscopy
ISS	ion scattering spectroscopy
LCAO	linear combination of atomic orbitals (theoretical method)
LDA	local density approximation (theoretical method)
LEED	low energy electron diffraction
LID	laser induced desorption (spectroscopy)
LITD	laser induced thermal desorption (spectroscopy)
MD	molecular dynamics (theoretical method)
MIES	metastable impact electron spectroscopy
MNDO	modified neglect of diatomic overlap (semi-empirical theoretical method)
MP2	Møller-Plesset theory truncated at 2 nd order
MSINDO	semi-empirical theoretical method
MSRI	mass spectroscopy of recoiled ions
NC-AFM	non-contact atomic force microscopy
NEXAFS	near edge X-ray absorption spectroscopy
PEEM	photoemission electron microscopy
PES	photoelectron spectroscopy
PID	photon induced desorption (spectroscopy)
PIRSS	polarization infrared surface spectroscopy
PM3	third parametrization of MNDO (semi-empirical theoretical method)
PSD	photon stimulated desorption (spectroscopy)
PhD	photoelectron diffraction
REMPI-TOFMS	resonantly enhanced multi-photon ionization - time of flight mass spectrometry
REMPI	resonantly enhanced multi-photon ionization (spectroscopy)
RHEED	reflection high energy electron diffraction
RT	room temperature
SCC-DV- $X\alpha$	self consistent charge discrete variational $X\alpha$ (theoretical method)
SCF- $X\alpha$ -SW	$X\alpha$ denotes a certain form of the exchange term, SW means scattered wave (theoretical method)
SCF	self-consistent field (theoretical method)
SEXAFS	surface extended X-ray absorption fine structure (spectroscopy)
SFG	sum frequency generation (spectroscopy)
SIMS	secondary ion mass spectrometry
SINDO	semi-empirical theoretical method
SPA-LEED	spot profile analysis - low energy electron diffraction
SSIMS	static secondary ion mass spectrometry
STM	scanning tunneling microscopy
TCS	total (target) current spectroscopy
TDS	thermal desorption spectroscopy
TOF	time of flight (spectroscopy)
UHV	ultra-high vacuum
UPS	ultra-violet photoelectron spectroscopy
UV	ultra-violet
XPS	X-ray photoelectron spectroscopy
XRD	X-ray diffraction
XSW	X-ray standing wave (spectroscopy)
ZINDO	semi-empirical theoretical method

3.9.3 Al₂O₃

Al₂O₃ surfaces have been prepared in different ways. α -Al₂O₃ surfaces may be prepared by cutting a α -Al₂O₃ single crystal along the desired surface (usually [0001]) with subsequent chemical cleaning. Preparation in UHV usually comprises annealing at high temperature and re-oxidation of the surface. Details of the procedure vary. It is also possible to prepare ordered Al₂O₃ surfaces as thin films on different substrates. NiAl(100) and NiAl(110) are often used substrates. Annealing in oxygen produces thin Al₂O₃ layers. On NiAl(110) formation of an incommensurate Al₂O₃ type layer with a well defined LEED pattern has been reported [91Jae1, 97Kuh1]. STM and surface X-ray diffraction studies [04Sti1, 00Sti2, 00Sti1, 03Kul1] led to the conclusion that the structure of the film is similar to that of θ -Al₂O₃, κ -Al₂O₃, or γ -Al₂O₃(111). On NiAl(100) formation of α -Al₂O₃, θ -Al₂O₃, α -Al₂O₃ and γ -Al₂O₃ has been observed [98Hsi1, 94Gas1]. On Mo(110) an aluminum oxide film with γ -Al₂O₃ or α -Al₂O₃ structure may be grown by evaporation of aluminum in an oxygen atmosphere [96Str1]. An overview of studies of adsorption on these systems is given in Table 2.

Table 2. Overview of investigations of the interaction of gases with well ordered Al₂O₃ surfaces.

Adsorbates	Method	References
Substrate: Single crystal α-Al₂O₃(0001)		
C ₈ H ₁₈ , CH ₄	Theory: DFT, united atom, explicit atom	99Bol1
C ₈ H ₁₈ , C ₁₆ H ₃₄ , C ₃₂ H ₆₆ , hydroxylated substrate	Theory: molecular dynamics	00Jin1
CH ₃ OH	TDS, isothermal desorption	98Nis1
phenanthrene	electronic absorption spectroscopy	91Hay1
Iodobenzene (C ₆ H ₅ I)	XPS, TDS, laser irradiation	98Slo1
CH ₃ I	Laser induced photochemistry, TDS	99Nis1
CO	Theory: DFT	00Cas1
C ₆₀	electronic absorption spectroscopy, TDS, isothermal desorption	91Tok1
C ₄ H ₁₀ , C ₈ H ₁₈ , C ₁₂ H ₂₆ +H ₂ O	Theory: molecular dynamics	97deS1
H ₂ O	LITD, TDS	98Nel1
H ₂ O, OH	XPS, thermodynamic calculations	98Liu1
H ₂ O, OH	molecular dynamics	98Has1, 00Has1
H ₂ O, OH	LITD, TDS	98Ela1
H ₂ O, OH	HREELS	94Cou2, 97Cou1
H ₂ O, HCl	LITD, TDS	01Nel1
OH	Theory: DFT	99DiF1
OH	Theory	97Nyg1
Substrate: Al₂O₃(111)/NiAl(110)		
CO	autoionization spectroscopy	96Kli1
CO	ELS, TDS	93Jae1, 94Kuh1, 93Jae2, 93Fre2, 96Fre2
O ₂	ARUPS, TDS, ELS	93Jae2
OH	SPA-LEED, XPS	97Lib1
Pd-carbonyl	IRAS	97Wol1
glycidyl isopropyl ether, epoxyhexane	IRAS	99Woo2
Substrate: α-Al₂O₃, γ-Al₂O₃, θ-Al₂O₃, α-Al₂O₃ on NiAl(100)		
CO	IRAS	98Hsi1
Substrate: Al₂O₃/Mo(110)		
C ₆ H ₆	TDS, HREELS	96Str1

3.9.3.1 CO adsorption

Several publications are found for CO on $\text{Al}_2\text{O}_3/\text{NiAl}(110)$. Using thermal desorption spectroscopy and electron energy loss spectroscopy two adsorption states could be identified with adsorption enthalpies of -170 meV and -140 meV [93Jae1, 93Jae2]. The corresponding desorption temperatures are 67 and 55 K. Also lifetimes, excitation energies and vibrational energies for the $a^3\Pi$ excited state are reported. Angular dependent autoionization spectra of the $\text{Cl}s \rightarrow 2\pi^*$ excitation are reported in [96Kli1]. For CO adsorption at 85 K onto $\alpha\text{-Al}_2\text{O}_3$, $\gamma\text{-Al}_2\text{O}_3$, $\theta\text{-Al}_2\text{O}_3$ and $\alpha\text{-Al}_2\text{O}_3$ on $\text{NiAl}(100)$ IRAS studies have been performed [98Hsi1]. On $\gamma\text{-Al}_2\text{O}_3$ no adsorption was observed. For the other three oxide surfaces CO desorption occurred at $T = 120$ K. Several C-O vibrational states have been observed depending on the type of oxide and the CO dose, with frequencies ranging from 1994 cm^{-1} to 2074 cm^{-1} . The highest frequencies were found for $\alpha\text{-Al}_2\text{O}_3$ and the smallest ones for $\alpha\text{-Al}_2\text{O}_3$.

3.9.3.2 H₂O adsorption

The interaction of H_2O with $\alpha\text{-Al}_2\text{O}_3(0001)$ was studied by several groups due to the importance of Al_2O_3 in catalysis. Special attention was paid to the formation and the properties of OH groups. These groups are formed by dissociative adsorption of water. The initial water sticking coefficient at $T = 300$ K is $S_0 \approx 0.1$. It decreases exponentially with increasing OH coverage [98Elal]. Saturation coverage is 0.5×10^{15} OH groups/ cm^2 at a dose of 10^{10} L [98Elal]. H_2O plasma hydroxylation leads to significantly higher coverages but roughens the surface and destroys the LEED pattern [98Elal]. H_2O desorption from hydroxylated $\alpha\text{-Al}_2\text{O}_3$ was observed at temperatures ranging from 300 to 500 K, corresponding to desorption energies between 23 and 41 kcal/mol $^{-1}$ [98Nel1]. The O-H vibrational energy is 3720 cm^{-1} and the O1s binding energy is 533.1 ± 0.2 eV [97Cou1]. According to molecular dynamics calculations the ideal Al-terminated (0001) surface of $\alpha\text{-Al}_2\text{O}_3$ is very reactive with respect to dissociation of water [00Has1]. The strong relaxation of the clean surface is partly removed by the OH adsorbate. According to the calculations spontaneous unimolecular dissociations as well as dissociation mediated by another H_2O molecule should occur [00Has1].

3.9.4 CaO

CaO exhibits rocksalt structure (like NiO, see Fig. 10) with a lattice constant of 4.8105 \AA [65Wyc1]. CaO may be cleaved along the (001) plane leading to high-quality surfaces, especially if the cleavage is performed in situ in vacuum. Another method comprises cutting the crystal along the desired plane and polishing it. After introduction into the vacuum system the sample is prepared by sputtering and annealing [83Sti1, 84Lee1]. CaO is an electrically insulating material. Therefore charge compensation may be needed when methods involving charged particles are applied. There is also a report of the epitaxial growth of $\text{CaO}(100)$ on $\text{NiO}(100)$ [00Xu1]. $\text{CaO}(100)$ surfaces have a high affinity towards formation of surface hydroxyls and carbonates [99Doy1, 97Kan1] upon interaction with H_2O and CO_2 , respectively. An overview of adsorption studies for this oxide is given in Table 3.

Table 3. Overview of investigations of the interaction of gases with well ordered CaO surfaces.

Adsorbates	Method	References
Substrate: Single crystal CaO(100)		
CO_2 , SO_2	Theory: <i>ab initio</i> cluster calculations	94Pac1
CO_2	XPS, NEXAFS	99Doy1
N_2O	Theory	97Kan1
N_2O_2 , NO	Theory	98Sni2
H_2O	XPS	98Liu3

Adsorbates	Method	References
H ₂ O	Theory: DFT	00deL1
O, O+CO	Theory: <i>ab initio</i> cluster calculations	94Nyg1
O	Theory: <i>ab initio</i> cluster calculations	92Str1
O ₂	Theory: <i>ab initio</i> cluster calculations	95Sni1
O ₂ ,O	Theory: DFT	97Kan2
OH	Theory: semiempirical slab calculations	95Gon1, 93Nog1
NO ₂ CH ₃	Theory: <i>ab initio</i> cluster calculations	96All1
SO ₂	XPS	84Lee1
SO ₂	XPS	83Sti1
Substrate: CaO(100)/NiO(100)/Mo(100)		
NO	TDS	00Xu1

3.9.4.1 CO₂ adsorption

CO₂ adsorption was studied with synchrotron based XPS and NEXAFS [99Doy1]. It was shown that carbonate forms on the surface at pressures $\geq 10^{-6}$ Torr applied for 15 min. In [94Pac1] the higher reactivity of CaO(100) as compared to MgO(100) is explained by the smaller Madelung potential of CaO which leads to a smaller stabilization of the O²⁻ ions on the CaO(100) surface.

3.9.4.2 H₂O adsorption

H₂O induces surface hydroxylation with an apparent sticking coefficient of ≈ 0.9 at room temperature for surface coverages below 0.8 monolayers [98Liu3]. At higher coverages the sticking coefficient is dramatically reduced to $\sim 3 \times 10^{-5}$. At H₂O pressures greater than 1×10^{-4} Torr bulk hydroxylation was observed [98Liu3].

3.9.4.3 SO₂ adsorption

SO₂ adsorption at room temperature leads to the formation of strongly bound sulfate (SO₄²⁻) with a desorption temperature beyond 673 K [84Lee1, 83Sti1]. It was shown that the initial sticking coefficient is about 0.4 and that the adsorption is of first order in surface coverage [83Sti1]. Similar to the case of CO₂ adsorption Pacchioni and coworkers [94Pac1] explain the higher reactivity of CaO(100) as compared to MgO(100) by the smaller Madelung potential of CaO which leads to a smaller stabilization of the O²⁻ ions on the CaO(100) surface.

3.9.5 CeO₂

CeO₂ exhibits fluorite structure with a lattice constant of 5.411 Å. The (111) and the (001) surface have been used for adsorption studies. The (001) surface is polar and thus energetically unstable if not stabilized by geometrical rearrangement at the surface, charge rearrangement, or adsorption. The stabilization mechanism for the (001) surface appears to be an open question. Termination of the surface by oxygen and cerium terminated patches, oxygen termination with a few percent of defects and oxygen termination with 50% of the oxygen atoms removed are named in [99Her1]. The two ideal terminations of the (100) surface and the (111) surface are displayed in Fig. 1. Ceria is a component of automotive emission control catalysts where it acts as a component for oxygen storage. It is also known to be active for the water-gas-shift reaction. CeO₂(111) is often prepared as a thin film on Ru(0001) whereas CeO₂(001) may be grown on SrTiO₃(001). Sub-stoichiometric oxide films may be grown by using smaller

oxygen pressures during oxidation or by annealing. CeO_2 is also commercially available in single crystal form. There is only a limited number of adsorption studies for ordered CeO_2 surfaces. An overview is given in Table 4

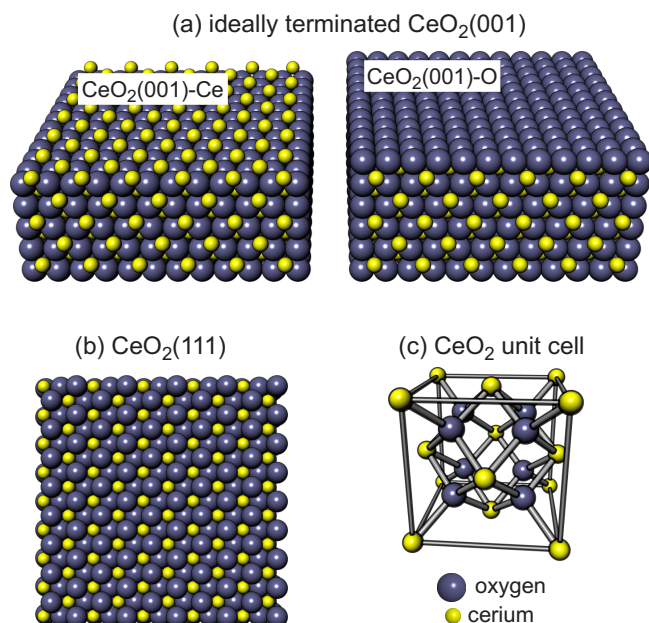


Fig. 1. Structure of the two polar $\text{CeO}_2(100)$ surfaces and the $\text{CeO}_2(111)$ surface.

3.9.5.1 CO adsorption on $\text{CeO}_2(111)$

For $\text{CeO}_2(111)/\text{Ru}(0001)$ the adsorption of CO was studied with XPS [99Mul1]. A state with a C1s binding energy of 290.5 eV was found to result from CO interacting with the $\text{CeO}_2(111)$ surface. This state vanishes between 600 and 700 K. It was suggested that the observed state corresponds to carbonate or carboxylate bonding to cerium sites.

Table 4. Overview of investigations of the interaction of gases with well ordered CeO_2 surfaces

Adsorbates	Method	References
Substrate: $\text{CeO}_2(001)/\text{SrTiO}_3(001)$		
NO	TDS, XPS, ion bombardment	97Ove1
D_2O	TDS, XPS	99Her1
Substrate: $\text{CeO}_2(111)/\text{Ru}(0001)$		
CO	XPS	99Mul1
CO, H_2O	XPS, TDS	00Kun1
O_2	TDS	96Put1
SO_2	TDS, XPS	99Ove1

3.9.5.2 H_2O and D_2O adsorption on $\text{CeO}_2(001)$ and $\text{CeO}_2(111)$

The adsorption of H_2O on $\text{CeO}_2(111)/\text{Ru}(0001)$ was investigated using TDS and XPS [00Kun1]. Water was found to desorb fully below 300 K from the fully oxidized surface. On reduced surfaces also H_2 desorption occurred at around 580 K. In this case additional H_2O desorption states at 250 K and 600 K were observed. The amount of desorbing H_2 was found to depend on the degree of reduction of the ceria substrate. Water adsorbed on the fully oxidized surface exhibits a O1s level with a binding energy of 531.8 eV which vanishes above 300 K. On reduced $\text{CeO}_2(111)$ H_2O adsorption leads to a O1s state at

532.5 eV at 200 K which shifts to 533 eV at 400 K. It was assumed that the O1s peak is composed of two peaks with binding energies of 532.4 and 533.1 eV resulting from chemisorbed water and hydroxyl groups, respectively. Hydrogen desorption as observed with TDS coincides with the disappearance of the O1s level of the hydroxyl groups.

D₂O adsorption on CeO₂(001)/SrTiO₃(001) was also investigated using XPS and TDS [99Her1]. With TDS desorption maxima at 152, 200 and 275 K were identified and assigned to desorption of multilayer water (152 K), first layer water (200 K) and recombination of hydroxyl groups (275 K). The O1s peak corresponding to the hydroxyl groups was found at 531.6 eV using XPS. From the intensity of the O1s peak a hydroxyl coverage of 0.9 ML was estimated. It was suggested that the hydroxyl groups might help to stabilize the polar CeO₂(001) surface. The O1s signal of the surface water could not be identified in the XPS data which was attributed to non-wetting adsorption of D₂O on CeO₂(001). This would lead to the formation of large clusters which would give a small O1s XPS intensity.

3.9.6 α -Cr₂O₃

Of all different chromium oxides α -Cr₂O₃ appears to be the most easily accessible oxide in well ordered form under UHV conditions. α -Cr₂O₃ exhibits corundum structure like α -Al₂O₃ with the hexagonal lattice constants $a=4.7628$ and $c=13.003$ Å [65Wyc1]. The (0001) surface is often prepared as a thin film by oxidation of Cr(110) [92Kuh2]. It has been shown that the surface may be terminated by a half layer of chromium atoms after annealing in UHV [97Roh2, 97Roh1] (see Fig. 2C) or by chromyl groups after treatment with oxygen [96Dil1]. We note that the surface shown in Fig. 2C is the only ideal surface of corundum(0001) which is non-polar and thus electrically stable. Figs. 2A and 2B are polar surfaces. Growth of α -Cr₂O₃(0001) by MBE onto α -Al₂O₃(0001) and Fe₂O₃(0001)/ α -Al₂O₃(0001) has also been reported [00Hen1]. Other authors describe the growth on Pt(111) [01Rod5, 97Rod1]. One adsorption study has also been carried out for a Cr₃O₄(111) film on Pt(111) [97Rod1]. In order to carry out adsorption studies on Cr₂O₃(10 $\bar{1}2$) a single crystal surface has been prepared by cutting a Cr₂O₃ single crystal along the (10 $\bar{1}2$) plane, polishing it and sputtering and annealing it in vacuo after insertion into the vacuum chamber [99Yor1]. Adsorption experiments performed for these surfaces are listed in Table 5.

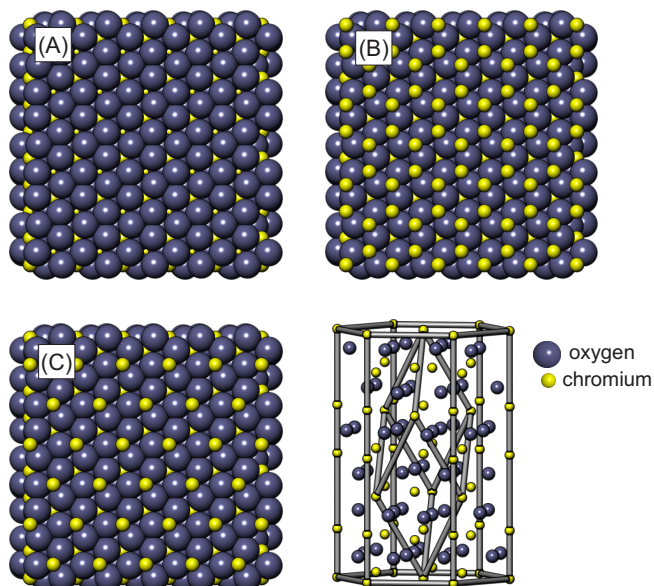


Fig. 2. (A), (B) and (C): three different ideal terminations of a corundum structure. (A): termination by an oxygen layer, (B): termination by a metal double layer, (C): termination by a single metal layer. In the lower right panel the non-primitive hexamolecular unit cell is displayed together with the primitive rhombohedral unit cell.

Table 5. Overview of investigations of the interaction of gases with well ordered Cr₂O₃ surfaces.

Adsorbates	Method	References
Substrate: Cr₂O₃(0001)/Cr(110)		
CO	TDS, IRAS, Theory: <i>ab initio</i> cluster calculations	01Pyk1
CO	TDS, REMPI, ELS	96Bea1
CO	autoionization spectroscopy	96Kli1
CO	ARUPS	91Xu1, 96Fre2
CO	HREELS	00Wol1
CO	LID	96AlS1, 96Bea2, 94AlS1, 95Bea1
CO	Theory: <i>ab initio</i> quantum dynamics	01Thi1
CO, NO, CO ₂	ELS, HREELS, NEXAFS	95Ben1, 92Kuh1
CO, NO, CO ₂ , NO ₂ , O ₂	ELS, HREELS, TDS, ARUPS, NEXAFS, XPS	92Kuh2, 94Kuh1, 93Kuh1, 93Fre2
CO ₂	IRAS	99Sei1
C ₂ H ₄	TDS, ELS, XPS	97Hem1
NO	LID	98Will1
NO	LID, TDS, IRAS	99Will1
NO	Theory: wavepacket calculations	98Thi1
O ₂ , C ₂ H ₄	TDS, IRAS, ELS	96Dil1, 96Fre1
O ₂ , NO, NO ₂	ELS, ARUPS, HREELS, NEXAFS	91Xu2
O ₂ , O ₂ +Cl ₂	TDS, XPS	86Foo1
OH, H ₂ O, O+H ₂ O	ARUPS	93Cap1
H ₂ O	Theory	98Bre1
Substrate: Cr₂O₃(0001)/Al₂O₃(0001), Cr₂O₃(0001)/Fe₂O₃(0001)/Al₂O₃(0001)		
H ₂ O, OH	TDS, XPS, HREELS	00Hen1
Substrate: Cr₂O₃(0001)/Pt(111)		
NO, N ₂ O, NO ₂	XPS, UPS, Theory: DFT	01Rod5
Substrate: Cr₂O₃(0001)/Pt(111), Cr₃O₄(111)/Pt(111)		
H ₂ S	XPS, ARUPS	97Rod1
Substrate: single crystal Cr₂O₃(10$\bar{1}$2)		
O ₂	LEED, XPS, AES	99Yor1

3.9.6.1 CO adsorption

The interaction of α -Cr₂O₃(0001)/Cr(110) with CO has been intensively studied both experimentally and theoretically. CO interacts only weakly with the chromyl-terminated surface but exhibits strong interaction with the chromium-terminated surface. For the chromium-terminated surface TDS exhibits a desorption maximum at 105 K which shows up after exposing the surface to doses of more than 4 Langmuirs and another maximum at 175-180 K which is visible already at low doses [01Pyk1]. According to infrared absorption spectroscopy the corresponding vibrational energies are 2132-2136 cm⁻¹, and 2170-2178 cm⁻¹ [01Pyk1]. Calculations suggest that CO molecules desorbing at $T = 175$ -180 K adsorb on oxygen threefold hollow sites with an angle of 55° between the molecular axis and the surface normal. For the more weakly bound CO molecules desorbing at 105 K it was suggested that they adsorb on oxygen on-top sites [01Pyk1]. In agreement with these results NEXAFS and ARUPS reveal the existence of a strongly tilted CO species on chromium-terminated α -Cr₂O₃(0001) [91Xu1, 92Kuh2]. Photoelectron spectroscopy reveals unusually high binding energies for the CO valence levels and the C1s core level which represents a still unexplained topic [91Xu1, 92Kuh2].

The photodesorption of CO from chromium-terminated α -Cr₂O₃ was studied by laser induced desorption with REMPI detection. In such an experiment the surface is exposed to short-time laser pulses to induce photodesorption. The desorbed molecules are detected by a second laser using resonantly enhanced multiphoton ionization via the B¹ Σ^+ state. This type of detection can be carried out fully state-selective. Time-of-flight measurements may be performed by varying the time-delay between the desorption laser pulse and the detection laser pulse. With experiments of this type it was shown that for rotationally hot molecules cartwheel rotation (J vector perpendicular to the surface normal) is the preferred rotational state after desorption whereas for rotationally cold molecules helicopter rotation (J vector parallel to the surface normal) is preferred. Using wave packet calculations based on three-dimensional potential energy surfaces it was shown that the corrugation of the excited and ground-state potential energy surfaces in the angular degrees of freedom are responsible for the experimental observation [01Thi1].

3.9.6.2 NO adsorption

NO is chemisorbed on chromium-terminated α -Cr₂O₃/Cr(100) with a desorption temperature of 340 K [91Xu2, 99Wil1] corresponding to a binding energy of about 1 eV according to the Redhead formula [62Red1]. At higher doses also a weakly bound species desorbing at 105 K (binding energy: 0.35 eV according to the Redhead formula) is detected which is attributed to the formation of NO dimers [99Wil1]. Desorption of the latter species is accompanied by the formation of N₂O, possibly forming a bilayer structure. According to IRAS experiments the N-O vibrational energy of the species desorbing at 340 K is 1759-1794 cm⁻¹ and the corresponding N-O symmetric stretching frequency of the NO dimers is at 1847-1857 cm⁻¹ [99Wil1].

Results of laser induced desorption studies of NO with REMPI detection are published in several papers [98Wil1, 99Wil1, 98Thi1]. For the high coverage regime two desorption channels are observed: a direct one where desorption occurs immediately after excitation of the adsorbate-substrate complex and a slow one where the NO molecules desorb after diffusion on the surface [99Wil1]. In the low-coverage regime the NO molecules desorb rotationally and vibrationally highly excited after irradiation with UV-laser pulses. The velocity distributions are non-Boltzmann like and bimodal with a strong dependence on the internal degrees of freedom.

3.9.6.3 CO₂ adsorption

CO₂ interacts strongly with the chromium-terminated α -Cr₂O₃(0001)/Cr(110) surface. At $T = 90$ K physisorbed as well as chemisorbed species are observed on the surface [99Sei1]. The physisorbed molecular species desorbs at 120 K and 180 K whereas the chemisorbed species desorbs at 330 K. IRAS spectra identify the chemisorbed species as a negatively charged bent CO₂ species (CO₂^{δ-}) bound to the metal ions of the surface. On the chromyl-terminated surface formation of the CO₂^{δ-} chemisorbate is strongly attenuated due to blocking of the metal ions by the oxygen atoms of the chromyl groups.

3.9.6.4 O₂ adsorption

O₂ adsorbs molecularly below room temperature onto α -Cr₂O₃(0001)/Cr(110) as a negatively charged species (O₂⁻) [96Di1]. Upon annealing part of the molecules desorb at temperatures between 290 K and 330 K. As evidenced by infrared spectroscopy the remaining O₂ molecules transform into a strongly bound chromyl species with an infrared absorption peak at 1005 cm⁻¹ which is still detected after annealing at 780 K. TDS data indicate that the chromyl species is stable up to about 1000 K [86Fool1]. As already noted in the previous paragraphs such a chromyl-terminated surface exhibits properties which are significantly different from those of the chromium-terminated surface. Due to the blocking of the chromium atoms on the chromyl-terminated surface, this surface is usually significantly less active. In the case of a α -Cr₂O₃(10 $\bar{1}$ 2) substrate O₂ adsorption was also found to lead to the formation of chromyl groups [99Yor1].

3.9.6.5 H₂O adsorption

H₂O adsorption has been investigated for α -Cr₂O₃(0001)/Cr(110) [93Cap1], α -Cr₂O₃(0001)/ α -Al₂O₃(0001) and α -Cr₂O₃(0001)/Fe₂O₃(0001)/ α -Al₂O₃(0001) [00Hen1]. Molecular as well as dissociative adsorption is reported for all three substrates. According to [00Hen1] molecular water desorbs at 295 K from α -Cr₂O₃(0001)/ α -Al₂O₃(0001) and from α -Cr₂O₃(0001)/Fe₂O₃(0001)/ α -Al₂O₃(0001) (see Fig. 3). Dissociated water desorbs at 345 K. TDS and XPS data suggest that every surface chromium atom has the capacity to bond one molecular and one dissociated water molecule [00Hen1]. The authors observe two distinct O-H vibrations of the hydroxyl groups which they attribute to terminal bonding onto a chromium atom ($\nu(\text{OH})=3600\text{ cm}^{-1}$) and to a bridging species with a O-H vibrational energy of $\nu(\text{OH})=2885\text{ cm}^{-1}$ [00Hen1].

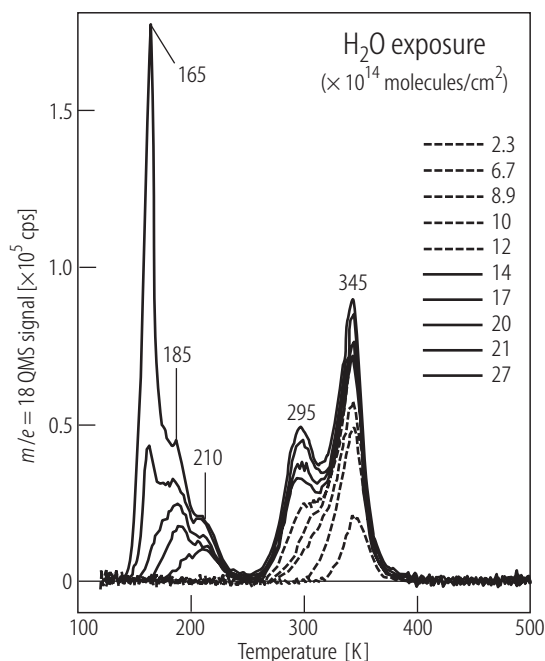


Fig. 3. TPD spectra of H₂O ($m/e = 18$) from various exposures at 120 K on the strained α -Cr₂O₃(0001)/ α -Fe₂O₃(0001)/ α -Al₂O₃(0001) surface. The dashed and solid line traces correspond to exposures above and below 1.3×10^{15} molecules/cm², respectively; [00Hen1]

3.9.7 CoO

CoO exhibits rocksalt structure (like NiO, see Fig. 10) with a lattice constant of 4.27 \AA [65Wyc1]. High-quality CoO(100) surfaces may be prepared by cleavage of CoO single crystals [95Has2, 89Mac1, 91Jen1]. At room temperature the electrical conductivity of cleaved single crystal surfaces may be high enough to allow application of electron spectroscopy without charging effects. Adsorption has also been studied on thin films of CoO. CoO(100) thin films may be prepared by oxidation of Co(11 $\bar{2}$ 0) [96Sch1, 95Has2] and the polar CoO(111) surface by oxidation of Co(0001) [96Sch1, 95Cap1, 95Has1]. Since ideal polar surfaces lead to diverging Madelung potentials [79Tas1] they must be stabilized. For CoO(111)/Co(0001) stabilization by a layer of hydroxyl groups has been reported [96Sch1, 95Cap1]. Due to the strong bond of the hydroxyl groups to the substrate they can not be removed by thermal treatment since this would significantly deteriorate the oxide film due to the high annealing temperature needed. Clean CoO(111) is stabilized by a layer of Co₃O₄ according to [00Moc1]. In the latter case the CoO(111) surface has been prepared from a CoO single crystal. Table 6 gives an overview of adsorption studies for ordered CoO surfaces.

Table 6. Overview of investigations of the interaction of gases with well ordered CoO surfaces

Adsorbates	Method	References
Substrate: Single crystal CoO(100)		
CO	ELS, HREELS	95Has2
CO, O ₂ , H ₂ O	UPS, ion bombardment	89Mac1
O ₂	UPS, ion bombardment	91Jen1
Substrate: CoO(100)/Co(11$\bar{2}$0)		
CO, NO, OH	HREELS	96Sch1
CO	ELS, HREELS	95Has2
Substrate: CoO(111)/Co(0001)		
CO, NO, OH	HREELS	96Sch1
D ₂ O, OH	HREELS	95Cap1
D ₂ O, OH, NO	HREELS, XPS	95Has1

3.9.7.1 CO adsorption

CO adsorbs molecularly on CoO(100)/Co(11 $\bar{2}$ 0) and CoO(111)/Co(0001) at 80 K [95Has2, 96Sch1] whereas at room temperature no adsorption is observed on regular surfaces [89Mac1]. The C-O vibrational energy as determined with HREELS is $\sim 2142\text{ cm}^{-1}$ for CO on CoO(100)/Co(11 $\bar{2}$ 0) and $\sim 2168\text{ cm}^{-1}$ for CO on CoO(111)/Co(0001). The latter value is higher than the gas phase value which is attributed to the so-called wall effect [95Cap2]. This is an increase of the C-O vibrational frequency due to a repulsive interaction with the electron density of the substrate during the vibrational movement. In the case of the CoO(111)/Co(0001) surface there was always a OH co-adsorbate which could not be removed.

With electron energy loss spectroscopy electronic excitations within the manifold of 3d electrons of CoO may be studied. The interaction of the surface with CO modifies the electronic surface excitation spectrum. Results of a study of this effect are published in [95Has2] together with theoretical calculations.

3.9.7.2 NO adsorption

At 80 K NO adsorbs molecularly on CoO(100)/Co(11 $\bar{2}$ 0) and CoO(111)/Co(0001) [96Sch1]. The N-O vibrational energies as determined with HREELS are $\sim 1813\text{ cm}^{-1}$ for CoO(100)/Co(11 $\bar{2}$ 0), and $\sim 1789\text{ cm}^{-1}$ for NO on CoO(111)/Co(0001) [96Sch1]. In the latter case a second feature is observed at $\sim 1650\text{ cm}^{-1}$ which is even more intense than the loss at $\sim 1789\text{ cm}^{-1}$. This vibration is attributed to NO molecules feeling the influence of neighboring hydroxyl groups [96Sch1, 95Has1].

3.9.7.3 H₂O adsorption

As already noted, the polar CoO(111) surface may be energetically stabilized by hydroxyl groups. Due to this the non-hydroxylated surface has a high affinity towards interaction with water, forming a layer of hydroxyl groups. The O-H vibrational energy is $\sim 3670\text{ cm}^{-1}$ [95Has1]. As shown with HREELS, OH groups may be exchanged for OD groups upon dosing D₂O at 450 K [95Has1].

3.9.8 Cu₂O

Cu₂O exhibits the cuprite structure with a lattice constant of 4.27 Å. The two polar (100) and the one nonpolar (111) surfaces are shown in Fig. 4. The two polar (100) surfaces are terminated by an oxygen layer or a copper layer, respectively. One of the (111) surfaces is non-polar (there are also other ones which are polar). Cu₂O(100) as well as Cu₂O(111) surfaces have been studied in the past with respect to adsorption. The surfaces have been prepared from single crystals by cutting along the desired plane, polishing the surface, and sputtering and annealing in vacuum [98Jon1, 91Sch1]. For the case of Cu₂O(100) this preparation method leads to a copper terminated surface which exhibits a $(3\sqrt{2}\times\sqrt{2})R45^\circ$ LEED pattern with missing spots [91Sch1]. Some details may be found in [91Sch1]. Adsorption experiments performed for these surfaces are listed in Table 7.

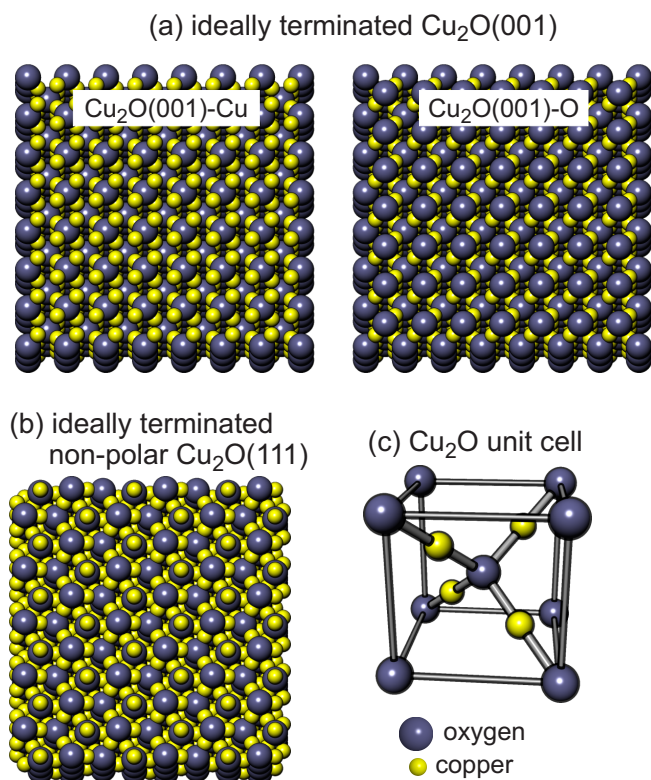


Fig. 4. Structure of the polar Cu₂O(100) surface and the non-polar Cu₂O(111) surface.

Table 7. Overview of investigations of the interaction of gases with well ordered Cu₂O surfaces

Adsorbates	Method	References
Substrate: Cu₂O(111)		
CO	Theory: DFT	99Bre1
CO	Theory: Hartree-Fock SCF, DFT	97Bre1
CO	UPS, Theory: SCF-X α -SW	98Jon2
CO, NO	Theory: DFT	97Cas3
CO, NO	Theory: LCAO-LDA	97Cas1
CO, NO	Theory: Hartree-Fock SCF	96Fer1
CH ₃ OH	XPS, NEXAFS, UPS, Theory: SCF-X α -SW	98Jon1
H ₂ O, H ₂ S	Theory: DFT	99Cas1
NH ₃	Theory: DFT	99Cas2
NO	Theory: <i>ab initio</i> cluster calculations	97Fer1, 94Fer1
O ₂	UPS, XPS, LEED	91Sch1

Adsorbates	Method	References
Substrate: Cu₂O(100)		
CO	TDS, UPS	91Cox1
H ₂	Theory: <i>ab initio</i> cluster calculations	96Nyg3
H ₂ O	Theory: <i>ab initio</i> cluster calculations	96Nyg1
H ₂ O	TDS, UPS	91Cox2
O ₂	UPS, XPS, LEED	91Sch1
Substrate: Cu₂O(110)		
CO, NO	Theory: SCC-DV-X α	94Dua1

3.9.8.1 CO adsorption

The interaction of Cu₂O(100) with CO has been studied using TDS and UPS [91Cox1]. After adsorption of CO at 120 K a complicated desorption pattern with desorption temperatures ranging from about 120 K to 320 K was observed. No CO₂ and no residual carbon were detected, indicating non-dissociative adsorption. Activation energies for desorption range from 8.4 kcal/mol to 16.7 kcal/mol as calculated with the Redhead equation [62Red1]. It was shown that doses in excess of 1000 Langmuirs are required to saturate the surface. For the case of CO adsorption on Cu₂O(111) a set of HeII UPS spectra is shown in [98Jon2]. The structures found in the spectra exhibit a shape typical for molecularly adsorbed CO which is indicative of non-dissociative adsorption. Most calculations for CO/Cu₂O listed in Table 7 agree that there are significant covalent contributions to the CO-substrate interactions and that the CO molecules bond to the Cu₂O surface with the carbon end.

3.9.8.2 H₂O adsorption

H₂O adsorption has been investigated experimentally using TDS and UPS [91Cox2] at 110 K and 300 K. At 110 K the adsorption was found to be molecular and dissociative with about 10% of a monolayer dissociated. At 300 K only dissociative adsorption occurs. The authors conclude that hydroxyl groups form on the surface [91Cox2]. In addition to the water multilayer desorption peak, TDS exhibits states at 300 K and 465 K which are assigned to recombination processes. Dissociation of H₂O is also proposed by theoretical calculations [96Nyg1].

3.9.8.3 CH₃OH adsorption

CH₃OH adsorption on Cu₂O(111) has been studied experimentally using XPS, UPS, and NEXAFS [98Jon1]. It was shown that low coverages of CH₃OH (dose 0.6 Langmuirs) are deprotonated at 140 K, forming chemisorbed methoxide. No other species is observed up to a temperature of 523 K.

3.9.8.4 O₂ adsorption

The adsorption of O₂ has been studied on the (100) and (111) surfaces of Cu₂O using UPS, XPS, and LEED [91Sch1]. On the non-polar non-reconstructed (111) surface an exposure of 10⁴ Langmuirs of oxygen at 300 K leads to a two-peak structure in UPS which was assigned to a molecular, possibly negatively charged oxygen species (O₂²⁻). For Cu₂O(100)-(3 $\sqrt{2}\times\sqrt{2}$)R45° and Cu₂O(100)-($\sqrt{2}\times\sqrt{2}$)R45° obtained after annealing at 900 K in vacuum the adsorption of oxygen was found to be atomic. For very high O₂ exposures (10⁹ Langmuirs) the (3 $\sqrt{2}\times\sqrt{2}$)R45° reconstruction is lifted and a (1 \times 1) oxygen terminated surface is observed. Annealing of the latter surface to 400-450 K leads to formation of a surface with ($\sqrt{2}\times\sqrt{2}$)R45° periodicity. Annealing at temperatures above 500 K re-establishes the (3 $\sqrt{2}\times\sqrt{2}$)R45° reconstruction.

3.9.9 FeO, Fe₃O₄ and α -Fe₂O₃

FeO (wüstite) exhibits rocksalt structure (like NiO, see Fig. 10) with lattice constants ranging from 4.28 to 4.32 Å, depending on the iron content [67Kat1], with the higher value being valid for stoichiometric FeO. The FeO phase is thermally not stable at room temperature and tends to disproportionate into Fe and Fe₃O₄ [96Cor1]. The (111) surface may be grown as a thin film on Pt(111). Typically one monolayer of iron is deposited onto the Pt(111) surface and subsequently oxidized at 1000 K for some minutes in an atmosphere of 10^{-6} mbar of oxygen, resulting in an oxygen-terminated double layer [02Wei1, 03Lei1]. According to Weiss and Ranke [02Wei1] ordered layers with a thickness of up to 2.5 ML can be grown for an annealing temperature of 870 K. The LEED pattern of the oxide film is characterized by a sixfold ring around each substrate spot which is due to a significant mismatch of the lattice constants of Pt and FeO (about 12%). This leads to a Moiré superstructure with a lattice constant of ~ 25 Å [02Wei1, 03Mey1]. The film is polar, which is energetically unfavorable in general, but stabilization of polar surfaces may be possible by charge redistribution and/or modified interlayer spacings in the surface region. Ranke and Weiss have published a review paper on iron oxide films [02Wei1] where an overview of the properties of thin iron oxide films on Pt(111) and ethylbenzene, water and styrene adsorption hereon is given. Growth of FeO(111) films has also been reported for Fe(111) [95Cap1] and Ag(111) [05Wad1] substrates.

Deposition and oxidation ($P \sim 10^{-6}$ mbar) or more iron on Pt(111) leads to Fe₃O₄(111) (magnetite) layers [02Wei1]. Fe₃O₄ exhibits the inverse spinel structure with a lattice constant of 8.396 Å [65Wyc1]. Layer thicknesses of 100 Å may easily be reached on Pt(111). At annealing temperatures of up to 920 K closed layers covering the whole surface form whereas annealing at 1000 K does not lead to closed layers. It was shown that an inward relaxed quarter layer of iron atoms on a close packed hexagonal oxygen layer [99Rit1] terminates films annealed at 1000 K (see Fig. 5). Layers prepared at lower annealing temperature may exhibit mixed termination (biphase). Here a mixture of Fe₃O₄(111) and FeO(111), and a rearranged oxygen terminated Fe₃O₄(111) surface were discussed [97Con1, 01Ket1]. Apart from preparation of Fe₃O₄(111) on Pt(111) also studies of polished natural (100) and (111) surfaces have been reported [00Ken1]. Also, thin films of Fe₃O₄(111) on single crystal α -Fe₂O₃(0001) [03Rim1] and Fe₃O₄(001) on MgO(100) [99Ped1] were prepared.

α -Fe₂O₃ (hematite) exhibits corundum structure (like Cr₂O₃, see Fig. 2) with hexagonal lattice constants of $a = 5.035$ Å and $c = 13.72$ Å [65Wyc1]. It can be prepared on Pt(111) by oxidizing at oxygen pressures of $P \sim 10^{-1}$ mbar or higher [02Wei1]. A termination by a layer of oxygen atoms (see Fig. 2c) or hydroxyl groups was proposed [02Wei1]. Oxidation at lower pressure ($P \sim 10^{-6}$ or 10^{-5} mbar) may lead to a mixed Fe₂O₃(0001) and FeO(111) termination [95Con1]. Apart from layers on Pt(111) also single crystal surfaces with (0001) and (012) orientation were studied. These surfaces were usually prepared by cutting a single crystal along the desired plane, followed by preparation in UHV using ion sputtering and annealing (see for instance [03Hen1, 01Tol1]).

Adsorption experiments performed on these iron oxide surfaces are listed in Table 8.

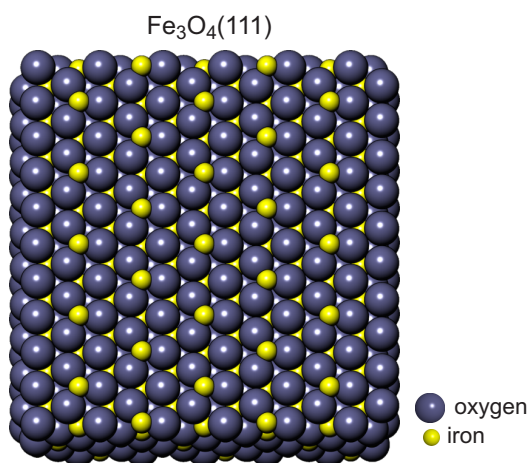


Fig. 5. Surface structure of Fe₃O₄(111)/Pt(111) according to reference; [99Rit1].

Table 8. Overview of investigations of the interaction of gases with well ordered α -Fe₂O₃ surfaces

Adsorbates	Method	References
Substrate: FeO(100)		
CO	Theory	99Che1
Substrate: FeO(111)/Pt(100)		
H ₂ O	TDS	92Vur1
Substrate: FeO(111)/Pt(111)		
ethylbenzene	UPS	98Ran1
ethylbenzene	UPS, TDS	98Zsc1
ethylbenzene	TDS, mass spectrometry	97Zsc1
ethylbenzene, styrene	NEXAFS	00Jos2
ethylbenzene, H ₂ O, styrene	UPS, adsorption isobars	02Ran1
styrene	NEXAFS, XPS, Theory: Hartree-Fock SCF	00Wuh1
H ₂ O	TDS, UPS	99Jos1, 99Sha1, 00Jos1
H ₂ O	TDS	92Vur1
D ₂ O	IRAS, TDS	03Lei1
Substrate: FeO(111)/Fe(111)		
H ₂ O	XPS	95Cap1
Substrate: Fe₃O₄(100)		
H ₂ O	XPS, NEXAFS	00Ken1
Substrate: Fe₃O₄(111)		
H ₂ O	XPS, NEXAFS	00Ken1
Substrate: Fe₃O₄(111)/Fe₂O₃(0001)		
D ₂ O	XPS, MSRI	99Her2
CCl ₄	STM	03Rim1
CCl ₄	TDS, XPS	03Adi1
CCl ₄	AES	02Cam1
Substrate: Fe₃O₄(001)/MgO(100)		
H ₂ O	TDS	99Ped1
Substrate: Fe₃O₄(111)/Pt(111)		
ethylbenzene	UPS	98Ran1
ethylbenzene	UPS, TDS	98Zsc1
ethylbenzene	TDS, mass spectrometry	97Zsc1
ethylbenzene	LEED, PEEM, TDS, mass spectrometry	98Wei1
ethylbenzene, styrene	TDS, GC	01Kuh1
ethylbenzene, styrene	NEXAFS	00Jos2
ethylbenzene, H ₂ O, styrene	TDS, UPS	99Sha1
ethylbenzene, H ₂ O, styrene	UPS, adsorption isobars	02Ran1
styrene	NEXAFS, XPS, Theory: Hartree-Fock SCF	00Wuh1
H ₂ O	TDS, UPS	99Jos1, 99Jos2
H ₂ O	TDS, UPS, XPS	00Jos1
D ₂ O	IRAS, TDS	03Lei1
unidentified (H ₂ O)	STM	00Sha1
Substrate: Fe₂O₃(0001)		
CH ₃ OH	HREELS	99Guo1
H ₂ O	XPS, thermodynamic calculations	98Liu1
H ₂ O	Theory: molecular modelling	00Jon1
H ₂ O	TDS, UPS	86Hen1
O ₂ , O	LID	98Laz1

Adsorbates	Method	References
O ₂ , H ₂ O, H ₂ , SO ₂	UPS, ion bombardment	87Kur1
OH, H	Theory	97Was1
SO ₂	UPS, XPS, UV irradiation	98To11
SO ₂	UPS, XPS, AES, UV irradiation	01To11
Substrate: Fe₂O₃(012)		
CH ₃ OH	TDS, HREELS	03Hen1
H ₂ O	TDS, SSIMS, LEED, HREELS	98Hen2
OH, H	Theory	97Was1
Substrate: Fe₂O₃(0001)/Pt(111)		
ethylbenzene	TDS, mass spectrometry	97Zsc1
ethylbenzene	LEED, PEEM, TDS, mass spectrometry	98Wei1
ethylbenzene, styrene	TDS	99Sha1
ethylbenzene, styrene	TDS, AES, LEED, STM	01Kuh1
ethylbenzene, styrene	NEXAFS	00Jos2
Substrate: Fe₂O₃(0001)+FeO(111) biphas/Pt(111)		
D ₂ O	IRAS, TDS	03Lei1
Substrate: Fe₂O₃(0001)+Fe_{1-x}O(111) biphas/Fe₂O₃(0001)		
CCl ₄	AES	02Cam1

3.9.9.1 Ethylbenzene, water and styrene adsorption

Ethylbenzene may be dehydrogenated over iron oxide catalysts to form styrene via the process [94Elv1]



This process is endothermic and therefore usually carried out at elevated temperature ($T \sim 600$ K). Water is added for different reasons, one of them being lowering of the educt partial pressure and another one is removal of coke. This reaction triggered a number of studies of styrene, ethylbenzene, and water adsorption on iron oxide, mainly performed by W. Weiss, W. Ranke and coworkers at the Fritz Haber Institute in Berlin. Adsorption was found to be molecular in all cases except in the case of water on Fe₃O₄(111)/Pt(111) which was found to dissociate, forming hydroxyl groups. This was correlated with the co-existence of iron and oxygen atoms on the Fe₃O₄(111) surface [02Wei1].

For ethylbenzene on Fe₃O₄(111) and α -Fe₂O₃(0001) a physisorbed state and a chemisorbed state were observed whereas for FeO(111) only physisorption was detected [see Fig. 6(top)]. Ethylbenzene was found to adsorb with the aromatic ring parallel to the surface plane for low coverages and with some tilt at higher coverage [02Wei1]. We note that reaction studies were undertaken where it was shown that the defective α -Fe₂O₃(0001) surface is able to catalyze the formation of styrene from ethylbenzene in the presence of steam [02Wei1] whereas the FeO(111) and the Fe₃O₄(111) surfaces are inactive. Water was found to adsorb only molecularly on FeO(111) and α -Fe₂O₃(0001) and dissociatively on Fe₃O₄(111). A set of thermal desorption spectra is shown in Fig. 6 (second row). From the measurement of kinetic isobars with UPS a number of thermodynamic data was obtained for water on the three oxide surfaces. These data are listed in Table 9.

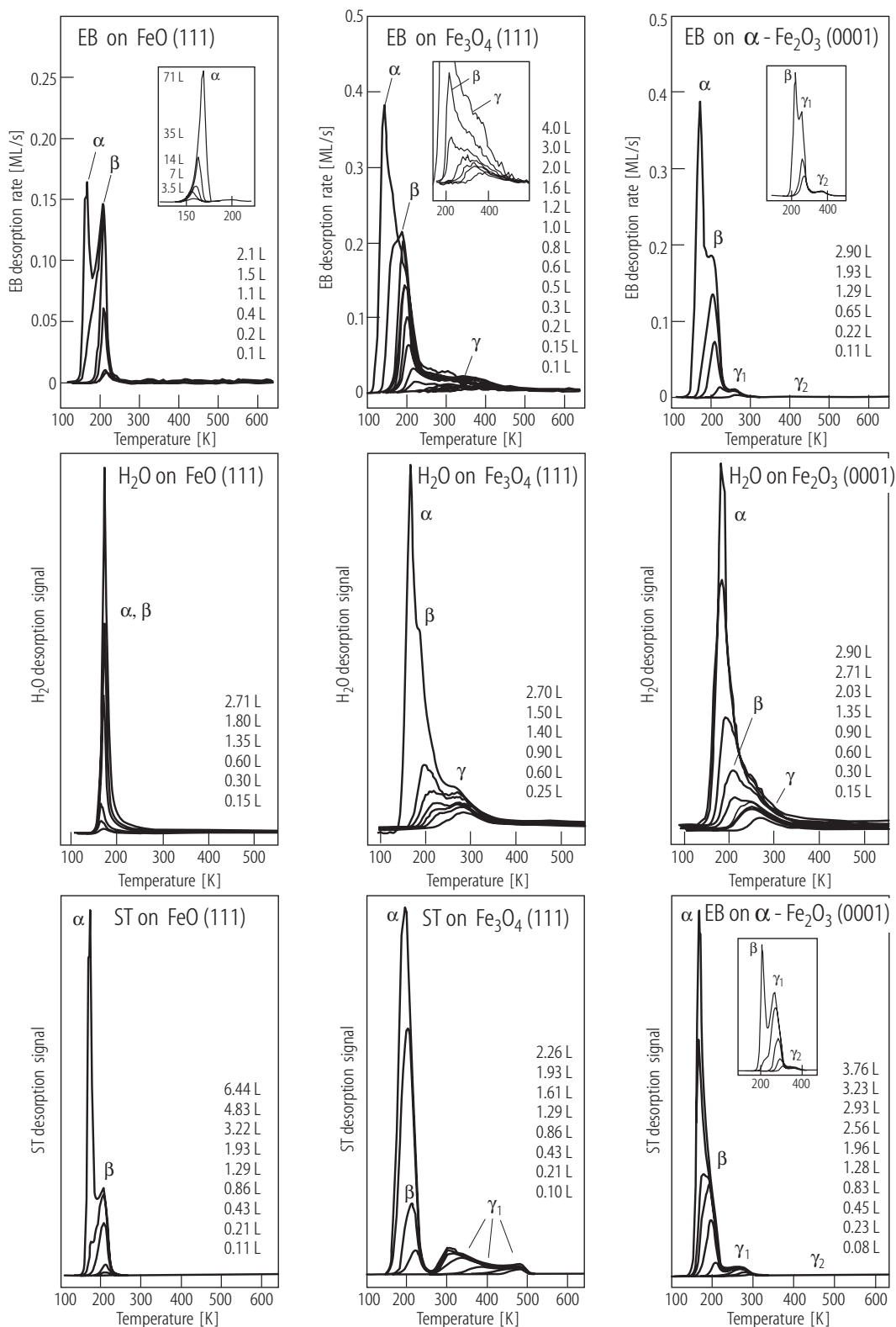


Fig. 6. TDS spectra of ethylbenzene (top), water (second row) and styrene (bottom) on FeO(111)/Pt(111) (1-2 ML thick), Fe₃O₄(111)/Pt(111) and α-Fe₂O₃(0001)/Pt(111); [02Wei1]. Exposures are given in Langmuirs.

Table 9. Saturation coverage θ_{sat} , isosteric heat of adsorption q_{st} , frequency factors ν_n and desorption order n of different water species adsorbed on epitaxial Fe-oxide films obtained from the kinetic fit of adsorption isobars measured by UPS. E_{des} is the desorption energy determined from TDS data. Data from [02Wei1].

Substrate	Adsorbate species	θ_{sat} in unit of d/l_e	q_{st} [kJ/mol]	ν_n from kinetic fit	n from kinetic fit	E_{des} [kJ/mol]
FeO(111)	β_1 (monom.)	0.55 ± 0.03	52 ± 2	$3 \pm 2 \times 10^{15} \text{ s}^{-1}$	1, mobile prec. $K = 0.13 \pm 0.04$	52^a
	β_2 (bilayer)	1.3 ± 0.2	47 ± 2	$3 \times 10^{(15 \pm 1)} \text{ s}^{-1}$	1, mobile prec. $K = 0.08 \pm 0.05$	
	α (ice)	> 1.3	40^b			48^c
Fe ₃ O ₄ (111)	γ (OH + H)	0.43 ± 0.03	65 ± 2	$(2.4 \pm 1) \times 10^{-6} \text{ cm}^2 \text{ s}^{-1}$	2	50 ± 10^d
	β_1 (monom.)	0.86 ± 0.03	50^c	$10^9 - 10^{14}$ (θ dep.) ^e	1	49^f
	α (ice)	> 0.86	38^b			48^c
α -Fe ₂ O ₃ (0001)	γ	$\sim 0.5^g$				63^h
	β	$\sim 1^g$				52^h
	α (ice)	$> 1^g$				48^c

^a Assuming first order desorption and $\nu_1 = 3 \times 10^{15} \text{ s}^{-1}$, the value deduced from the kinetic fit. ^b Lower limit. ^c From direct analysis of the Polanyi-Wigner equation using $\nu_1 = 4 \times 10^{15} \text{ s}^{-1}$ from [96Spe1]. ^d From TDS peak shift analysis assuming second order which also yields $\nu_2 = 10^{-(5 \pm 2)} \text{ cm}^2 \text{ s}^{-1}$. ^e Assuming first order desorption with constant q_{st} and fitting the frequency factor ν_1 . ^f Assuming first order desorption and $\nu_1 = 10^{13} \text{ s}^{-1}$, the mean value deduced from the kinetic fit. ^g Estimated values. ^h Redhead analysis assuming $\nu_1 = 10^{13} \text{ s}^{-1}$.

TDS spectra for styrene adsorption on the three iron oxides are shown in Fig. 6 (bottom). Similar to what was observed for water and ethylbenzene, the interaction is weakest for FeO(111), intermediate for α -Fe₂O₃(0001), and strongest for Fe₃O₄(111). With NEXAFS the orientation of the styrene molecules was determined leading to the conclusion that the phenyl group of styrene is approximately parallel to the surface plane whereas there is a significant tilting angle for FeO(111) [02Wei1]. An overview of the thermodynamic data of water, ethylbenzene and styrene on the three oxides is given in Table 10.

Table 10. q_{st} : Isosteric heat of adsorption for ethylbenzene (EB), water and styrene (ST) on FeO(111)/Pt(111), Fe₃O₄(111)/Pt(111) and α -Fe₂O₃(0001)/Pt(111). Energies in kJ/mol. ν in s^{-1} , if not stated otherwise. (CC): from Clausius-Clapeyron analysis of isobars. (kin. fit): from a kinetic fit of isobars; reaction order n for adsorption and desorption is given. (TDS): from analysis of thermal desorption data; reaction order for desorption is given. (R): Redhead method, first order, ν assumed. (LE): Leading edge method, large uncertainty in ν . (NE): Ads.-des. equilibrium not established; data uncertain. (Frag): observation of partial adsorbate fragmentation and coke formation; measurement in ads.-des. equilibrium not possible. Data from [02Wei1].

Subst.	Ads.	q_{st} (CC)	ν, n (kin. fit)	E_{des} (TDS)	ν, n (TDS)
FeO(111)	H ₂ O(phys.)	52 (β_1)	3×10^{15} (β_1), 1/1	52 (R)	3×10^{15} (A), 1
	H ₂ O(phys.)	47 (β_2)	-	-	-
	EB (phys.)	58	4.8×10^{14} , 1/1	55 (LE)	5×10^{12} , 1
	ST (phys.)	55	3×10^{10} , 1/1	-	-
Fe ₃ O ₄ (111)	H ₂ O (chem.)	65	$2.4 \times 10^{-6} \text{ cm}^2 \text{ s}^{-1}$, 2/2	50 ± 10	$10^{(-5 \pm 2)} \text{ cm}^2 \text{ s}^{-1}$, 2
	H ₂ O (phys.)	50	$10^9 - 10^{14}$, 1/1	49 (R)	10^{13}
	EB (chem.)	94-74	$5 \times 10^{12} - 2 \times 10^{10}$, 1/1	86 (LE)	10^{12} , 1
	EB (phys.)	65-52	$10^{13} - 5 \times 10^{15}$, 1/1 (NE)	47 (LE) (NE)	8×10^{11} , 1
	ST (chem.)	(Frag)	-	118 (LE)	3×10^{11}
	ST (phys.)	-	-	46 (LE)	6×10^{10} , 1

Subst.	Ads.	q_{st} (CC)	ν, n (kin. fit)	E_{des} (TDS)	ν, n (TDS)
α -Fe ₂ O ₃ (0001)	H ₂ O (chem.)	-	-	63 (R)	10 ¹³
	H ₂ O (phys.)	-	-	52 (R)	10 ¹³
	EB (chem.)	-	-	64 (LE)	1×10 ¹²
	EB (phys.)	-	-	50 (LE)	1×10 ¹¹ , 1
	ST (chem.)	-	-	73 (LE)	5×10 ¹²
	ST (phys.)	-	-	48 (LE)	4×10 ¹⁰ , 1

3.9.10 MgO

MgO(100) is one of the most often studied oxide surfaces. MgO exhibits rocksalt structure (like NiO, see Fig. 10) with a lattice constant of 4.2112 Å [65Wyc1]. The usually studied surface is MgO(100) which may be prepared by cleavage of a MgO single crystal. Another common way to produce a MgO(100) surface is the evaporation of magnesium onto Mo(100) in the presence of oxygen [92Wu2]. MgO(100) is a non-polar surface with equal numbers of cations and anions in the surface layer. Table 11 lists adsorption studies performed for ordered MgO surfaces.

Table 11. Overview of investigations of the interaction of gases with well ordered MgO surfaces

Adsorbates	Method	References
Substrate: MgO(100)		
C ₂ H ₂	LEED structure analysis	98Van1, 97Fer4
C ₂ H ₂	LEED, isosteric heat, phase diagram	96Fer3
C ₂ H ₂	LEED, thermodynamics, Theory: potential energy calculations	97Fer5
C ₂ H ₂	Theory: DFT cluster calculations	01Cai1
C(CH ₃) ₄	Adsorption isotherms	03Sai1
CH ₄ , CH ₃	Theory: <i>ab initio</i> cluster calculations	99Tod1
CH ₄ , He on CH ₄	Theory: CH ₄ hindered rotor motion, He bound state analysis	99Pic1
HCOOH	Theory: <i>ab initio</i> cluster calculations	95Nak1
HCOOH	Theory: DFT-pseudopotential	96Szy1
HCOOH	TDS, SFG, AFM	97Yam1
CH ₃ COOH, CD ₃ COOD	IR, TDS	95Xu2
acetone, keto-enol	Theory: <i>ab initio</i> cluster calculations	98Ovi2
CH ₃ I	TDS	94Hol1
CH ₃ I	UV photodissociation, REMPI-TOFMS	95Fai1
CH ₃ I	Theory: MD study of photodissociation	95Set1
CH ₃ I	Theory: photodissociation, time-dependent Hartree	95Fan1
CH ₃ Br	TDS, 193 nm photodissociation, TOF	97Gar1
CO	Theory: periodic Hartree-Fock	96Min1
CO	Theory: periodic Hartree-Fock, B3LYP	01Dam1
CO	Theory: FLAPW	98Che1
CO	Theory: interaction potential calculations, structure optimization	96Gir1
CO	Theory: <i>ab initio</i> cluster calculations	95Mej1, 96Nyg2
CO	Theory: Monte Carlo simulations	00Sal1
CO	polarization dependent FTIR	95Hei1
CO	Theory: <i>ab initio</i> cluster calculations	96Nyg2
CO	Theory: <i>ab initio</i> cluster calculations: IR shifts	91Pac1, 92Pac1

Adsorbates	Method	References
CO	Overview: theory and experiment	00Pac1
CO	Theory: BEG spin-lattice model	98Bur1
CO	Theory: SINDO1	96Jug1
CO	Theory: DFT	00Sny1
CO	Theory: DFT cluster calculations	95Ney1
CO	IR, Theory: model calculations	96Hoa1
CO	HAS	95Ger2
CO, NH ₃	Theory: IR profiles	98Gir2
CO, NO	TDS	99Wic1, 99Wic2
CO, H ₂ , O ₂	Theory: <i>ab initio</i> cluster calculations	99Pac1
CO ⁻ , O ₂ ⁻	Theory: <i>ab initio</i> cluster calculations	97Fer2
CO ₂	LEED	93Suz1, 94Pan1
CO ₂	XPS, NEXAFS	99Car1
CO ₂	Theory: <i>ab initio</i> cluster calculations	93Pac1
CO ₂	IR, Theory: interaction potential calculations	95Pic1, 95Bri1
CO ₂	polarization FTIR spectroscopy, SPA-LEED	93Hei1
CO ₂ , CO, H ₂ O	Theory: SINDO1	97Jug1
CO ₂ , SO ₂	Theory: <i>ab initio</i> cluster calculations	94Pac1
CO ₂ , N ₂ , HCl, HOCl	Theory: electric field calculations	99Tou1
CO ₂ , N ₂ O	PIRSS, LEED	96Hei1
CO ₂ , NH ₃	Theory: IR profile	96Lak1
D ₂ O, OD	ESD	97Sor1
H ₂ O, OH	LEED, PES	98Liu2
H ₂ O, OH	XSW	98Liu5
H ₂ O, OH	XPS, AFM	99Abr1
H ₂ O, OH	PES, defects	98Liu4
H ₂ O, OH	Theory: molecular dynamics	99Ode1
H ₂ O, OH	Theory: DFT	98Gio1
H ₂ O, OH	MIES, Theory: Hartree-Fock, MP2	99Joh2
H ₂ O, OH	Theory: MP2, Hartree-Fock	96Anc1
H ₂ O, OH, defects	Theory: Car-Parrinello molecular dynamics	95Lan1, 94Lan1
H ₂ O, OH, defects	Theory: periodic Hartree-Fock	94Sca1
H ₂ O, OH, defects	Theory: MSINDO	00Ahl1
H ₂ O, OH, defects	Theory: DFT, molecular dynamics	01Fin1
H ₂ O, OH	PES, defects	98Liu4
H ₂ O, OH	Theory: SINDO1	97Tik1
H ₂ O, OH, H ⁺	Theory: tight binding calculations	93Gon1
H ₂ O	tensor LEED	98Fer1
H ₂ O	Theory: MP2, Hartree-Fock	98Joh1
H ₂ O	Theory: MP2, Hartree-Fock	03Sha1
H ₂ O, D ₂ O	LEED, PIR	95Hei2
H ₂ O, D ₂ O	HAS	97Fer3
H ₂ O	UPS	99Bro1
H ₂ O	TDS	00Ahm1
H ₂ O	Theory: HF slab calculations	98Ahd1
H ₂ O	LEED, HAS	96Fer2
H ₂ O	FTIR	04Fos1
H ₂ O	Theory: molecular dynamics	96McC1, 98Gir1, 98Soe1, 98Mar1
H ₂ O	Theory: IMPT	99Eng1

Adsorbates	Method	References
H ₂ O, CH ₃ OH, CO ₂ , CH ₃ COOH, HCOOH	XPS, UPS	87Oni1
H ₂ O, H ₂ O+ N ₂ , CO ₂ , HCl, HOCL	Theory: electric field	99Tou1
D ₂ O	TDS, defects	96Sti1
D ₂ O	TDS, FTIR	05Haw1
H ₂	Theory: DFT	97And1
H ₂	Theory: <i>ab initio</i> embedded cluster	95Ste1
HCl	Theory: mixed quantum/classical time- dependent SCF (photolysis)	96Hin1
HCl	photoexcited molecular beam	00Kor1
HCl	Theory: photodissociation	95Sei1, 95Hin1
H ₂ S	XPS, Theory: DFT	99Rod1
liquid water	Theory: molecular dynamics	98deL1
NH ₃	Theory: <i>ab initio</i> cluster calculations	95Fer1
NH ₃	Theory: DFT-pseudopotential	94Pug1
NH ₃	Theory: SFG calculation	98Pou1
NH ₃	Theory: DFT	96Nak1
NH ₃	Theory: Car-Parrinello	96Lan1
NH ₃	Theory: Hartree-Fock, vibrational IR spectrum	95All1
NH ₃	Theory: interatomic potential, vibrational IR spectrum	95Lak1
NO ₂ CH ₃	Theory: <i>ab initio</i> cluster calculations	96All1
N ₂ O dissociation	Powder samples: mass spectrometry; Theory: <i>ab initio</i> cluster calculations	98Sni1
N ₂ O	Theory: DFT	99Lu1
NO, N ₂ O, NO ₂	XPS, UPS, Theory: DFT	01Rod5
NO	Theory: DFT	99Lu2
OH	Theory: slab calculations	95Gon1, 93Nog1
OH	Theory: Hartree-Fock, molecular dynamics	98Ovi1
O ₂ , O	Theory: DFT	97Kan3, 97Kan2
O ₂ ⁻	Theory: <i>ab initio</i> cluster calculations	96Pac2
O, O+CO	Theory: <i>ab initio</i> cluster calculations	94Nyg1
SO ₂	XPS, NEXAFS, Theory: DFT	01Rod4
SO ₂ , SO ₃	Theory: DFT	01Sch1
Substrate: MgO powder (preferentially MgO(100) surfaces)		
C ₂ D ₂	neutron diffraction	94Cou1
CH ₄	neutron diffraction and spectroscopy	98Lar1
N ₂	neutron diffraction	97Tra1
ND ₃	neutron diffraction	96Pan1
NH ₃	volumetric adsorption isotherms	99Joh1
NH ₃	neutron spectroscopy	96Hav1, 97Pra1, 97Pra2, 98Pra1
Substrate: MgO(110)		
OH	Theory: slab calculations	95Gon1
Substrate: MgO(111)		
H ₂ O	Theory: <i>ab initio</i> cluster calculations	95Ref1
H ₂ O, CH ₃ OH, CO ₂ , CH ₃ COOH, HCOOH	XPS, UPS	87Oni1

Adsorbates	Method	References
H ₂	Theory: molecular dynamics, Hartree-Fock	98Her1
OH	Theory: slab calculations	95Gon1
Substrate: MgO(100)/Mo(100)		
C ₆ H ₆	MIES, UPS	98Gun1
C ₆ H ₆	TDS, HREELS	96Str1
CH ₄ +O ₂	HREELS	92Wu4, 93Wu1
CH ₃ OH	HREELS	96Goo1, 92Wu1
HCOOH, CH ₃ COOH, H ₂ O, CH ₃ OH, C ₂ H ₄ , C ₂ H ₆	HREELS	92Wu3
CO	IRAS, TDS, Clausius-Clapeyron	92He2
CO	HREELS, XPS, TDS	92He1
CO	TDS	01Doh1
CO	UPS, TDS, Theory: DFT	01Rod3
D ₂ O, CH ₃ OH	MIES, UPS	99Gun1
D ₂ O, D ₂ O+Na	MIES, UPS	98Gun2
D ₂ O	TDS, IRAS, LEED	97Xu1
H ₂ O, D ₂ O, CH ₃ OH	HREELS	91Wu1, 92Wu2
H ₂ O, OH	HREELS, UPS	03Yu1
D ₂ O, CH ₃ OH	TDS, MIES, UPS	00Gun1
Mn ₂ (CO) ₁₀	Laser irradiation, mass spectrometry, IRAS, TDS	98Van2
Mn ₂ (CO) ₁₀	IRAS, TDS	97Van1
SO ₂	XPS, NEXAFS, Theory: DFT	01Rod4
Substrate: MgO(100)/NiO(100)/Mo(100)		
NO	TDS	96Xu2

3.9.10.1 H₂O adsorption

Water is the most often studied adsorbate on MgO(100). The main reason for this is likely the unclear situation with respect to water dissociation and surface hydroxylation. Most of the theoretical studies agree that water does not dissociate on regular surface sites whereas many experimental studies find that water dissociates (see references in Table 11). However, one problem concerning the experimental studies is that several different methods for preparation of the MgO(100) were employed: cleavage in UHV, cleavage in air, cutting and polishing of a single crystal disk, and thin film growth. This influences the defect density and impedes comparison of the results. Currently there appears to be some kind of agreement that water may easily hydroxylate defect sites whereas hydroxylation of regular sites requires higher water pressures (see for instance [04Fos1, 98Liu2]). Liu et al [98Liu2] report that significant hydroxylation of regular sites starts at a pressure of $\sim 1 \times 10^{-4}$ mbar.

Using helium atoms scattering (HAS) two commensurate superstructures of molecular water on regular MgO(100) were identified: a $c(4 \times 2)$ phase at temperatures below 185 K and a (3×2) phase at higher temperatures [97Fer3, 96Fer2]. The transition from the $c(4 \times 2)$ phase to the (3×2) phase was accompanied by partial desorption of water which means that the $c(4 \times 2)$ phase is more dense than the (3×2) phase. For the (3×2) phase an isosteric heat of adsorption of 85.3 ± 2.1 kJ/mol and a lateral interaction energy of 35.1 ± 9.6 kJ/mol were determined via LEED spot intensity analysis [97Fer3, 96Fer2]. Heidberg et al [95Hei2] report vibrational data for the $c(4 \times 2)$ phase. The authors observe a very broad absorption band in the range from 3050 cm^{-1} to 3500 cm^{-1} , pointing towards a significant contribution of hydrogen bonds. The dependence of the IR intensities on the light polarization led the authors to the conclusion that the molecular plane of the water molecules should be oriented essentially parallel to the surface plane. A model of the $c(4 \times 2)$ phase as proposed by Heidberg et al [95Hei2] is displayed in Fig. 7.

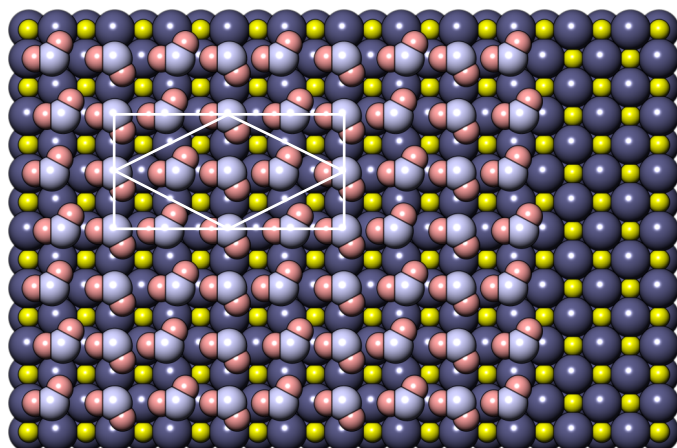


Fig. 7. Model of the $c(4\times 2)$ structure of water on $\text{MgO}(100)$ as proposed by Heidberg et al [95Hei2]. The primitive and a non-primitive unit cell are indicated.

3.9.10.2 CO adsorption

The adsorption of carbon monoxide on $\text{MgO}(100)$ has been studied by a number of groups with different methods. Thermal desorption spectroscopy has been used to study the binding energy of CO adsorbed on $\text{MgO}(100)$. Wichtendahl et al [99Wic1, 99Wic2] investigated $\text{MgO}(100)$ surfaces cleaved in UHV and obtained a binding energy of 0.14 eV by using the Redhead equation [62Red1] for a frequency factor of 10^{13} s^{-1} . The maximum of the desorption peak was found to be at 57 K (see Fig. 8). Additional structures in the thermal desorption spectra point towards the existence of a detectable number of defects even on the cleaved surface. For CO on a $\text{MgO}(100)$ film on $\text{Mo}(100)$ Dohnhálek and coworkers reported similar results (17 kJ/mol for a frequency factor of 10^{15} s^{-1}) [01Doh1]. From the intensities of the desorption peaks attributed to CO adsorbed on surface defects they estimated the density of surface defects to be ~ 0.25 monolayers for $\text{MgO}(100)/\text{Mo}(100)$ and ~ 0.15 monolayers for the UHV-cleaved surface using the data of Wichtendahl et al [99Wic1, 99Wic2].

Gerlach et al investigated CO adsorption on UHV-cleaved $\text{MgO}(100)$ at temperatures between 36 and 59 K with helium atom scattering [95Ger2]. At temperatures below 40 K a $c(4\times 2)$ phase was identified on the surface which transformed into a (1×1) phase after warming up to 51 K. Since the phase transition was only reversible when CO was offered from the gas phase, the authors concluded that the coverage of the (1×1) phase was below that of the $c(4\times 2)$ phase. Time of flight measurements revealed only a dispersion-free mode at 9 meV for the (1×1) phase whereas for the $c(4\times 2)$ phase an additional dispersion-free mode at 10.5 meV and some dispersing modes were found. It was suggested that the $c(4\times 2)$ unit cell contains three molecules, one on-top and two occupying bridging sites. The (1×1) phase was attributed to a lattice gas. These phases were studied with polarization dependent infrared spectroscopy by Heidberg et al [95Hei1]. The authors observe three different C-O vibrational modes for the $c(4\times 2)$ phase at 2152.2 cm^{-1} , 2137.2 cm^{-1} and 2132.5 cm^{-1} . The latter two modes were attributed to Davydov splitting of the modes of the two tilted CO molecules and the first mode was assigned to CO molecules adsorbed on-top. For the (1×1) structure only a single mode at 2150.5 cm^{-1} was observed.

3.9.10.3 CO_2 adsorption

Similar to H_2O , CO_2 seems to react with $\text{MgO}(100)$, forming carbonate (CO_3^{2-}) on the surface. Carrier et al [99Car1] investigated carbon dioxide adsorption with NEXAFS and XPS. Based on thermodynamic considerations (a calculation of the pressure dependence of the equilibrium $\text{MgO} + \text{CO}_2 \leftrightarrow \text{MgCO}_3$) they suggest that carbonate formation on regular surface sites occurs at pressures $P > 2.3 \times 10^{-6} \text{ mbar}$ or $P \geq 3.3 \times 10^{-9} \text{ mbar}$, depending on the input data. Below the calculated pressure (i.e. under typical UHV conditions) CO_3^{2-} formation is expected to occur on defect sites only.

Molecularly adsorbed CO_2 forms a $(2\sqrt{2}\times\sqrt{2})\text{R}45^\circ$ structure at low temperature on $\text{MgO}(100)$ as determined with LEED and SPA-LEED [96Hei1, 94Pan1, 93Suz1]. The structure has at least one glide plane and two molecules in the unit cell. From this one would expect two asymmetric stretching vibrations split by vibrational correlation forces, but three vibrations at 2334 cm^{-1} , 2308 cm^{-1} , and 2306 cm^{-1} were observed by Heidberg et al [96Hei1, 93Hei1] (see Fig. 9), one of them possibly being due to adsorption on defect sites.

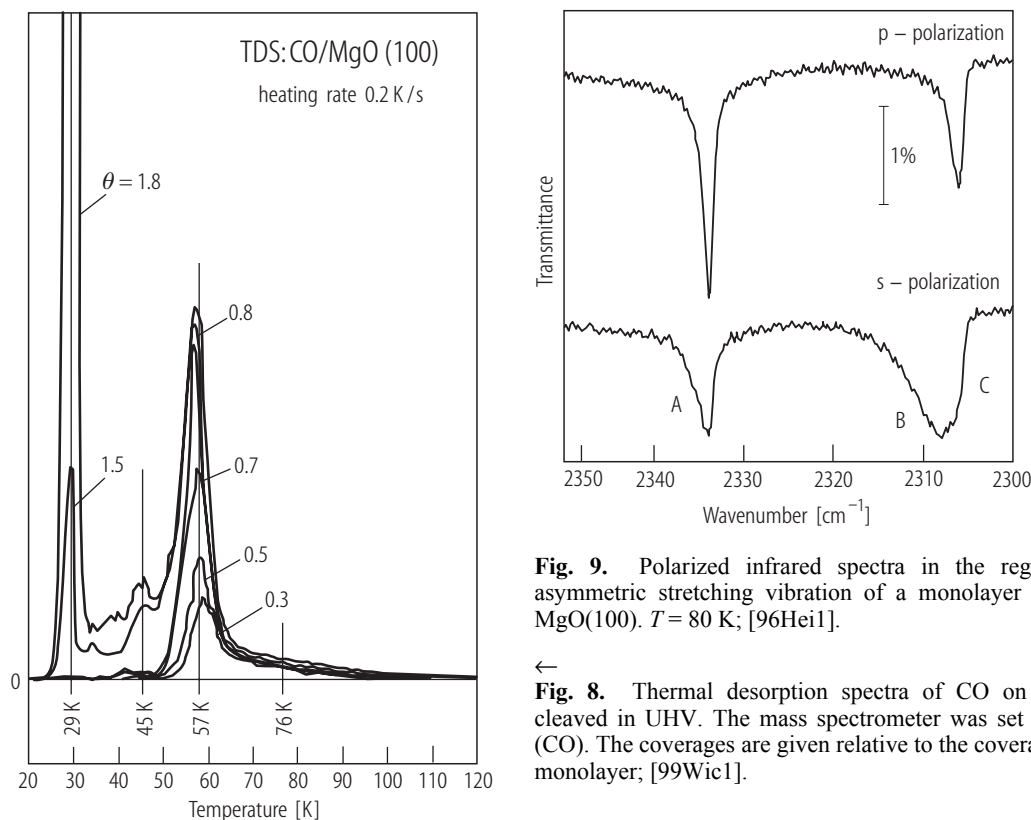


Fig. 9. Polarized infrared spectra in the region of the asymmetric stretching vibration of a monolayer of CO_2 on $\text{MgO}(100)$. $T = 80\text{ K}$; [96Hei1].

← **Fig. 8.** Thermal desorption spectra of CO on $\text{MgO}(100)$ cleaved in UHV. The mass spectrometer was set to mass 28 (CO). The coverages are given relative to the coverage of a full monolayer; [99Wic1].

3.9.11 NiO

NiO exhibits rocksalt structure with a lattice constant of 4.1684 Å [65Wyc1]. The $\text{NiO}(100)$ and $\text{NiO}(111)$ surfaces belong to the most often used substrates for adsorption studies among the oxides. $\text{NiO}(100)$ surfaces may be prepared with high quality by in-situ cleavage of single crystals in vacuum [99Wic1]. Also methods for the preparation of thin films have been established. A standard method is growth by oxidation of a $\text{Ni}(100)$ single crystal surface [91Kuh1]. It has been shown that films grown this way consist of crystallites ($\sim 50\text{ Å}$ diameter) which are tilted by some degrees with respect to the surface plane [91Bau1]. This effect was attributed to the large mismatch between the $\text{Ni}(100)$ and $\text{NiO}(100)$ lattice constants ($\sim 18\%$). The defective area between the crystallites was estimated to cover about 20% of the surface. To avoid these problems $\text{Ag}(100)$ substrates have been used [98Rei1, 00Rei1, 01Sch2]. The lattice constant of silver is 4.0853 Å [73Liu1] which is only by about 2% different from that of NiO which means that the oxide layer should be less strained. $\text{NiO}(100)$ films on $\text{Ag}(100)$ exhibit a better order than those grown on $\text{Ni}(100)$ [01Sch2, 96Mar2, 96Ber1, 99Seb1]. Films with thicknesses of up to some ten monolayers have been studied. Several adsorption experiments have also been performed for $\text{NiO}(100)$ films grown on $\text{Mo}(100)$ [93Wu2, 94Ves1, 92Tru1, 96Xu1, 93Tru1, 93Wu3]. The usual film

thickness was around 20 to 30 monolayers. It was reported that the films exhibit excellent LEED patterns indicative of long-range order [93Wu3].

NiO(111) is a polar surface and therefore intrinsically unstable [79Tas1]. An unstable ideal surface may be terminated either by a nickel or an oxygen ion layer (see Fig. 10). A NiO(111) surface may be stabilized by a so-called octopolar reconstruction [92Wol1] (see Fig. 11) which has experimentally been verified with grazing incidence X-ray scattering (GIXS) [00Bar2, 00Bar1]. A non-reconstructed NiO(111) surface may be stabilized by a layer of charged adsorbates like hydroxyl groups as reported in references [94Roh1, 98Kit1, 98Bar1]. NiO(111) surfaces may be prepared from single crystals by cutting along the (111) plane, polishing and annealing in an oxygen atmosphere [00Bar2], but adsorption experiments are reported for thin film substrates only. Most adsorption experiments have been performed for NiO(111) grown on Ni(111). These films exhibit rather broad LEED spots with significant background, indicative of only moderate crystalline quality [94Roh1, 98Kit1] which may at least partly be due to the significant mismatch of the lattice constants of the oxide film and the substrate. Some details of the film properties may be found in [98Kit1]. NiO(111) films may also be grown by oxidation of Ni(100) at room temperature. The films are hydroxyl-terminated and exhibit a LEED pattern with significant background, indicative of an appreciable number of defects [94Lan2, 91Kuh1]. Preparation of NiO(111) on Mo(110) has also been reported [96Xu1, 95Xu1]. Here the order of the films may be somewhat better as judged from the LEED pattern [95Xu1]. There is also one adsorption study for NiO(111) grown on Au(111) [97Kat1]. Due to the small lattice mismatch such films may exhibit high crystalline quality as concluded from surface sensitive X-ray scattering experiments [00Bar1]. Table 12 gives an overview of adsorption studies for ordered NiO surfaces.

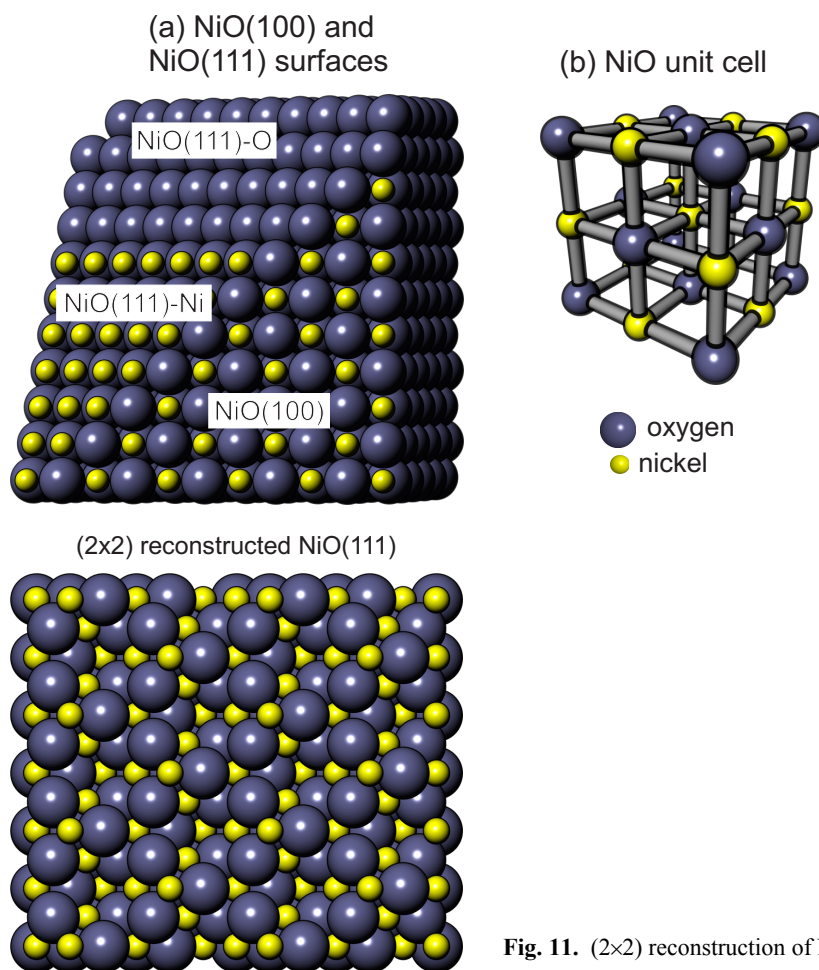


Fig. 10. (a): structure of NiO(100), oxygen terminated NiO(111) and nickel terminated NiO(111). (b) unit cell of NiO.

Fig. 11. (2x2) reconstruction of NiO(111).

Table 12. Overview of investigations of the interaction of gases with well ordered NiO surfaces

Adsorbates	Method	References
Substrate: NiO(100)		
C ₂ H ₄	AES, XPS, hydrogen reduction	85Fur1
CH ₃ OH	HREELS	92Wul2
CO	Theory: <i>ab initio</i> cluster calculations	92Poh1
CO	Theory: <i>ab initio</i> cluster calculations: IR shifts	91Pac1
CO	Theory: DFT, Hartree-Fock, hybrid methods	02Bre1
CO	Theory: DV-X	95Xu3
CO, C ₂ H ₄ , H ₂ O	AES, XPS, hydrogen reduction	86Lan1
CO, NO	TDS	99Wic1, 99Wic2
CO, NO	Theory: multiple scattering NEXAFS calculations	00Zhu1
CO, NO, NH ₃	PhD, Theory: DFT	01Hoe1, 02Kit1
H ₂	AES, XPS, LEED	85Fur2
H ₂	UPS	92Wul1
H ₂	XRD, NEXAFS, EXAFS, Theory: DFT	02Rod1
H	Theory: <i>ab initio</i> cluster calculations	80Wep1
H ₂ S	SEXAFS	99Woo1, 89Tho1
H ₂ S	RHEED, LEED, AES	78Ste1
SO ₂	XPS, UPS, ion bombardment	93Li1
NO	TDS, XPS, Theory: <i>ab initio</i> cluster calculations	91Kuh1
NO	TDS, XPS	92Bau1
NO	PhD	99Lin1
NO, OH	ELS	93Cap1
NO	Theory: <i>ab initio</i> cluster calculations	94Pet1
NO	LID, Theory	98Klu1, 97Klu1, 96Klu1, 98Klu2, 03Bac1
NO	Theory: DFT, wave function based methods	02DiV1
O ₂ , H ₂ O	UPS, XPS	85McK1
Substrate: NiO(100)/Ni(100)		
CO	TDS, NEXAFS, ARUPS	95Cap2
CO	Autoionization	96Kli1
CO, NO	TDS	99Wic1, 99Wic2
C ₂ H ₅ COOH, HCOOH	SFG	98Yuz1
azomethane (methyl groups)	TDS, XPS	98Dic1
D ₂ O, OH, OD, NO	ELS, ARUPS, XPS, TDS	93Cap1
H ₂	HREELS	91Che1
NO	TDS, XPS, HREELS, NEXAFS, Theory: <i>ab initio</i> cluster calculations	91Kuh1
NO	PhD	99Pol1
NO	HREELS, XPS, TDS	92Bau1
NO	HREELS, TDS	93Kuh1
NO	LID	96Eic1, 98Eic1, 99Eic1, 96AlS1, 90Mul1, 94Men1, 99Zac1

Adsorbates	Method	References
OH, NO	ELS, Theory: <i>ab initio</i> cluster calculations	93Fre1
perfluorodiethoxymethane	TDS, HREELS	94Jen1
Substrate: NiO(100)/Mo(100)		
CH ₃ OH, C ₂ H ₅ OH, CH ₃ OD	HREELS, TDS	93Wu2
CO	IRAS, Clausius-Clapeyron	94Ves1
HCOOH	TDS, HREELS	92Tru1
HCOOH, CO	TDS, HREELS	96Xu1
H ₂ CO	TDS, HREELS	93Tru1
NH ₃	HREELS, TDS	93Wu3
Substrate: NiO(100)/Ag(100)		
H ₂ O	TDS, UPS	98Rei1, 00Rei1
H ₂ O	TDS, XPS, UPS	01Sch2
Substrate: NiO(111)		
HCOOH	Theory: DFT, cluster model	01Miu1
Substrate: NiO(111)/Ni(111)		
C ₂ H ₂	UPS	77Dem1
HCOOH, CO, D ₂ O, OD	IRAS, TDS	98Mat1
HCOOH	IRAS	96Kub1
HCOOH	SFG, pulsed laser irradiation	99Dom1
HCOOH	TDS	96Ban1
HCOOH	TDS, IRAS	96Ban2
HCOOH	IRAS, mass spectrometry	97Ban2
C ₅ H ₅ N ⁺	ion scattering	95Wai1
CO	LID	92Ass1
CO	SFG, pulsed laser irradiation	99Ban1
CO	Autoionization	96Kli1
CO, NO	SFG, IRAS	97Ban1
CO, NO, OH	HREELS, NEXAFS	96Sch1
CO ₂	TDS, XPS, UPS	93Gor1
CO ₂ , OD	IRAS	99Mat1
H ₂ O, OH	SPA-LEED, ELS	94Roh1, 95Cap1
H ₂ O, OH	STM, LEED, thermal decomposition	98Kit2
H ₂ O, OH	STM, XPS	98Kit1
D ₂ O, OH, OD, NO	ELS, ARUPS, XPS, TDS	93Cap1
NO, OH	ELS, TDS	94Cap1
NO, OH	TDS, XPS	94Win1
NO	LID	96AlS1, 94Men1, 94Men2
Substrate: NiO(111)/Ni(100)		
CH ₃ COOH, OH	HREELS, XPS	94Lan2
NO	LID	90Mul1
H ₂ O, OH	HREELS	78And1
Substrate: NiO(111)/Mo(110)		
HCOOH, CO	TDS, HREELS	96Xu1
HCOOH	TDS, ELS, HREELS	95Xu1
Substrate: NiO(111)/Au(111)		
Di- <i>tert</i> -butylnitroxide	ESR, TDS	97Kat1

3.9.11.1 CO adsorption

NiO(100)

The binding energy of CO on NiO(100) has been studied for NiO(100) single crystals cleaved in UHV [99Wic1, 99Wic2], NiO(100)/Ni(100) [99Wic1, 99Wic2, 95Cap2] and NiO(100)/Mo(100) [96Xu1, 94Ves1] with TDS and IRAS. For the high-quality single crystal surfaces a binding energy of 0.30 eV was obtained for low coverage [99Wic1, 99Wic2], decreasing with increasing coverage due to lateral interactions of the CO molecules. A set of data for the cleaved single crystal surface is shown in Fig. 12.

There are no significant differences between the results for UHV-cleaved single crystal surfaces and the thin films although in the thin film case the TDS peaks are somewhat broader and exhibit additional structures which may be attributed to the influence of surface defects. In [94Ves1] Vesecky et al report a C-O vibrational energy of 2156 cm⁻¹ for small CO coverages on NiO(100)/Mo(100). This value is higher than the CO gas phase frequency (2143 cm⁻¹) which the authors attribute to the so-called “wall effect” and/or donation of CO 5σ charge to the substrate. The “wall effect” arises from the repulsion which the CO molecules feel when they stretch in the presence of the rigid surface as discussed by Pacchioni and Cogliandro [91Pac1]. Angular dependent NEXAFS investigations revealed that the C-O molecular axis is oriented perpendicular to the surface plane and from angular resolved valence band photoemission data it was concluded that the CO molecules bond to the substrate via their carbon lone pair [95Cap2]. Later on the CO molecular geometry was determined in much more detail with C1s scanned-energy mode photoelectron diffraction [01Hoe1, 02Kit1]. It was found that the molecules adsorb in an essentially perpendicular geometry (12±12° with respect to the surface normal) on top of the nickel surface atoms, interacting with the surface via their carbon atoms. The determined C-Ni distance was 2.07±0.02 Å. ARUPS valence band spectra of CO/NiO(100)/Ni(100) are reported in [95Cap2]. These data reveal rather high binding energies of the CO valence levels: ~10.6 eV, ~11.2 eV and ~13.9 eV for the 5σ, 1π and 4σ ionizations, respectively. The angular dependence of the intensity of the levels is consistent with a perpendicular orientation of the molecular axis. According to NEXAFS data reported in [95Cap2] the energy of the C1s → 2π ionization is about 287.4 eV.

NiO(111)

Some data also exist for CO adsorption on NiO(111). Thermal desorption spectra for NiO(111)/Mo(111) reveal broad structures between 100 and 250 K [96Xu1]. The maximum shifts from 205 K for low coverage to 155 K for saturation coverage which is somewhat larger than the corresponding values for NiO(100) (137 K and 115 K) [99Wic1, 99Wic2].

Infrared absorption spectra of CO on NiO(111)/Ni(111) are reported in [97Ban1, 98Mat1]. Matsumoto et al [98Mat1] find a doublet at 2146 cm⁻¹ and 2079 cm⁻¹. The two peaks are assigned by the authors to CO adsorption on fully (2146 cm⁻¹) and on less oxidized (2079 cm⁻¹) Ni cation sites. The SFG spectra reported in [97Ban1, 99Ban1] reproduce the high-energy vibration observed in the infrared spectra whereas the low energy vibration could not be observed due to a small cross section.

NEXAFS data reported in [96Sch1] indicate that the C-O molecular axis of CO on NiO(111)/Ni(111) is tilted by ~46° which was attributed to the octopolar reconstruction of the NiO(111) surface. The energy of the C1s → 2π resonance was found to be ~287.8 eV.

3.9.11.2 NO adsorption

NiO(100)

NO adsorption has been studied with several methods by a number of authors for single crystals as well as for thin film substrates. The NO-NiO(100) binding energy has been determined with TDS [99Wic1, 99Wic2, 91Kuh1] for a NiO(100) single crystal surface cleaved in UHV and for NiO(100) thin films grown on Ni(100). The data for the cleaved single crystal surface are shown in Fig. 13. The results for both substrates are similar, but the desorption peaks of NO on the thin film oxide are broader and exhibit significant additional intensity due to adsorption on defects. The maximum shifts from 220 to 216 K with

increasing coverage [99Wic1, 99Wic2]. Evaluation of the TDS data with the leading edge method and complete analysis gave a NO-NiO(100) binding energy of 0.57 eV for low coverage which dropped to ~0.12 eV at a coverage near to 1.

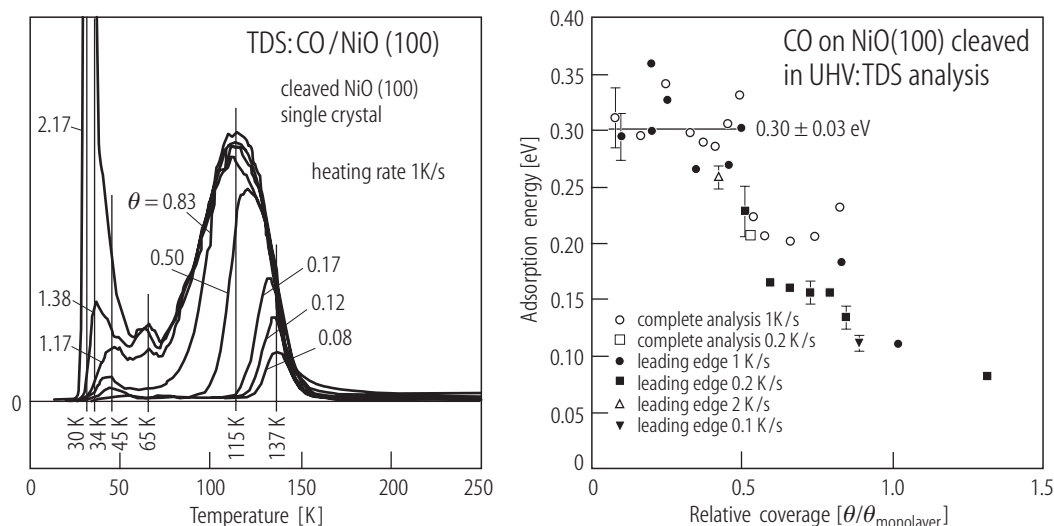


Fig. 12. Thermal desorption spectroscopy of CO on vacuum-cleaved NiO(100). Left: raw data. Right: CO-NiO binding energy as a function of coverage as obtained with the evaluation methods *complete analysis* and *leading edge*; [99Wic1, 99Wic2].

N1s XPS data are published in [92Bau1, 91Kuh1, 99Lin1, 99Pol1]. The N1s feature consists of two peaks at 402.8 and 407.2 eV for UHV-cleaved NiO(100) and at 403.1 and 407.5 eV for NiO(100) on Ni(100) [91Kuh1]. It was suggested that the two peaks are not due to different species but to a final state effect, i.e. to the distribution of the intensity between a screened and a non-screened final state [91Kuh1]. Angular dependent N1s NEXAFS data revealed that the NO molecular axis is tilted by an angle between 20 and 45° with respect to the surface normal [91Kuh1]. The tilting was attributed to be due to an interaction between the NO 2 π electron and the Ni 3d $_{x^2-y^2}$ level which is only possible in the reduced symmetry of a tilted geometry. A more detailed investigation of the adsorption geometry has been performed with photoelectron diffraction (PhD) [99Lin1, 99Pol1, 01Hoe1, 02Kit1]. From this investigation it was concluded that the NO molecules bond via their nitrogen end to the nickel surface atoms. The Ni-N distance was determined to be 1.88±0.02 Å and for the tilt angle a value of 59° (+31°/–17°) was obtained. The bonding of NO to NiO(100) leads to characteristic electronic surface excitations at 0.9 eV and ~1.8 eV as observed with medium resolution electron energy loss spectroscopy and modelled with *ab initio* cluster calculations [93Fre1]. For NO on NiO(100)/Ni(100) the N-O vibrational energy has been determined to be 1797 cm⁻¹ with HREELS [91Kuh1, 92Bau1, 93Kuh1, 96Sch1].

A number of laser induced desorption studies has been performed for NO on NiO(100)/Ni(100) with resolution of the vibrational and rotational states as well as the kinetic energy of the desorbing molecules [96Eic1, 98Eic1, 99Eic1, 96AIS1, 90Mul1, 94Men1, 99Zac1]. It was assumed that the primary excitation step occurs in the substrate. One electron may be captured by a NO molecule which starts moving away from the ground state minimum. After the electron has returned into the substrate the molecule eventually has gained enough energy to desorb. A characteristic feature of the system is that it exhibits bimodal velocity distributions with a distinct dependence on vibration, rotation, and the spin-orbit state. A number of theoretical publications [98Klu1, 97Klu1, 96Klu1, 98Klu2, 03Bac1] have dealt with this problem.

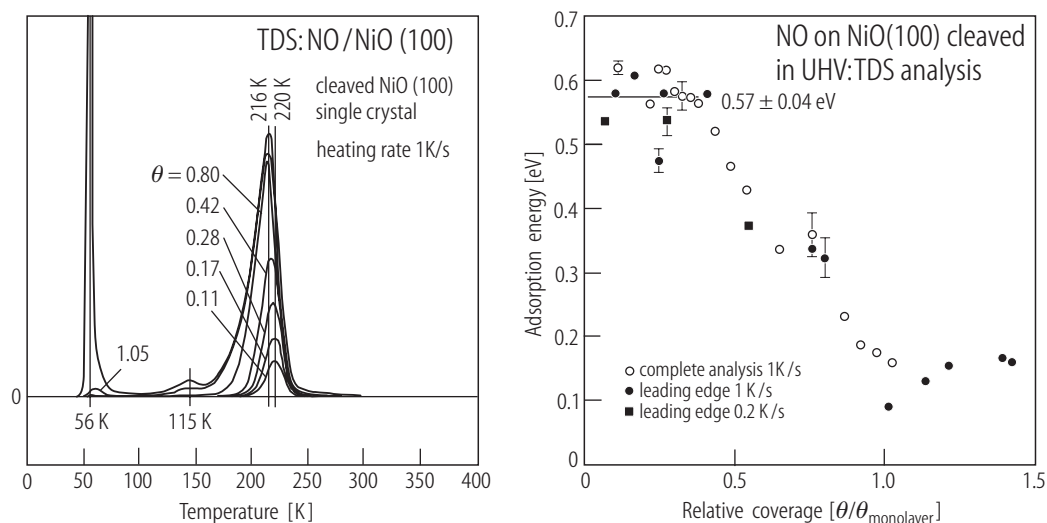


Fig. 13. Thermal desorption spectroscopy of NO on vacuum-cleaved NiO(100). Left: raw data. Right: NO-NiO binding energy as a function of coverage as obtained with the evaluation methods *complete analysis* and *leading edge*; [99Wic1, 99Wic2].

NiO(111)

Less data exist for NO adsorption on NiO(111). HREELS spectra of NO on NiO(111)/Ni(111) reveal that the energy of the N-O stretching vibration is 1772 cm^{-1} for the hydroxylated surface. This value shifts to 1805 cm^{-1} after dehydroxylation of the oxide film [96Sch1]. For dehydroxylated NiO(111) films on Ni(111) Bandara et al studied the N-O vibration with SFG and IRAS [97Ban1] and found a vibrational energy of 1800 cm^{-1} with SFG and 1805 cm^{-1} with IRAS. These energies are near to that found for NO on NiO(100) which was attributed to the octopolar reconstruction of the dehydroxylated surface: the reconstructed surface exhibits microfacets with (100)-type termination. From the polarization dependence of the SFG spectra the authors concluded that the molecular axis is oriented more or less perpendicularly to the surface which would be the case for tilted molecules on the microfacets if all molecules would be bent towards the (111) direction. This result is somewhat at variance with a NEXAFS investigation where it was shown that the NEXAFS spectra of the system are nearly independent of the light incidence angle which was attributed to rotation of the molecules around the surface normal of the microfacets [96Sch1]. The energy of the $\text{N}1s \rightarrow 2\pi$ resonance is 406.5 eV and the $\text{N}1s \rightarrow 6\sigma$ is centered at about 421 eV .

For NO on NiO(111)/Ni(111) also UV-laser induced desorption experiments have been performed [96AlS1, 94Men1, 94Men2]. Similar to the case of NO on NiO(100) the velocity distributions are bimodal, but the intensity distribution between the two modes and the dependence on the internal degrees of freedom is different.

3.9.11.3 H₂O adsorption

NiO(100)

First studies of water adsorption on NiO(100) have been reported in the eighties. McKay and Henrich [85McK1] report that water adsorbs dissociatively at room temperature on ion-bombarded NiO(100) covered with pre-adsorbed oxygen, forming hydroxyl groups. Langell and Furstenau [86Lan1] conclude that water does not interact with stoichiometric NiO(100) at temperatures between 200 and 300 K whereas at 500 K a not clearly identified layer formed on the surface. Water adsorption on thin NiO(100) films on Ag(100) was studied using XPS, TDS and UPS by R. Reissner, M. Schulze and coworkers [98Rei1, 00Rei1, 01Sch2]. TDS revealed three desorption states at 140 K, 200 K and 210-270 K. The low-temperature peak was attributed to multilayer desorption and the other two states to the monolayer. For

the state at 200 K a desorption energy of 52 kJ/mol and a pre-exponential factor of 10^{14} s^{-1} was determined using the leading edge method and for the state ranging from 210 to 270 K the calculated desorption energy is 65 kJ/mol assuming a frequency factor of 10^{13} s^{-1} . The state at 200 K was attributed to desorption from well-ordered flat NiO(100) whereas the state between 210 and 270 K was identified as originating from an ensemble of energetically different adsorption sites. Hydroxyl groups could not be observed for this substrate. For the case of NiO(100) films on Ni(100) Cappus and coworkers [93Cap1] conclude that hydroxyl groups form only on defect sites whereas vacuum-cleaved NiO(100) surfaces seem to be inert with respect to hydroxyl formation.

NiO(111)

The interaction of NiO(111) with H₂O is strong since NiO(111) is a polar surface which may be stabilized by a layer of hydroxyl groups. For NiO(111) grown by oxidation of Ni(100) references [78And1, 94Lan2] report that the oxide films are covered by hydroxyl groups directly after oxide film preparation. Rohr and coworkers [94Roh1] report a SPA-LEED study for the interaction of water with NiO(111)/Ni(111). They find that removal of the OH groups from the NiO(111) surface leads to the formation of a (2×2) superstructure in the LEED pattern which was attributed to a octopolar reconstruction as proposed by Wolf [92Wol1]. This reconstruction stabilizes the hydroxyl-free NiO(111) surface which would not be stable without this reconstruction due to its polar nature. Since a negatively charged layer of hydroxyl groups may also stabilize the surface the reconstruction is not observed for the hydroxyl-covered surface. The O-H vibrational energy is 460 meV as reported by [78And1, 95Cap1]. Kitakatsu and coworkers investigated the interaction of NiO(111)/Ni(111) with H₂O using XPS, AES and STM [98Kit1]. They observe that the film is covered by 0.85 ± 0.1 monolayers of OH⁻ after preparation at 300 K. The O1s binding energy of the hydroxyl groups was determined to be 531.4 ± 0.1 eV. Exposing the hydroxylated surface to 150 L of H₂O leads to the formation of a second layer of hydroxyl groups with the sequence OH-Ni-OH⁻, i.e. to a surface β -Ni(OH)₂ film. Oxidation of the Ni(111) surface at 500 K leads to a mixture of NiO(100) (93±3%) and NiO(111) crystallites (7±3%). Here exposure to water induces a lateral extension of the NiO(111) crystallites at the expense of the NiO(100) crystallites.

3.9.11.4 HCOOH adsorption on NiO(111)

Formic acid adsorption on NiO(111)/Ni(111) was studied with different methods. Domen, Hirose and coworkers published results of TDS, IRAS and SFG studies on this system [96Ban1, 96Ban2, 97Ban2, 96Kub1, 99Dom1, 98Mat1]. Formic acid is transformed into a tilted bidentate formate species under UHV conditions. This occurs already at 163 K, and at 250 K all molecular formic acid has disappeared. Further heating leads to decomposition of the surface formate groups into H₂+CO₂ at 340, 390 and 520 K and CO+H₂O (water undetected) at 415 and 520 K [96Ban2]. The reactions at temperatures between 340 and 415 K and at 520 K are attributed to interaction with surface nickel atoms in different oxidation states [98Mat1]. At higher formic acid pressure ($P \geq 5 \times 10^{-5} \text{ Pa}$) also monodentate formate forms under steady state conditions and the bidentate species was found to be non-tilted. The latter result was attributed to the transformation of the reconstructed NiO(111)(2×2) surface into a non-reconstructed one due to the formation of surface hydroxyl groups. Again, two formate dissociation paths are observed: formation of H₂ and CO₂ starting at 373 K with an activation energy of $22 \pm 2 \text{ kJ/mol}$ and formation of CO and H₂O above 423 K with an activation energy of $16 \pm 2 \text{ kJ/mol}$. In both cases the reaction order is 0.5 with respect to the pressure of HCOOH. From pressure dependent IRAS spectra it was concluded that the monodentate formate species acts as an intermediate for dissociation [97Ban2]. This was later substantiated by picosecond SFG spectroscopy in combination with transient laser induced heating [99Dom1]. An overview of vibrational energies observed for formate on NiO(111) and NiO(100) is given in Table 13.

Table 13. Vibrational energies of HCOOH on NiO(100) and NiO(111) in cm^{-1} . For monodentate formate $\nu_a(\text{OCO})$ and $\nu_s(\text{OCO})$ are the stretching modes of C=O not interacting with the surface and C-O bound to the surface, respectively. The table has been adapted from [96Kub1].

Vibrational mode	NiO(111) in HCOOH flow (IRAS)		NiO(111) in vacuum (IRAS)	NiO(100) (HREELS)
$\nu(\text{CH})$	2940	2850	2860	2901
$\nu_a(\text{OCO})$	-	-	1570	1594
$\nu_s(\text{OCO})$	1253	1355	1360	1377
Assignment	monodentate	bidentate	bidentate	monodentate
Reference	96Ban1	96Ban1	96Ban1	92Tru1

3.9.11.5 H₂ adsorption on NiO(100)

Hydrogen causes reduction of NiO(100) [85Fur2, 92Wul1, 02Rod1, 80Wep1]. It was shown that there is an induction period during which oxygen vacancies are created which act as hydrogen dissociation sites [02Rod1, 85Fur2]. High-quality NiO(100) crystals exhibit only negligible reactivity towards H₂ [02Rod1]. The reduction process was shown to lead to the formation of metallic nickel [85Fur2, 92Wul1, 02Rod1].

3.9.11.6 H₂S adsorption on NiO(100)

H₂S reacts with a cleaved NiO(100) single crystal surface, causing the formation of Ni rafts with a sulfur overlayer. Using EXAFS, the in-plane Ni-Ni distance was determined to be 2.77 ± 0.09 Å [99Woo1], representing a $6 \pm 4\%$ contraction with respect to the distance in NiO(100) which is also visible in LEED [78Ste1]. For the S-Ni bond length a value of 2.21 ± 0.02 Å was obtained with the S atoms occupying four-fold hollow sites in a $c(2 \times 2)$ structure.

3.9.11.7 CO₂ adsorption on NiO(111)

The interaction of CO₂ with NiO(111)/Ni(111) has been studied using IRAS, TDS, XPS and UPS [99Mat1, 93Gor1]. For the hydroxyl-free $(2 \times 2)\text{NiO(111)/Ni(111)}$ surface adsorption of CO₂ at 123 K leads to vibrations at 1263 and 910 cm^{-1} whereas for the OD covered surface a vibration at 1267 cm^{-1} was observed with IRAS [99Mat1]. The vibrations at 1263 and 1267 cm^{-1} were assigned to the symmetric O-C-O vibration and the one at 910 cm^{-1} to the out-of-plane deformation of monodentate carbonate. On the hydroxylated surface the latter vibration was much weaker which was attributed to a tilted configuration on $(2 \times 2)\text{NiO(111)/Ni(111)}$ in contrast to an upright geometry on OD/NiO(111)/Ni(111). The different molecular orientations were attributed to the different surface structures: the hydroxyl-covered surface is flat whereas the hydroxyl-free surface exhibits the micro-facets of the octopolar reconstruction. For both surfaces the vibrational signals vanished around 248 K [99Mat1]. Results for adsorption at room temperature are reported in [93Gor1]. CO_3^{2-} and CO_3^- were identified on the surface. The TDS spectra exhibit desorption peaks at 395 and 645 K [93Gor1].

3.9.12 RuO₂

RuO₂ exhibits rutile structure like TiO₂ with lattice parameters $a = 4.51$ Å and $c = 3.11$ Å [65Wyc1]. The unit cell is displayed in Fig. 14. Ruthenium oxide exhibits high catalytic activity for oxidation reactions like CO oxidation to CO₂ or methanol oxidation to formaldehyde which is one of the reasons why this oxide has been studied intensively in recent years. Other reasons are the high electric conductivity which

enables the application of electron spectroscopy and the simplicity of preparation of a $\text{RuO}_2(110)$ surface by oxidation of a $\text{Ru}(0001)$ single crystal surface. Exposure of $\text{Ru}(0001)$ to several 10^6 L of O_2 at 760 K leads to formation of a stoichiometric $\text{RuO}_2(110)$ surface [02Wen1] which is structurally similar to $\text{TiO}_2(110)$ (see Fig. 14a). Reduction with CO at 410 K leads to a slightly different surface where the oxygen rows at the surface are missing [02Wen1]. A structural model is displayed in Fig. 14b.

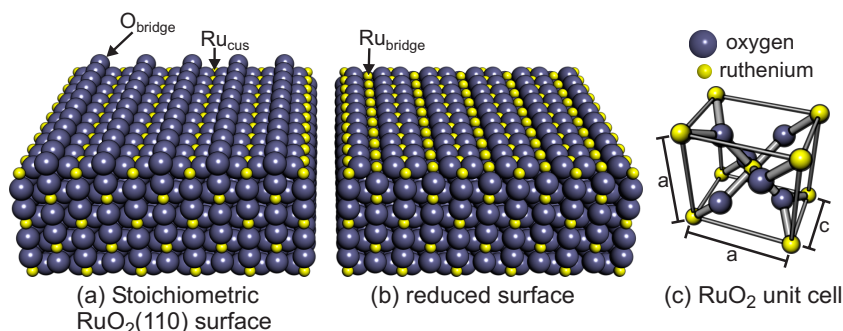


Fig. 14. Structure of the stoichiometric (a) and the mildly reduced (b) $\text{RuO}_2(110)$ surface. Panel (c) displays the rutile type unit cell of RuO_2 .

Table 14. Overview of investigations of the interaction of gases with well ordered RuO_2 surfaces

Adsorbates	Method	References
Substrate: $\text{RuO}_2(110)$		
CO, O_2	Theory: DFT	03Reu1
Substrate: $\text{RuO}_2(110)/\text{Ru}(0001)$		
C_2H_4	TDS, HREELS, isotopic labeling	04Paul
CO	STM	00Ove1
CO	STM, TDS, HREELS	03Kim1
CO	HREELS, TDS	01Wan2, 01Fan1, 03Paul
CO	TDS	03Ove1, 02Wen1
CO	TDS, LEED IV analysis, Theory: DFT	02Sei1
CO, N_2	LEED IV analysis, Theory: DFT	01Kim1
$\text{CO}, \text{CH}_3\text{OH}, \text{O}_2$	LEED, TDS	02Ove1, 01Mad1
CO_2	HREELS, TDS	02Wan1, 02Laf1
NO	HREELS, TDS	03Wan2
H_2O	TDS, HREELS	03Lob1
O_2	TDS, HREELS, LEED IV analysis, Theory: DFT	01Kim2

For RuO_2 mainly the adsorption of CO was studied which will also be the system discussed in the following. For the remaining systems the reader may consult the references listed in Table 14.

3.9.12.1 CO adsorption

Most of the adsorption studies performed for $\text{RuO}_2(110)$ dealt with CO [03Reu1, 00Ove1, 03Kim1, 01Wan2, 03Ove1, 02Wen1, 01Kim1, 02Ove1, 01Mad1, 02Sei1]. Other adsorbates have also been studied, but the CO adsorption system was surely in the focus which may be due to the high catalytic activity of $\text{RuO}_2(110)$ for CO oxidation. For the $\text{RuO}_2(110)$ surface it could be shown that CO interacts already at room temperature with the weakly bound oxygen atoms of the oxygen rows on the surface (O_{bridge} in Fig. 14), forming CO_2 . After removal of the oxygen atoms CO molecules may adsorb directly on the underlying ruthenium atoms ($\text{Ru}_{\text{bridge}}$ in Fig. 14). With HREELS two C-O vibrations at 234.5 meV and 248.5 meV are observed for this species and a CO-Ru vibration at 53.5 meV [01Wan2]. The two C-O vibrations have been attributed to CO molecules adsorbed on a symmetric bridge site and to CO bonding

to one Ru atom in a bent geometry [02Sei1]. The corresponding TDS spectrum exhibits two peaks at 415 and 470 K [03Kim1]. If the stoichiometric RuO₂(110) surface is exposed to CO at 85 K CO molecules may bond to the Ru_{cus} sites (see Fig. 14). With HREELS vibrations at 39 meV and 262 meV are detected [01Wan2]. In the TDS spectra desorption peaks at 270, 320 and 470 K show up [03Kim1]. The first two of them are attributed to desorption of CO molecules from Ru_{cus} sites whereas the third state is attributed to desorption from a Ru_{bridge} site which was formed by reduction of the surface due to the interaction with the CO molecules [03Kim1]. With STM (2×1) and c(2×2) structures were observed for CO bonded to Ru_{cus} sites which may explain the two different desorption peaks observed with TDS [03Kim1]. Reuter and Scheffler calculated the binding energies for CO on Ru_{cus} and Ru_{bridge} and obtained values of 1.26 eV and 1.58 eV, respectively [03Reu1]. An experimental value of 0.9 - 1.0 eV was given for the CO molecules on the Ru_{cus} sites [03Kim1].

We note that a somewhat different TDS spectrum of CO on a reduced surface has been published by Seitsonen et al [02Sei1]. Desorption peaks were identified at ~300 K, ~350 K and ~560 K. These peaks were attributed to CO molecules on Ru_{cus} sites, asymmetrically bridging CO molecules on Ru_{bridge} sites, and symmetrically bridging CO molecules on Ru_{bridge} sites, respectively. The differential heats of adsorption as calculated with density functional theory are reported to be 1.00 eV, 1.33 eV and 1.85 eV, respectively [02Sei1].

3.9.13 SnO₂

SnO₂ (cassiterite) exhibits rutile structure (like TiO₂, see Fig. 15) with lattice parameters of $a = 4.59373 \text{ \AA}$ and $c = 3.186383 \text{ \AA}$ [65Wyc1]. Usually the (110) surface is studied. A single crystal surface may be prepared by cutting off a piece from a single crystal needle and polishing it followed by sputtering and annealing in combination with O₂ or N₂O treatment. Depending on the preparation conditions stoichiometric as well as reduced surfaces may be prepared [95Ger1]. With increasing surface reduction a sequence of 4×1, 1×1 and 1×2 surface LEED patterns may be observed. Due to the tendency of this oxide to undergo gas-induced changes of the electrical conductivity it has important applications in gas-sensing applications. Table 15 gives an overview of adsorption studies for ordered SnO₂ surfaces.

Table 15. Overview of investigations of the interaction of gases with well ordered SnO₂ surfaces

Adsorbates	Method	References
Substrate: SnO₂(110)		
CH ₃ OH	Theory: MNDO	94Mar
CH ₃ OH	Theory: DFT, HF	99Cal1
CH ₃ OH	XPS	00Kaw1
CH ₃ OH	TDS, XPS	94Ger1
HCOOH	ARUPS, AES, LEED	96Irw1
H ₂	Theory: MNDO, AM1, PM3	95Mar1
H ₂ O	Theory: DFT	96Gon1, 02Bat1, 00Lin1
H ₂ O	TDS, UPS	95Ger1
H ₂ O, O ₂	TDS, UPS, band bending	87Sem1
O ₂	PYS	97Szu1, 94Szu1
O ₂	ARUPS, TDS, $\Delta\Phi$	92She1
O ₂	surface conductivity	87Eri1
O ₂	Theory: DFT	01Ovi1, 00Yam1
O ₂ , CO	Theory: LDA cluster calculations	95Ran1
CO	TDS, UPS	95Ger1
CO	Theory: DFT	00Mel1
CO ₂	Theory: DFT	01Mel1

3.9.13.1 O₂ adsorption

The interaction of SnO₂(110) with O₂ has been studied by several authors due to the oxygen-induced conductivity changes of SnO₂. Results of surface conductivity investigations have been published by Erickson and Semancik [87Eri1]. The authors concentrate on the influence of the surface preparation, i.e. oxygen exposure and annealing and find variations of more than two orders of magnitude of the surface sheet conductivity which was mainly attributed to variations of the concentration of oxygen vacancies. Oxygen exposure changes the concentration of vacancies and thus the conductivity. ARUPS and TDS studies indicated that oxygen adsorption at low temperature occurs molecularly. O₂ thermal desorption peaks were found at about 200 and 250 K [92She1].

3.9.13.2 H₂O adsorption

Water adsorption on stoichiometric and defective SnO₂(110) was experimentally studied using TDS and UPS [95Ger1]. Molecular desorption of water was found at 200 and 300 K and a desorption state at 435 K was attributed to OH disproportionation. It was shown that the water dissociation probability was highest on a moderately defective surface. For this surface it was assumed that all bridging oxygen atoms at the surface were removed while 80% of the surface in-plane oxygen anions did still exist.

3.9.13.3 CH₃OH adsorption

The interaction of SnO₂(110) with methanol depends also on the surface structure. Methanol may be oxidized to form formaldehyde on SnO₂(110) [94Ger1]. The conversion of methanol was found to exhibit a maximum for intermediate surface reduction. Using XPS it was shown that on the pre-oxidized surface methanol decomposition occurred via the abstraction of a hydrogen atom while on the reduced surface the methanol C-O bond was cleaved [00Kaw1]. For a list of XPS binding energies see [00Kaw1].

3.9.13.4 HCOOH adsorption

Formic acid adsorption on reduced SnO₂(110) exhibiting (1×1) and (1×2) LEED patterns was studied with ARUPS, AES and LEED [96Irw1]. At 105 K formic acid adsorbs molecularly and after annealing at 375 K it is fully desorbed, leaving no carbon residue behind. While the (1×1) LEED pattern was unaffected by this process, the (1×2) pattern was transformed into a (1×1) pattern. It was assumed that oxygen atoms from the HCOOH molecules re-oxidize the surface.

3.9.14 TiO₂

Three different modifications of TiO₂ may be found at ambient conditions: rutile, anatase and brookite. Rutile and anatase are the technically more important ones and have thus been employed for surface science studies. Both are electrically insulating in pure form. Rutile exhibits the tetragonal cassiterite structure with lattice constants $a = 4.59$ and $c = 2.96$ Å [65Wyc1]. The lattice of anatase is tetragonal; here the lattice parameters are $a = 3.88$ and $c = 9.51$ Å [65Wyc1]. The (110) surface of rutile is the most stable one of this TiO₂ modification. An image of this surface and the rutile unit cell are shown in Fig. 15. Together with MgO(100), the rutile TiO₂(110) surface is probably the most often studied oxide surface in surface science. It has been characterized extensively and well established methods for its preparation do exist. In order to establish a sufficiently high electrical conductivity for STM or electron spectroscopy the sample is usually annealed at elevated temperature and bombarded with ions which leads to a bulk reduction of the oxide as documented by a color change from colorless transparent to yellowish or bluish or even black [00Die1]. A common defect occurring upon annealing is the removal of oxygen atoms from

the rows of bridging oxygen atoms, leaving behind vacancies in these rows. Especially for the strongly reduced samples, high defect densities at the surface have to be expected. The stoichiometric (110) surface is not reconstructed, but under reducing conditions a (1×2) superstructure may form. Exposing the reduced surface to oxygen leads to re-oxidation. An overview of the properties may be found in U. Diebold's review article [03Die1]. Much less studies have been performed for $\text{TiO}_2(100)$ and $\text{TiO}_2(001)$. Both surfaces are less stable than the (110) surface. For $\text{TiO}_2(100)$ (1×1) and (1×3) surface structures have been observed with the latter one corresponding to a reduced, micro-faceted surface [93Har1]. Due to its high surface energy the (001) surface also exhibits a tendency to form microfacets as revealed by STM and LEED studies [82Fir1, 03Ter1].

Large high-quality rutile single crystals are readily commercially available which is not the case for anatase. Therefore, most studies have been performed on the rutile modification of TiO_2 although anatase appears to exhibit higher catalytic activity. Investigations have been performed for the (101) and (001) surfaces of anatase. Usually natural single crystals or thin films (grown on natural crystals) were used for the studies [03Die1].

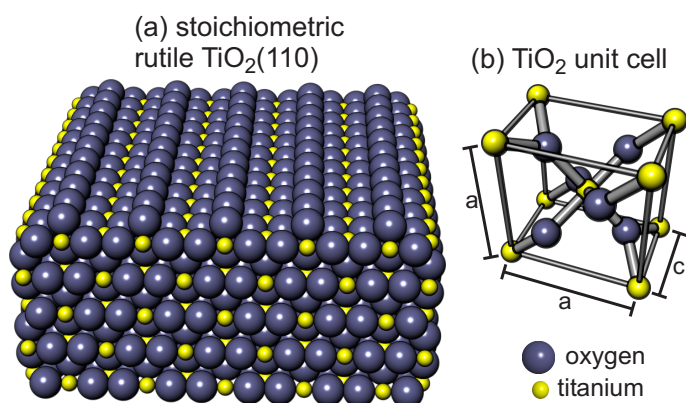


Fig. 15. (a) structure of the rutile $\text{TiO}_2(110)$ surface. (b) unit cell of rutile TiO_2 .

Table 16. Overview of investigations of the interaction of gases with well ordered TiO_2 surfaces

Adsorbates	Method	References
Substrate: anatase $\text{TiO}_2(001)$		
HCOOH	STM, NC-AFM	02Tan2
HCOOH, CH_3COOH	STM, TDS	02Tan1
HOOC-COOH , HOOC-COO^- , $\text{C}_2\text{O}_4^{2-}$	Theory: periodic Hartree-Fock calculations	95Fah1
H_2O	Theory: SINDO1	95Bre1
H_2O	Theory: DFT	98Vit1
Substrate: anatase $\text{TiO}_2(010)$		
HOOC-COOH , HOOC-COO^- , $\text{C}_2\text{O}_4^{2-}$	Theory: periodic Hartree-Fock calculations	95Fah1
Substrate: anatase $\text{TiO}_2(101)$		
HCOOH, $\text{HCOOH}+\text{OH}$	Theory: DFT	00Vit1
H_2O , H_2S , HI	Theory: molecular dynamics	98Sel1
H_2O , CH_3OH	TDS, XPS	03Her1
H_2O	Theory: DFT	98Vit1, 03Til1
<i>cis</i> (CO)- <i>trans</i> (I)-Ru-(4,4'-dicarboxylate-2,2'-bipyridine)(CO) $_2\text{I}_2$	Theory: DFT	02Hau1
Substrate: rutile $\text{TiO}_2(100)$		
$\text{C}_4\text{H}_4\text{S}$	AES, UPS, XPS, electron and X-ray irradiation	97Raz1

Adsorbates	Method	References
C ₆ H ₆	AES, UPS, XPS, electron and X-ray irradiation	98Raz1
CO ₂	UPS, MIES	01Bra1
H ₂ O	UPS, XPS	99Wan1
H ₂ S, MeSH	Theory: periodic Hartree-Fock calculations	96Fah1
HOOC-COOH, HOOC-COO ⁻ , C ₂ O ₄ ²⁻	Theory: periodic Hartree-Fock calculations	95Fah1
maleic anhydride	TDS, Theory: PM3	00Will
NH ₃	Theory: periodic Hartree-Fock calculations	96Mar1
NH ₃ , (CH ₃) ₂ NH, C ₂ H ₅ NH ₂	XPS, TDS	03Far1
SO ₂	NEXAFS	96Raz1
Substrate: rutile TiO₂(001)		
acrylic acid	TDS, XPS, scanning kinetic spectroscopy	01Tit1
CH ₃ COOH	photoreaction	03Will
H ₂ O	TDS	96Hen1
<i>tert</i> -butylacetylene	TDS	95Pie1
trimethylsilyl acetylene	TDS, XPS	02She1
cyclooctatetraene	TDS, NEXAFS	01She1
benzaldehyde	NEXAFS, TDS	00She1
Substrate: rutile TiO₂(110)		
2,2'-bipyridine-4,4'-dicarbocyclic acid	XPS, NEXAFS, Theory: INDO	99Pat1
2,2'-bipyridine-4,4'-dicarbocyclic acid	NEXAFS, Theory: ZINDO	00Per1
2,2'-bipyridine-4,4'-dicarbocyclic acid	NEXAFS, Theory: DFT	03Ode1
isonicotinic acid, nicotinic acid, picolinic acid	XAS, STM	03Sch2, 03Sch1
2-propanol+oxygen	photocatalysis, molecular beam, XPS	98Bri3, 98Bri1, 00Bri1
CD ₃ I	photon irradiation, REMPI	96Hol1
C ₂ H ₅ OD, tetraoxysilane, pre and post-adsorption of H ₂ O	TDS	96Gam1
CH ₃ I, CH ₃ Br	UV photodesorption, mass spectrometry	98Kim1
CH ₃ I	TDS, UV photodesorption	00Kim1
CH ₃ OH	TDS, ESD, electron irradiation	98Hen3
CH ₃ OH	TDS, XPS	03Far2
CH ₃ OH	Theory: DFT, pseudopotential	98Bat1
CH ₃ OH, CH ₃ OH+H ₂ O, CH ₃ OH+O ₂	TDS, HREELS, LEED	99Hen2
CH ₃ OH, HCOOH	STM	03Ter1
HCOOH	XPS	96Idr1
HCOOH	XPD	98The1, 97Cha1
HCOOH	XPD, XPS, LEED, TDS, HREELS	98Cha1
HCOOH	TDS, SSIMS, HREELS	97Hen1
HCOOH	XPS, IRAS, LEED	99Hay1
HCOOH	HREELS	00Cha1
HCOOH	molecular beam, STM, LEED	02Bow1
HCOOH	STM	00Ben1
HCOOH	UPS, XPS, Theory: <i>ab initio</i> cluster calculations	97Wan1

Adsorbates	Method	References
HCOOH	Theory: DFT	00Kac1, 00Kac2
HCOOH, O ₂ , C ₅ H ₅ N	STM	98Iwa1
HCOOH, OH	STM, NC-AFM	01Iwa1, 96Oni1
HCOOH, CH ₃ COOH, C ₂ H ₅ COOH	NEXAFS	01Gut3
HCOOH, CH ₃ COOH	NC-AFM	99Fuk1, 01Sas1
DCOOD	XPS, TDS	03Wan1
DCOOD	TDS, LEED, AES, XPS, UPS	94Oni1
CH ₃ COOH, C ₆ H ₅ COOH	STM, LEED	99Guo2
CH ₃ COOH, CF ₃ COOH	NC-AFM	01Sas2
CH ₃ COOH	UPS	97Coc1
CH ₃ COOH	LEED, ESDIAD	97Guo1
CH ₃ COOH, DCOOH	STM	98Egd1
CH ₃ COOH	NC-AFM	00Fuk1
CH ₃ COOH	Temperature jump STM	96Oni3
C ₆ H ₅ COOH	STM, ESDIAD, LEED	97Guo2
C ₅ H ₅ N	STM, NC-AFM	99Suz1
C ₁₇ H ₃₅ COOH	AFM, photo degradation	99Saw1
benzene, naphtalene, anthracene	NEXAFS, XPS, TDS	02Rei1
glycine	PES, photon damage	99Sor1, 00Sor2
C ₄ H ₄ S	XPS, TDS, Theory: DFT	03Liu1
Cl ₂	STM	98Die1
CO	Theory: <i>ab initio</i> cluster calculations, band structure calculations	96Pac1
CO	Theory: FLAPW	01Yan1
CO	Theory: DFT, pseudopotential	98Sor1
CO	Theory: periodic Hartree-Fock	96Rei1
CO	ESD, AES	95Tor1
CO	TDS	95Lin1
CO	molecular beam	03Kun1
CO+O ₂	TDS, PID	96Lin2
CO, H ₂ O	Theory: DFT	99Cas4
CO, H ₂ O, H ₂ S	Theory: DFT	98Cas2
CO ₂ +H ₂ O	TDS, SSIMS, HREELS	98Hen1
CO ₂	TDS	03Tho1
CrO ₂ Cl ₂	TDS, $\Delta\Phi$, AES, SSIMS, XPS	98Ala1
FPTS[(3,3,3- trifluoropropyl)trimethoxysilane]	TDS, XPS, SSIMS	98Gam1
H ₂ O	Theory: DFT	97Lin1, 96Gon1
H ₂ O	Theory: DFT, molecular dynamics, slab	96Lin1, 98Lin1
H ₂ O	Theory: SINDO1	95Bre1
H ₂ O	Theory: HF slab calculations	98Ahd1
H ₂ O	Theory: FLAPW	98Vog1
H ₂ O	Theory: Hartree-Fock, DFT	99Ste1
H ₂ O	Theory: MP2, Hartree-Fock	03Sha1
H ₂ O	Theory: DFT	03Zha2
H ₂ O	Theory: Hartree-Fock, MP2	02Sha1
H ₂ O	UPS	77Hen1
H ₂ O	TDS, HREELS	96Hen2
H ₂ O	TDS	96Hen1

Adsorbates	Method	References
H ₂ O	TDS, XPS,	94Hug1
H ₂ O, O ₂	TDS	98Ep11
H ₂ O, CO ₂ , NH ₃ , OH	Theory: Hartree-Fock	99Ahd1
H ₂ O, liquid and vapor	UPS, XPS	95Wan1
H ₂ O	TDS, molecular beam scattering	98Bri2
H ₂ O, CH ₃ OH, H ₂ O ₂ , HCOOH	Theory: DFT	98Bat2
HOOC-COOH, HOOC-COO ⁻ , C ₂ O ₄ ²⁻	Theory: periodic Hartree-Fock calculations	95Fah1
N ₂	Theory: <i>ab initio</i> cluster calculations	98Rit1, 99Rit3
N ₂	Theory: Monte Carlo simulations	99Rit2
NO	UV photochemistry, TOF mass spectrometry	00Rus1
NO, CO, H ₂ CO	Theory: Hartree-Fock, MP2	01Li1
NO	TDS, Theory: DFT, pseudopotential	00Sor1
NH ₃	Theory: periodic Hartree-Fock calculations	96Mar1
NH ₃	APECS	00Siu1
N ₂ O	SHG, XPS	97Shu1
NO ₂	XPS, NEXAFS, Theory: DFT	01Rod2
NO ₂	PES	02Cha1
O ₂	SHG, XPS	95Shu1
O ₂	STM	96Oni2, 98Die2
O ₂	TDS, ELS, isotopic labeling, sticking coefficient	99Hen1
O ₂ , O ₂ +H ₂ O	TDS, SSIMS, EELS	01Per1
O ₂	Theory: DFT	99Shu1
OH	XPS	96Bul1
OH	Theory: slab calculations	95Gon1, 93Nog1
OH, H	ion scattering	01Fuj1
H ₂ S	UPS	89Smi1
H ₂ S, MeSH	Theory: periodic Hartree-Fock calculations	96Fah1
SO ₂	NEXAFS	89Tho1
SO ₂	XPS	01Say1
SO ₂	XPS, UPS, PSD	97Rom1
SO ₂ Theory: DFT	03Zha1	
{Rh(CO) ₂ Cl} ₂ +H ₂	IRAS, XPS	98Hay1
{Rh(CO) ₂ Cl} ₂	STM	01Ben1
Rh((CH ₃ CO) ₂ CH) ₂ (CO) ₂ , Rh(CO) ₂ Cl	XPS, TDS	00Eval
merocyanine dye	NEXAFS, STM	02Mat1

For TiO₂ a number of adsorbates has been studied, partly in great detail. Some systems will be discussed in the following and for the remaining systems the reader may consult the references listed in Table 16.

3.9.14.1 CO adsorption

Only a limited number of adsorption studies has been performed for CO on TiO₂. Linsebigler et al [95Lin1] performed a TDS study for CO adsorption on stoichiometric and reduced rutile TiO₂(110). CO desorption was found to occur at 170 K for low coverage. With increasing coverage the desorption temperature shifted to about 135 K as shown in Fig 7.16a. From these data an adsorption energy of 9.9

kcal/mol was determined for the zero coverage limit. CO was found to desorb molecularly and no CO_2 formation was observed (if CO is co-adsorbed with O_2 on a $\text{TiO}_2(110)$ surface with oxygen vacancies, CO_2 may be formed upon irradiation with light with $h\nu \geq 3.1$ eV [96Lin2]). The shift of the CO desorption peak with increasing coverage was attributed to lateral interactions which were found to have an energy of about 2.2 kcal/mol at a relative coverage of 0.68 ML. The authors estimated that the maximum CO density at the surface is about half of the density of in-plane titanium atoms which were named as the CO adsorption sites.

Fig 7.16b demonstrates that defects on the surface lead to more strongly bound CO molecules. The desorption peaks tail up to 350 K. Pre-adsorbed oxygen was found to suppress these desorption states. Since the CO maximum coverage was the same as for the stoichiometric surface the authors of the TDS study [95Lin1] concluded that the CO adsorption sites are the same in both cases and that the additional binding energy observed for the reduced surface is provided by interaction of the oxygen end of the CO molecules with a neighboring vacancy site. A molecular beam study for CO on rutile $\text{TiO}_2(110)$ was performed by Kunat and Burghaus [03Kun1] as a function of incidence angle, kinetic energy and surface temperature. For an impact energy of 0.05 eV an initial sticking probability (this is the sticking coefficient for vanishing coverage) of $S_0 = 0.84 \pm 0.05$ was obtained. The sticking coefficient was found to decrease with increasing kinetic energy towards a value of $S_0 = 0.1 \pm 0.05$ for a kinetic energy of 0.57 eV. Temperature dependent measurements revealed that the initial sticking coefficient is independent of the temperature which was interpreted as an indication of non-activated adsorption. The dependence of the initial sticking coefficient on the angle is a function of the kinetic energy: for small kinetic energies the initial sticking coefficient is only weakly dependent on the incidence angle whereas for energies above 0.5 eV normal energy scaling takes place. For normal incidence the sticking coefficient $S(\theta)$ is nearly independent of the coverage θ : $S(\theta) \sim S_0$ independent of the incidence energy. For grazing incidence and a kinetic energy of 0.52 eV auto-catalytic behavior (increase of $S(\theta)$ with increasing θ) was observed for incidence along $[1\bar{1}0]$ whereas for incidence along $[001]$ the adsorption probability was found to decrease slightly with increasing incidence angle. From the temperature dependence of the saturation coverage the authors derived a heat of adsorption of $E_d = (7.2 - 1.6\theta)$ kcal/mol using a frequency factor of $\nu_d = 1 \times 10^{-13} \text{ s}^{-1}$ which is not far from the value determined with thermal desorption spectroscopy [95Lin1].

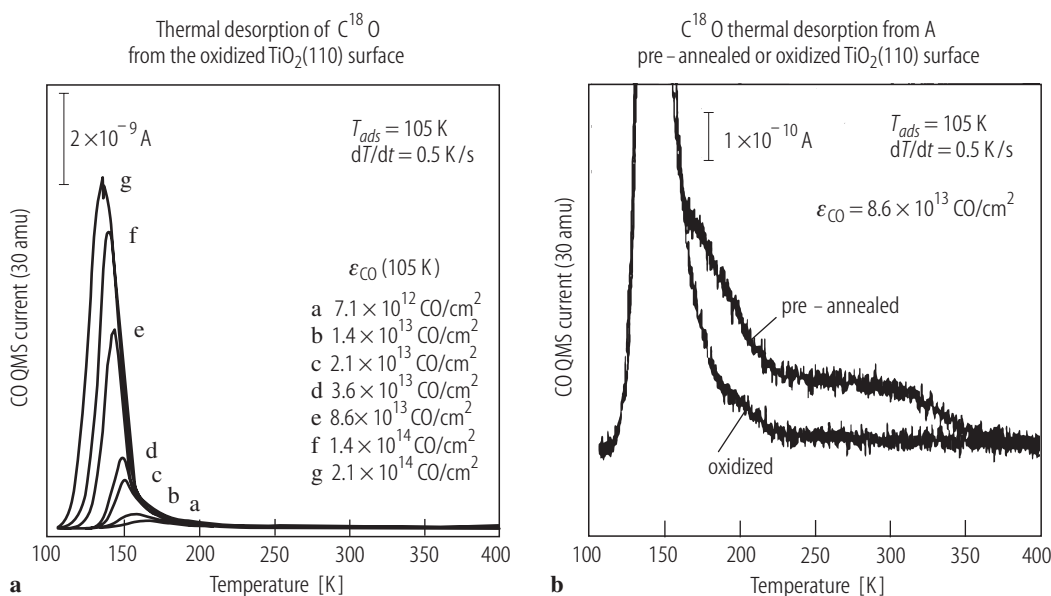


Fig. 16. (a): Thermal desorption spectra of C^{18}O on rutile $\text{TiO}_2(110)$ after adsorption at 105 K. (b): Comparison of TDS spectra of CO on stoichiometric and annealed $\text{TiO}_2(110)$; [95Lin1].

3.9.14.2 H₂O adsorption

The interaction of water with TiO₂ is technologically interesting since TiO₂ is active for water photolysis. The chemical activity of TiO₂(110) for water dissociation (without photon irradiation) is low according to most experimental results. It appears that there is some activity for dissociation at defect sites whereas the regular surface is inert with respect to H₂O dissociation.

Henderson [96Hen2], Brinkley et al [98Bri2] and Hugenschmidt et al [94Hug1] have published TDS data of water on TiO₂(110). The data provided by Henderson are shown in Fig. 17. The desorption maxima at 155 K, 174 K and 270 K are attributed to multilayer, bilayer, and monolayer water, respectively. According to [98Bri2] the monolayer coverage is $5.2 \times 10^{14} \text{ cm}^{-2}$ and the condensation coefficient of water is about 1. Water vibrations are found at 1625 and 3420-3505 cm⁻¹ [96Hen2]. The three publications agree that only a very small concentration of hydroxyl groups forms on the surface. According to [94Hug1] surface hydroxyl groups were detected with a concentration of ~1%, desorbing at 500 K. With HREELS the O-H vibrational energy was determined to be 3690 cm⁻¹ [96Hen2]. It was suggested that the hydroxyl groups bond to oxygen vacancies. The experimentally observed low activity of TiO₂(110) for water dissociations is at variance with many theoretical publications which propose that water should dissociate also on regular TiO₂(110) sites (see the references in Table 16).

3.9.14.3 HCOOH adsorption

The adsorption of a number of organic molecules on TiO₂(110) has been studied and formic acid was surely one of the most often investigated molecules which is at least partially due to the activity of titania for the photo-assisted decomposition of organic molecules. An electron-hole pair may be created in TiO₂ upon irradiation with sunlight. The charge carriers may travel to the surface and attack water and oxygen forming radicals which may oxidize adsorbed organic molecules. Such a process may be used for purification, environmental cleaning, etc.

On TiO₂(110) formic acid decomposition into formate+hydrogen occurs already at low temperature:

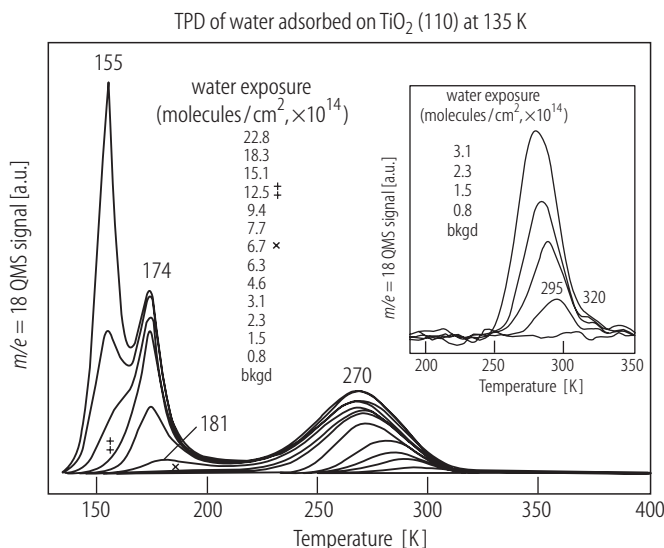


Fig. 17. TDS spectra of H₂O on TiO₂(110); [96Hen2].

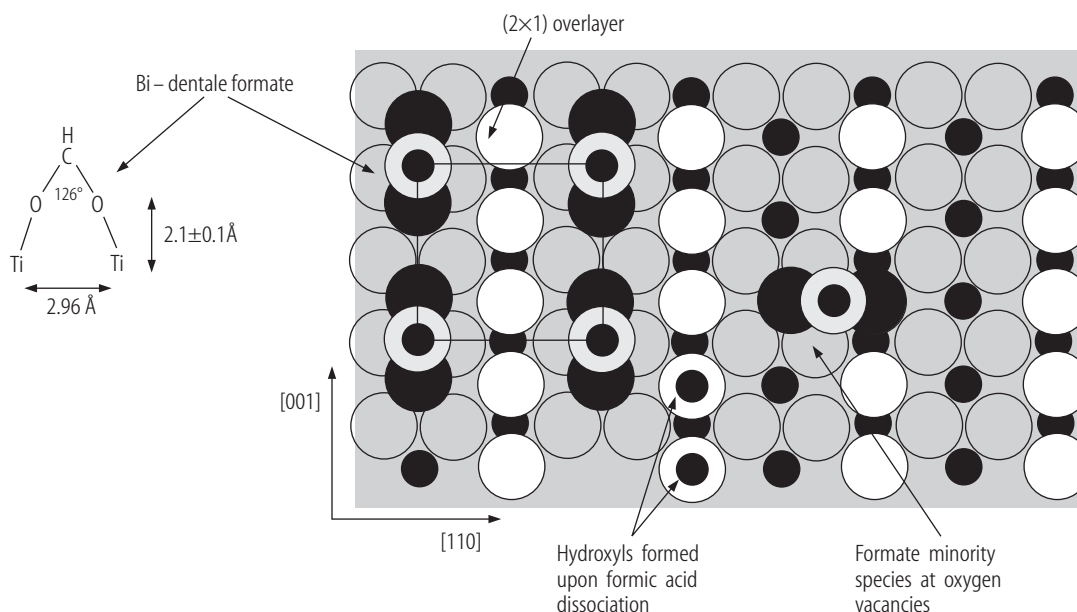
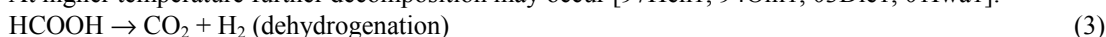


Fig. 18. Structure of HCOO ions on TiO₂ (110); [03Die1].

At higher temperature further decomposition may occur [97Hen1, 94Oni1, 03Die1, 01Iwa1]:



and



Formate forms a (2×1) phase on TiO₂(110) with a nominal coverage of 0.5 molecules per TiO₂(100) surface unit cell. The geometrical parameters of this layer have been investigated with NEXAFS and XPD [97Cha1, 01Gut3] (for the intermolecular angles and distances see Fig. 18). Apart from molecules adsorbing on regular (2×1) sites also defect adsorption as shown in Fig. 18 has been observed. The latter molecules are adsorbed with their molecular plane parallel to $[1\bar{1}0]$ and bind to oxygen defects. With infrared spectroscopy the vibrational energies of the HCOO groups were determined to be $\nu_{\text{asym}}(\text{OCO}) = 1566 \text{ cm}^{-1}$ and $\nu_{\text{sym}}(\text{OCO}) = 1363 \text{ cm}^{-1}$ for the molecules with their molecular plane parallel to the [001] direction and $\nu_{\text{asym}}(\text{OCO}) = 1535 \text{ cm}^{-1}$ and $\nu_{\text{sym}}(\text{OCO}) = 1393 \text{ cm}^{-1}$ for the other species [99Hay1]. Deviations in the NEXAFS data [01Gut3] from the expected results for the ideal (2×1) structure were also explained by the existence of the minority species. Co-adsorbed molecular HCOOH which is found at formate coverages above 0.5 was shown to desorb at 164 K [97Hen1].

Formate groups on TiO₂(110) were imaged with STM and non-contact-AFM [98Iwa1, 00Ben1, 01Iwa1, 99Fuk1, 01Sas1]. Fig. 19 shows a set of STM images obtained by Onishi et al [96Oni1] at room temperature. Here scanning with high bias voltage was used to remove part of the formate molecules. Fig. 19 shows that the hole is mainly filled up by diffusion of molecules along the titanium rows. The bottom row of images shows the mobilization of a single formate ion by the moving formate ion front.

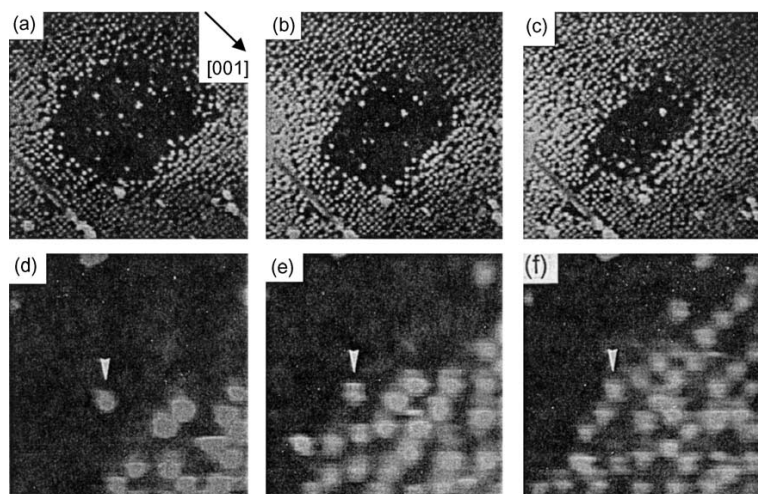


Fig. 19. Serial topographs of a manipulated (2×1) formate layer. Before the first image was recorded the sample was scanned with a high voltage to form a hole in the covered area and the scans (a), (b) and (c) were taken 15, 26, and 35 minutes later. The small area scans show the incorporation of an isolated molecule into the migrating monolayer. (e) and (f) were recorded 296 and 666 s after (d) was recorded. Large areas: (29×28 nm²); small areas: (6.8×6.8 nm²); [96Oni1].

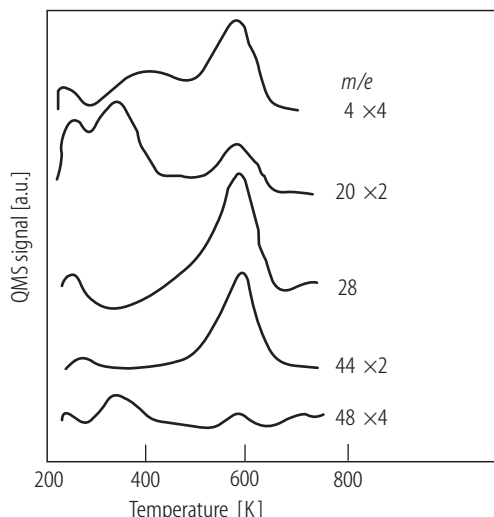


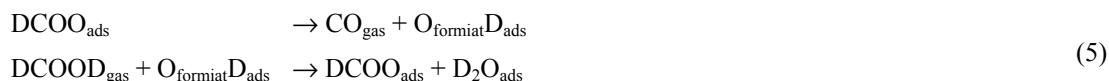
Table 17. The relative amount of desorbing species observed with TDS (see Fig. 20) of a (2×1) formate overlayer on TiO₂(110); [94Oni1].

Temperature [K]	Product	Relative amount
350	DCOOD	16
	D ₂ O	10
400	D ₂	5
570	CO	16
	CO ₂	11
	D ₂ O	5
	D ₂	6
	DCOOD	7

Fig. 20. Thermal desorption spectra of DCOOD on TiO₂(110). *m/e*=4: D₂, 20: D₂O, 28: CO, 44: CO₂, 48: DCOOD; [94Oni1].

Thermal desorption spectra of DCOOD on TiO₂(110) are displayed in Fig. 20 [01Iwa1]. These data show that the formate layer decomposes via the dehydration pathway (equation 4) as well as via dehydrogenation (equation 3) with the main desorption occurring at about 570 K. The relative intensities of the desorbing species are listed in Table 17.

Iwasawa et al [01Iwa1] investigated the catalytic decomposition of DCOOD on TiO₂(110) by determining turnover frequencies as a function of temperature for different pressures (see Fig. 21). The figure shows that for temperatures below ~500 K dehydrogenation is dominant whereas at higher temperature dehydration is more important. The dehydration process was assumed to be unimolecular with an activation energy of 120 kJ/mol and a pre-exponential factor of $2 \times 10^{-9} \text{ s}^{-1}$. Since the dehydrogenation rate depends significantly on the gas pressure this process was assumed to be bimolecular (under the participation of another DCOOD molecule) with an activation energy of 15 kJ/mol. According to Diebold [03Die1] these processes are



for dehydration with the unimolecular decomposition of DCOOD being the rate determining step and for dehydrogenation the following process was proposed:



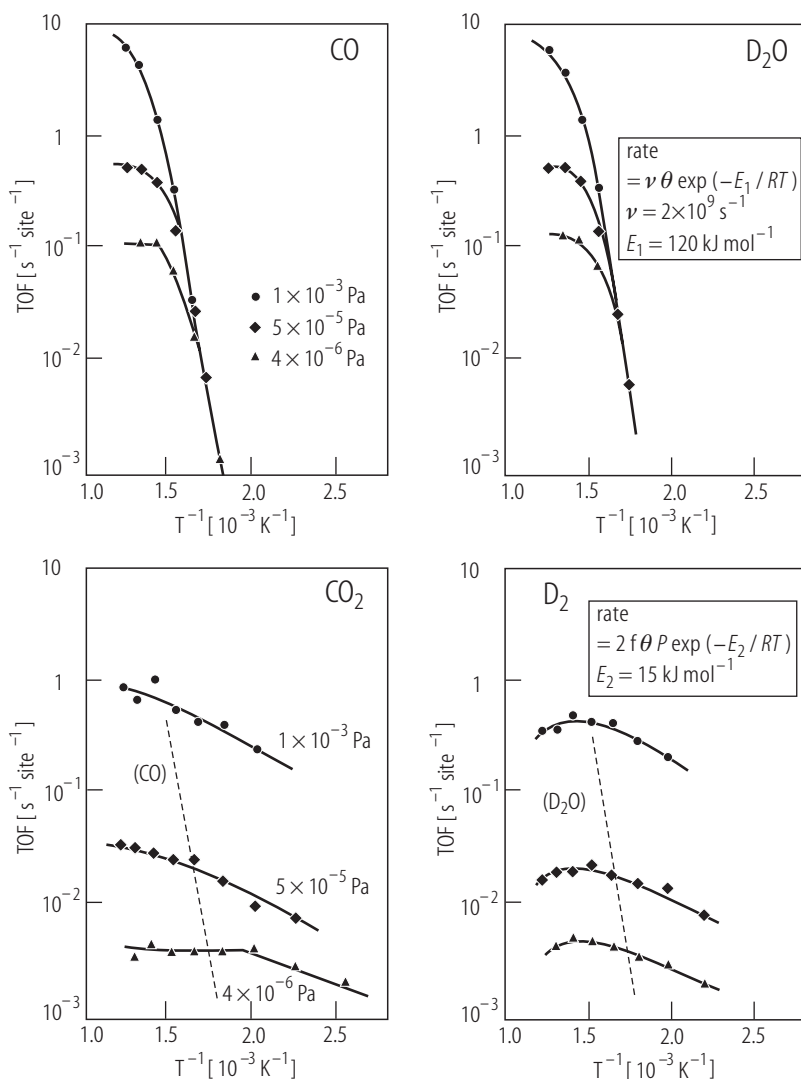


Fig. 21. Left: Arrhenius plot for the catalytic dehydration (according to equation 4) of DCOOD on TiO₂(110) at different pressures. Right: Arrhenius plot for the catalytic dehydrogenation (according to equation 3) of DCOOD on TiO₂(110) at different pressures; [01Iwa1].

3.9.14.4 CH₃COOH adsorption

Similar to the case of HCOOH, CH₃COOH decomposes on TiO₂(110), forming a (2×1) superstructure of acetate ions. Structural properties of the adsorbate were studied with ESDIAD by Guo et al [97Guo1]. In the angular distribution of desorbing H⁺ ions contributions due to hydrogen bonded to the substrate and to hydrogen resulting from C-H bond rupture could be identified. It was proposed that the acetate ions bond to the fivefold-coordinated surface Ti⁴⁺ ions in a bridging geometry (bidentate) with the molecular plane parallel to the surface normal. It was also proposed that the adsorbate induced forces lead to a pairing of surface Ti⁴⁺ cations along [001]. NEXAFS investigations performed by Gutiérrez-Sosa and coworkers [01Gut3] indicate that the acetate groups stand upright on the surface with an overall twist angle of 26±5° of the molecular plane with respect to [001].

Onishi et al [96Oni3] monitored the decomposition of acetate with STM as a function of time at different temperatures. From the time dependent decrease of the acetate induced features in the STM images the authors computed a unimolecular reaction rate of (4±1)×10⁻³ s⁻¹. The authors assumed decomposition via ketene formation according to



3.9.15 V_2O_3

V_2O_3 exhibits corundum structure (like Cr_2O_3 , see Fig. 2) with lattice parameters of $a = 5.105 \text{ \AA}$ and $b = 14.449 \text{ \AA}$ for the non-primitive hexagonal unit cell [65Wyc1]. The oxidation state of the vanadium ions is 3+ which means that formally two 3d electrons are left to the vanadium ions. Thin films grown on Au(111), Pd(111) or W(110) are (0001) oriented and show good crystalline order [03Dup1, 04Sch1]. Cutting a single crystal along (0001) followed by sputtering and annealing in UHV has also been used to prepare a (0001)-oriented surface [01Tol2]. $V_2O_3(10\bar{1}2)$ has been prepared by cleavage of a V_2O_3 single crystal in UHV [89Smi1]. A large part of the studies of V_2O_3 was motivated by its physical properties, especially the phase transition from antiferromagnetic insulating below 150 K to paramagnetic metallic at room temperature. This phase transforms into a paramagnetic insulating phase above 500 K [02DiM1, 70McW1, 69McW1]. Studies of the chemical activity of V_2O_3 surfaces are largely motivated by the use of vanadium oxide based catalysts for different reactions.

Only a few adsorption studies have been performed for V_2O_3 surfaces. Some of them are discussed in the following. An overview is given in Table 18.

Table 18. Overview of investigations of the interaction of gases with well ordered V_2O_3 surfaces

Adsorbates	Method	References
Substrate: $V_2O_3(0001)$		
H_2O	XPS, UPS, work function	01Tol2
Substrate: $V_2O_3(0001)/W(110)$		
O_2	HREELS, IRAS, ARUPS, XPS, NEXAFS	03Dup1
Substrate: $V_2O_3(10\bar{1}2)$		
SO_2	UPS, XPS	89Smi1
H_2O, O_2	UPS	83Kur1

3.9.15.1 O_2 adsorption

Dupuis et al [03Dup1] have shown that $V_2O_3(0001)$ is terminated by a layer of vanadyl groups under typical UHV conditions. These groups are strongly bonded and cannot be removed thermally, but by electron irradiation. The vanadyl layer may be re-established by dosing the surface with oxygen followed by annealing. At low temperature a molecular negatively charged oxygen species was found on the surface. $V_2O_3(10\bar{1}2)$ prepared by in-vacuo cleavage was found to interact strongly with oxygen [83Kur1]. It was reported that oxygen increases the surface oxidation state, possibly by forming O_2^- ions.

3.9.15.2 H_2O adsorption

Water adsorption on $V_2O_3(0001)$ was studied between 180 K and room temperature [01Tol2]. Molecular adsorption was observed at 180 K for doses less than 1000 L whereas at larger doses also OH formation became obvious. At room temperature only hydroxyl formation was observed. Newer results for H_2O on $V_2O_3(0001)$ layers on W(110) and Au(111) [06Abu1] show that the interaction with water depends on the termination of the $V_2O_3(0001)$ surface: a surface terminated by vanadyl groups does not dissociate water to form hydroxyl groups whereas a surface where the vanadyl groups have been removed prior to water adsorption dissociates water and hydroxyl groups are observed. For $V_2O_3(10\bar{1}2)$ it was found that water dissociates to form hydroxyl groups on nearly perfect as well as on ion-bombarded surfaces [83Kur1].

3.9.16 V₂O₅

The unit cell of the V₂O₅ lattice is orthorhombic with lattice constants of $a = 11.519 \text{ \AA}$, $b = 3.564 \text{ \AA}$ and $c = 4.373 \text{ \AA}$ [65Wyc1]. Three different types of oxygen atoms are found in the V₂O₅ lattice: singly coordinated vanadyl oxygen atoms [O(1)] twofold [O(2)] and threefold bridging [O(3)] atoms (see Fig. 22). The oxidation state of the vanadium atoms is 5+ which means that formally no 3d electrons are left to the vanadium ions. All adsorption studies discussed here have been performed for the (001) surface. V₂O₅ cleaves easily along this plane since the lattice consists of weakly interacting planes parallel to (001). Therefore, and because no simple recipe for the preparation of well-ordered V₂O₅ surfaces under UHV conditions is known, most studies have been performed for cleaved single crystal surfaces. Vanadium oxides are catalytically active for a number of oxidation reactions which was the motivation for most of the performed adsorption studies.

Only a few adsorption studies have been performed for V₂O₅ surfaces. Some of them are discussed in the following. An overview is given in Table 19.

Table 19. Overview of investigations of the interaction of gases with well ordered V₂O₅ surfaces

Adsorbates	Method	References
Substrate: V₂O₅(001)		
C ₃ H ₆	XPS, SEM	79Fie1
CO, SO ₂	UPS, XPS	94Zha1
CH ₃ OH	Theory: extended Hückel	99Sam1
CH ₃ OH oxidation	Theory: extended Hückel	97Sam1
C ₃ H ₈ , C ₂ H ₆	Theory: molecular mechanics	00Kam1, 00Kam2
H ₂ , H	ARUPS, Theory: DFT	99Her3
H ₂ , H	ARUPS, HREELS, XPS	02Tep1
H, H ⁺ , C ₃ H ₆ , C ₇ H ₈	Theory: DFT, ZINDO	99Wit1
H ₂ , C ₃ H ₆	Theory: DFT, Hartree-Fock, INDO-type	96Wit1
H ₂ O	Theory: ZINDO/1	99Ran1
H ₂ O	TDS: poly-crystalline V ₂ O ₅ , Theory: ZINDO/1	00Ran1
NH ₃	Theory: DFT	00Yin1
Substrate: V₂O₅(010)		
CH ₃ OH	Theory: extended Hückel	99Sam1

3.9.16.1 CO and SO₂ adsorption

Zhang and Henrich [94Zha1] used XPS and ARUPS to study the interaction of CO and SO₂ with V₂O₅(001) for UHV-cleaved V₂O₅(001) with a low density of defects and for reduced V₂O₅(001). Both adsorbates interact only weakly with the UHV-cleaved surface at room temperature. CO seems to induce some reduction of the surface after dosing large amounts ($>10^5 \text{ L}$). O₂ was found to partially re-oxidize the reduced surface and molecular as well as dissociative adsorption were observed for SO₂ on the reduced surface. The reduced surface appeared to be inert with respect to interaction with CO at room temperature.

3.9.16.2 H₂ and H adsorption

The interaction of molecular and atomic hydrogen with UHV-cleaved V₂O₅(001) was studied by Tepper et al using HREELS, ARUPS and XPS [02Tep1]. Both adsorbates led to a reduction of the surface: while a few Langmuirs of atomic hydrogen were sufficient to induce a considerable surface reduction, ten thousands of Langmuirs of molecular hydrogen were needed to induce significant effects. Formation of

hydroxyl groups was not observed in these experiments. From vibrational data of the reduced surface and from a comparison of an ARUPS spectrum of the reduced surface with a calculated density of states [99Her3] indications could be found that preferentially twofold bridging oxygen atoms are removed from the $V_2O_5(001)$ surface during the first stage of reduction by hydrogen atoms.

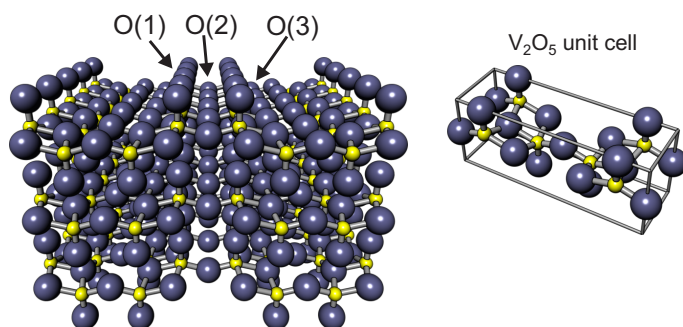


Fig. 22. Left: structure of the $V_2O_5(001)$ surface. Right: unit cell of V_2O_5 .

3.9.17 ZnO

Zinc oxide crystallizes in the hexagonal wurtzite structure. Since this structure does not exhibit an inversion center, a disk cut from a single crystal along the hexagonal basal plane has two structurally different surfaces. The hexagonal surfaces $ZnO(0001)\text{-O}$ (often also called $ZnO(000\bar{1})\text{-O}$) and $ZnO(0001)\text{-Zn}$ are the most often studied ones (see Fig. 23a and b). Some studies have also been performed for the $ZnO(10\bar{1}0)$ surface. The $ZnO(0001)\text{-Zn}$ and the $ZnO(000\bar{1})\text{-O}$ surface are terminated by zinc and oxygen layers, respectively, and exhibit different chemical properties. A special point to note is that these surfaces are polar which means that they are energetically unstable if not special surface conditions like adsorption, reconstruction, charge-rearrangement or similar stabilizes them. There are reports that under typical UHV conditions the non-reconstructed $ZnO(000\bar{1})\text{-O}$ surface may be terminated by a layer of hydrogen atoms which stabilizes it [02Kun1, 03Sta1, 03Kun2]. The hydrogen-free surface was found to exhibit a (1×3) reconstruction. For the zinc terminated surface STM revealed the presence of nanosized islands with triangular holes exhibiting oxygen terminated step edges [03Dul1, 02Dul1]. It was suggested that the oxygen terminated step edges provide the necessary stabilization for the $ZnO(0001)\text{-Zn}$ surface.

Usually disks cut off from a single crystal rod are used as samples. These are prepared by polishing followed by sputtering and annealing cycles as well as oxygen treatment after introduction into the UHV chamber. Since the oxygen and the zinc terminated surfaces behave chemically different they may be differentiated by chemical methods. Chemical etching with HCl may be employed [65Kle1].

ZnO is one of the most often studied oxides which is due to its importance in the field of catalysis. Cu/ZnO catalysts are widely used for the synthesis of methanol via CO hydrogenation and for the water-gas shift reaction.

In the following we give an overview of results for some adsorption systems. For the remaining systems the reader may consult the references listed in Table 20.

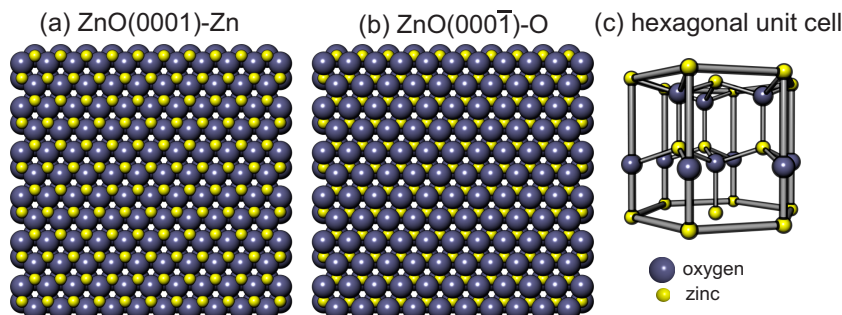


Fig. 23. Structure of ZnO. (a): zinc terminated $ZnO(0001)\text{-Zn}$. (b): oxygen terminated $ZnO(000\bar{1})\text{-O}$. (c): hexagonal unit cell of ZnO.

Table 20. Overview of investigations of the interaction of gases with well ordered ZnO surfaces

Adsorbates	Method	References
Substrate: ZnO(0001), ZnO(000$\bar{1}$)		
CH ₃ , H-C≡C, Cl, PF ₃	Theory: INDO/S	89Rod1
C ₂ H ₂ , methylacetylene, allene	UPS	90Voh1
methylacetylene, allene	HREELS	93Pet1
CH ₃ OH	XPS, NEXAFS, CFS, Theory: SCF-X α -SW	98Jon1
CH ₃ OH, OH	Waveguide CARS	94Wij1
HCOOH	HREELS	97Cro1, 98Tho1
HCOOH	NEXAFS	01Gut2
HCOOH, HCOOD	TDS, XPS	94Lud1
C ₅ H ₅ N	TDS, XPS, NEXAFS	00Hov1
C ₆ H ₆ , phenol	NEXAFS	01Gut1
Cl	LEED, AES, $\Delta\Phi$	76Hop1
Cl, HCOOH	ISS, XPS, work function, TDS	00Gra1
Crystal violet	Photocurrent measurements	84Cla1
CO	molecular beam	00Bec1
CO	HAS, molecular beam	00Bec2
CO, C ₄ H ₁₀	HAS, molecular beam, XPS	00Bec3
CO	Theory: Monte Carlo	01Bur1
CO	EELS, TCS	94Mol1, 95Mol1
CO, CO ₂	NEXAFS, IRAS	96Gut1
CO, NH ₃	Theory: DFT	94Cas1, 95Cas2
CO, HCOOH	TDS	98Yos1
CO, CO ₂ , HCOOH	STM, XPS	02Lin1
CO	ARUPS	81McC1
CO, CO ₂	UPS, XPS	88Au2
CO	Theory: INDO	87Rod1
CO	Theory: MNDO, AM1, PM3	96Mar3
CO	NEXAFS	99Lin2
CO	Theory: SCF-X α -SW	98Jon2
NH ₃ , C ₅ H ₅ N, H ₂ CO, HCOO, H ₃ CO	Theory: INDO/S	88Rod1
H ₂ O, H ₂ S, HCN	Theory: DFT	95Cas1
H ₂ O, H ₂ S, HCN, CH ₃ OH, CH ₃ SH	Theory: LCAO-LDF	96Cas1
H ₂ O, H ₂ S	Theory: DFT	97Cas2
H ₂ O, H ₂ S, HCN, CH ₃ OH, CH ₃ SH	Theory: DFT	97Cas2
H ₂ O, D ₂ O	TDS, ARUPS	83Zwi1
H ₂ O	Theory: INDO/S	88Rod2
H ₂ O	Theory: DFT	01Wan1
H ₂	Theory: <i>ab initio</i> cluster calculations	96Nyb1
H ₂	LEED, HAS	01Bec1
SO ₂	XPS, NEXAFS	99Rod2
SO ₂ , NO ₂	XPS, NEXAFS	01Rod1
Xe	LEED, TDS, ARUPS	84Gut1
Substrate: ZnO(10$\bar{1}$0)		
HCOOH	HREELS	97Cro1
HCOOH, CO ₂ , H+CO ₂	UPS, XPS	88Au1

Adsorbates	Method	References
C ₆ H ₆	TDS, LEED, UPS	81Pos1
C ₆ H ₆ , C ₅ H ₅ N	NEXAFS	93Wal1
CH ₃ OH	XPS, NEXAFS, CFS, Theory: SCF-X α -SW	98Jon1
benzotriazole, Indazole, benzimidazole, 1- methylbenzotriazole	NEXAFS	95Wal1
Cl	Theory: INDO/S	89Rod1
CO	ARUPS	80Say1
CO	TDS	94Ge1
CO, H, CO+H	ARUPS, UPS	80DAm1
CO, CO+H	HREELS, AES	97Guo3
CO, H ₂	Theory: DFT	97Cas2
CO, CO ₂	surface conductivity, surface potential, TDS, LEED	79Hot1
CO, CO ₂ , O ₂ , H ₂ , H	surface conductivity, charge transfer, Theory: SINDO	82Gop1
CO, H ₂	Theory: DFT	99Cas3, 98Cas1
CO	Theory: MNDO, AM1, PM3	96Mar3
CO ₂	UPS	80Gop2
H ₂	Theory: <i>ab initio</i> cluster calculations	96Nyb1
H ₂	Theory: periodic Hartree-Fock calculations	99Zap1
H ₂ O, D ₂ O	TDS, ARUPS	83Zwi1
O ₂ , CO, CO ₂	TDS, adsorption isotherms, UPS, XPS, ESR, conductivity	80Gop1, 85Gop1
NO	TDS, UPS	84Zwi1
O ₂	TDS, LEED, ESR, AES, $\Delta\Phi$, surface conductivity	77Gop1, 78Gop1, 76Gop1
NH ₃	Theory	99Cas2
OH+ Rh(CO) ₂ (π -C ₃ H ₅)	HREELS	90Yam1
S ₂	XPS, Theory: SCF cluster calculations	97Cha2
Xe	LEED, TDS, ARUPS	84Gut1
Substrate: ZnO(11$\bar{2}$0)		
H ₂	Theory: <i>ab initio</i> cluster calculations	96Nyb1

3.9.17.1 CO adsorption

CO adsorption on the basal surfaces of ZnO as well as on Zn(10 $\bar{1}$ 0) has been studied employing different methods. CO adsorbs weakly on ZnO(000 $\bar{1}$)-O and ZnO(0001)-Zn with the heat of adsorption being (7–2 θ_{CO}) kcal/mol (θ_{CO} = CO coverage) on both surfaces as revealed by molecular beam studies employing the King and Wells method [00Bec2, 00Bec1, 00Bec3]. From He reflectivity measurements it was concluded that CO prefers defect sites, but with increasing coverage also regular sites are occupied. Precursor mediated adsorption was found to occur for both surfaces as concluded from the coverage dependence of the sticking coefficient. A sticking coefficient which increases with coverage was observed for both surfaces, but the effect was found to be especially pronounced for ZnO(0001)-Zn. This observation was interpreted as an indication of adsorbate-assisted adsorption. For ZnO(0001)-Zn the angular dependence of ARUPS intensities has been employed to study the molecular orientation of molecules adsorbed at 80 K [81McC1]. It was found that the molecules are standing upright on the surface. With XPS C1s and O1s binding energies of 291.8 eV and of 537.9 eV, respectively, were determined for CO on ZnO(0001)-Zn for an adsorption temperature of 73 K [00Bec3].

Carbonate formation following CO dosage onto ZnO(000 $\bar{1}$)-O was observed at 120 K [02Lin1, 88Au2] and 130 K [99Lin2, 96Gut1]. The surface coverage is small at 130 K. Using XPS the maximum CO coverage was determined to be 0.04 ML [99Lin2]. For carbonate resulting from CO dosage the coverage was studied as a function of substrate annealing temperature and oxygen treatment, leading to the result that carbonate formation from adsorbed CO mainly occurs on defect sites [02Lin1]. The coverage varied from 0.2 ML for a surface annealed at 1070 K to nearly zero for 1370 K annealing temperature. With angular dependent NEXAFS it was shown that the CO molecular axis is tilted by $17\pm 10^\circ$ with respect to the surface normal for CO adsorbed at 130 K [99Lin2]. With NEXAFS the C1s $\rightarrow\pi^*$ excitation energy for CO was found to be 287.7 ± 0.2 eV and for carbonate an energy of 290.4 ± 0.2 eV has been reported [99Lin2]. Reported corelevel binding energies as obtained with XPS are 288.6 eV for the C1s level of adsorbed CO and 290 eV and 532.5 eV for the C1s and O1s level of carbonate, respectively [88Au2].

Less studies have been performed for CO adsorption onto ZnO(10 $\bar{1}$ 0). For low temperature adsorption ($T \sim 77$ K) at an ambient CO pressure of 1×10^{-6} Torr the formation of a dense layer with near-monolayer coverage was reported [80Say1]. The heat of adsorption was reported to be ~ 12 kcal/mol [80Say1, 80DAm1]. The adsorption geometry of the CO molecules was determined via the angular dependence of the CO 4 σ intensity in angular resolved photoelectron spectra which gave a tilting angle of about 30° with respect to the surface normal [80Say1, 80DAm1].

The adsorption of CO on ZnO(10 $\bar{1}$ 0) has also been studied at room temperature. After exposing the surface to 100 Pa of CO for 15 min a CO desorption peak was detected around 360 K [94Ge1]. In contrast to the results of Ge and Möller [94Ge1] who only found small amounts of desorbing CO₂, Hotan, Göpel and Gaul [79Hot1] detected exclusively CO₂ with TDS. However, in the latter case the applied CO pressure was much smaller (1.3×10^{-5} Pa). Coverage and chemical identity of the adsorbed species were not studied.

3.9.17.2 CO₂ adsorption

The adsorption of carbon dioxide on ZnO(000 $\bar{1}$)-O was studied with XPS and NEXAFS [02Lin1, 88Au2, 96Gut1]. CO₂ was found to be transformed into carbonate at the oxygen vacancies at step edges [02Lin1]. Above 150 K all physisorbed CO₂ is desorbed and at temperatures above 400 K the carbonate signal vanishes [88Au2]. The carbonate molecules stand upright on the surface with an angle of about 30° between the surface normal and the molecular plane as concluded from NEXAFS data obtained after exposing ZnO(000 $\bar{1}$)-O to CO₂ at 130 K [96Gut1]. The C1s $\rightarrow\pi^*$ resonance was found at 290 ± 0.2 eV. With XPS the carbonate C1s binding energy was determined to be 290.3 eV [88Au2]. The C1s binding energy of physisorbed CO₂ was found to be 291.8 eV.

CO₂ adsorption on ZnO(10 $\bar{1}$ 0) was studied with XPS and UPS [88Au1, 80Gop2]. Formation of a surface carbonate occurs already at 100 K. Physisorbed CO₂ was observed up to about 150 K and the carbonate was found to disappear until 400 K. As determined from XPS intensities the carbonate coverage was $\theta = 0.1$ ML. C1s binding energies of 290.4 and 291.8 eV were measured for the carbonate and the physisorbed CO₂, respectively.

3.9.17.3 CH₃OH adsorption

Methanol adsorption on ZnO(0001)-Zn and ZnO(10 $\bar{1}$ 0) was studied using NEXAFS and XPS. On both surfaces a methoxide species characterized by a C1s binding energy of 290.2 eV was observed [98Jon1]. Formate forms on ZnO(0001)-Zn after annealing above 220 K. This species was found to be stable even at 523 K which is the methanol synthesis temperature. No formate formation was observed on ZnO(10 $\bar{1}$ 0). From the energy of the σ shape resonance (295.5 eV) as determined with NEXAFS a C-O bond length of the methoxy groups of 1.39 Å was estimated [98Jon1].

3.9.17.4 HCOOH adsorption

HCOOH adsorption was studied on ZnO(0001)-Zn, ZnO(000 $\bar{1}$)-O and ZnO(10 $\bar{1}$ 0). On ZnO(000 $\bar{1}$)-O HCOOH was found to adsorb dissociatively ($\text{HCOOH} \rightarrow [\text{HCOO}]^- + \text{H}^+$) on surface defects [02Lin1, 01Gut2]. With XPS the saturation coverage was studied as a function of the annealing temperature of the substrate and oxygen treatment [02Lin1]. For an annealing temperature of 1070 K a surface coverage of about 0.3 was found which dropped to 0.1 for an annealing temperature of 1370 K. This observation was explained as to result from the decreasing number of surface defects with increasing substrate annealing temperature. From STM results the authors concluded that adsorption preferably occurs on *cus* zinc cations at step edges. The C1s corelevel of the surface formate was detected at 289.6 ± 0.3 eV.

NEXAFS was used to study the geometry of the adsorbed formate ions [01Gut2] on ZnO(000 $\bar{1}$)-O. From the dependence of the intensity of the C1s 2b₂ resonance at 288.3 eV on the light incidence angle a tilting angle of $55 \pm 5^\circ$ with respect to the surface normal was estimated. Other (weaker) C1s resonances were identified at 291.8 eV (7a₁), 297.8 eV (8a₁) and 301.4 eV (5b₁).

Ludviksson et al investigated the adsorption of formic acid on ZnO(000 $\bar{1}$)-O with thermal desorption spectroscopy [94Lud1]. Desorption of molecularly adsorbed HCOOH was found to occur below 200 K with a small tail extending to higher temperatures. CO and CO₂ formation due to the decomposition of adsorbed formate ($\text{HCOO} \rightarrow \text{CO}_2 + \text{H}$ and $\text{HCOO} \rightarrow \text{CO} + \text{OH}$) was found at 550 K. A large part of the hydrogen resulting from the formic acid decomposition was assumed to dissolve into the bulk.

HREELS data for HCOOH adsorption onto ZnO(000 $\bar{1}$)-O at 300 K have been obtained by Crook et al [97Cro1] and Thornton et al [98Tho1]. Vibrational modes of formate were observed at ~ 750 cm⁻¹ ($\delta(\text{OCO})$), 1080 cm⁻¹ ($\pi(\text{CH})$), 1371 cm⁻¹ ($\nu_s(\text{OCO})$), 1605 cm⁻¹ ($\nu_a(\text{OCO})$) and 2928 cm⁻¹ ($\nu(\text{CH})$). A hydroxyl vibration was not observed which was supposed to result from hydrogen dissolution into the bulk.

For the zinc terminated ZnO(0001)-Zn surface HCOOH adsorption was studied with TDS by Yoshihara et al [98Yos1] and Grant et al [00Gra1]. HCOOH desorption occurs at 200 K (multilayer) and 370 K (molecularly chemisorbed formic acid) [98Yos1]. Between ~ 350 K and 450 K also H₂ adsorption was observed which was attributed to desorption of hydrogen originating from the decomposition of formic acid on the surface ($\text{HCOOH} \rightarrow \text{HCOO} + \text{H}$). At about 575 K desorption peaks of CO, H₂O, CO₂ and H₂ showed up which was attributed to the dissociation of formate via the reactions $\text{HCOO} \rightarrow \text{CO}_2 + \text{H}$ and $\text{HCOO} \rightarrow \text{CO} + \text{OH}$.

The HCOOH adsorption on ZnO(10 $\bar{1}$ 0) at 300 K was studied with HREELS by Crook et al [97Cro1]. Again formate formation was observed. Vibrational losses of the adsorbed formate were found at 1040 cm⁻¹ ($\pi(\text{CH})$), 1363 cm⁻¹ ($\nu_s(\text{OCO})$), 1573 cm⁻¹ ($\nu_a(\text{OCO})$) and 2895 cm⁻¹ ($\nu(\text{CH})$). The fate of hydrogen atoms originating from the formic acid decomposition was not clear. An increase of the OH-induced IR absorption-intensity was observed after dosage of HCOOH but no comparably strong OD vibration was found in the spectra after exposure to DCOOD. The authors argued that this observation may be due to isotopic exchange effects and to the fact that the OD vibration would be partially hidden by the $\nu_s(\text{OCO})$ overtone. XPS spectra for HCOOH adsorption onto ZnO(10 $\bar{1}$ 0) were published by Au et al [88Au1]. Upon adsorption a species with a C1s binding energy of 289.9 eV was observed. The position of the C1s peak did not depend on the dose nor on the annealing temperature and was visible even at 590 K, but with significantly reduced intensity.

3.9.18 Tables of selected adsorbate properties

Selected results of the studies discussed in the previous sections are summarized in the following tables. Table 21 gives an overview of desorption temperatures and adsorbate-substrate binding energies, Table 22 lists sticking coefficients and coverages, Table 23 collects vibrational data and Table 24 lists corelevel binding energies and NEXAFS excitation energies.

Table 21. Desorption temperatures and adsorbate-substrate binding energies.

Substrate	Desorption temperature [K]	Activation energy [eV]	Notes (method, etc)	References
Adsorbate: CO				
Al ₂ O ₃ /NiAl(110)	55, 67	0.14, 0.17	TDS	93Jae1, 93Jae2
θ-Al ₂ O ₃ /NiAl(100)	120, 318, 395		TDS	98Hsi1
α-Al ₂ O ₃ /NiAl(100)	120, 375		TDS	98Hsi1
α-Cr ₂ O ₃ (0001)/Cr(110)	105, 175	0.47 (175 K)	TDS, Cr term. surf.	01Pyk1
Cu ₂ O(100)	120- 320 (complicated pattern)	≤0.36-0.72	TDS	91Cox1
MgO(100)	57	0.14	TDS	99Wic1, 99Wic2
MgO(100)/Mo(100)	~60, ~80 and ~100 (defect ads.)	0.17 (60 K)	TDS	01Doh1
NiO(100)	115-137	0.30 (low coverage), 0.1 (high coverage)	TDS	99Wic1, 99Wic2
NiO(111)/Mo(111)	broad structures between 100 and 250		TDS	96Xu1
reduced RuO ₂ (110)/Ru(0001)	415 (CO on asym. Ru _{bridge}), 470 (CO on sym. Ru _{bridge})		TDS, see Fig. 14	03Kim1
reduced RuO ₂ (110)/Ru(0001)	~300 (CO on Ru _{cus}), ~350 (asym. bridging CO on Ru _{bridge}), ~560 (sym. bridging CO on Ru _{bridge})		TDS, see Fig. 14	02Sei1
RuO ₂ (110)/Ru(0001)	270, 320 (CO on Ru _{cus}), 470 (CO on Ru _{bridge})		TDS, see Fig. 14	03Kim1
rutile TiO ₂ (110)	135-170	0.43 (lateral interactions: ~0.1 at θ _{CO} = 0.68)	TDS	95Lin1
rutile TiO ₂ (110)		0.31-0.07×θ _{CO} (θ _{CO} =CO coverage)	molecular beam	03Kun1
ZnO(0001)-O-, ZnO(0001)-Zn		0.3-0.087×θ _{CO} (θ _{CO} =CO coverage)	molecular beam	00Bec2, 00Bec1, 00Bec
Adsorbate: CO₂				
α-Cr ₂ O ₃ (0001)/Cr(110)	120 (CO ₂), 180 (CO ₂), 330 (CO ₂ ^{δ-})		TDS, Cr term. surf.	99Sei1
NiO(111)/Ni(111)	395, 645		TDS	93Gor1
Adsorbate: D₂O				
CeO ₂ (001)/SrTiO ₃ (001)	152 (mult. D ₂ O), 200 (first layer D ₂ O), 275 (OD)		TDS	99Her1
Adsorbate: DCOOD				
rutile TiO ₂ (110)	350 (DCOOD, D ₂ O), 400 (D ₂), 570 (CO, CO ₂ , D ₂ O, D ₂ , DCOOD)		TDS, DCOO+OD	01Iwa1
Adsorbate: H₂O				
α-Al ₂ O ₃ (0001)	300-500	0.99- 1.78	TDS, OH groups	98Ela1

Substrate	Desorption temperature [K]	Activation energy [eV]	Notes (method, etc)	References
CeO ₂ (111)/Ru(0001)	<300		TDS, fully oxidized surface	00Kun1
CeO ₂ (111)/Ru(0001)	180, 250, 600 (580: H ₂)		TDS, reduced surface	00Kun1
α -Cr ₂ O ₃ (0001)/Al ₂ O ₃ (0001)	185 (phys. water), 210 (phys. water), 295 (chem. water), 345 (hydroxyl groups)	0.92 (hydroxyl groups)	TDS	00Hen1
Cu ₂ O(100)	300 and 465: hydroxyl recombination		TDS	91Cox2
FeO(111)/Pt(111)	165-170	0.54	TDS	02Wei1
Fe ₃ O ₄ (111)/Pt(111)	185-215, 265-280 (OH recombination)	0.51(185- 215 K), 0.52±0.1(265- 285K)	TDS	02Wei1
Fe ₂ O ₃ (0001)/Pt(111)	240-260	0.65	TDS	02Wei1
MgO(100)		0.88±0.02 (isosteric heat of adsorption), 0.36±0.1 (lateral interaction energy)	LEED	97Fer3, 96Fer2
NiO(100)/Ag(100)	140 (multilayer), 200 (regular sites), 210-270 (nonreg. sites)	0.54 (200 K), 0.67 (210- 270 K)	TDS	98Rei1, 00Rei1, 01Sch2
SnO ₂ (110)	200, 300, (435: OH disprop.)		TDS	95Ger1
rutile TiO ₂ (110)	155 (multilayer), 174 (bilayer), 270 (monolayer)		TDS	96Hen2
Adsorbate: HCOOH				
ZnO(0001)-O	200 (molec. HCOOH), 550 (CO, CO ₂)		TDS	94Lud1
ZnO(0001)-Zn	200 (multilayer HCOOH), 370 (mol. ads. chem. HCOOH), 350- 450 (H ₂), 575 (CO, H ₂ O, CO ₂ , H ₂)		TDS	98Yos1, 00Gra1
NiO(111)/Ni(111)	195 and 210 (molec HCOOH), 340, 390 and 520 (H ₂ , CO ₂), 415 and 520 (CO)		TDS	96Ban2
Adsorbate: NO				
α -Cr ₂ O ₃ (0001)/Cr(110)	105, 340	0.35, 1.0	TDS, Cr term. surf.	91Xu2, 99Will
NiO(100) (NiO(100) /Ni(100) similar)	216-220	0.57 (low coverage), 0.12 (high coverage)	TDS	99Wic1, 99Wic2
Adsorbate: O₂				
α -Cr ₂ O ₃ (0001)/Cr(110)	290- 330		TDS, Cr term. surf.	96Dil1
SnO ₂ (110)	200, 250		TDS	92She1

Substrate	Desorption temperature [K]	Activation energy [eV]	Notes (method, etc)	References
Adsorbate: ethylbenzene				
FeO(111)/Pt(111)	200-210	0.57	TDS	02Wei1
Fe ₃ O ₄ (111)/Pt(111)	190-210, 250-400	0.49 (190-210 K), 0.89 (250-400 K)	TDS	02Wei1
Fe ₂ O ₃ (0001)/Pt(111)	200-210, 250-275, 300- 450	0.52 (200-210 K), 0.66 (250-275 K)	TDS	02Wei1
Adsorbate: styrene				
FeO(111)/Pt(111)	~210	0.52	TDS	02Wei1
Fe ₃ O ₄ (111)/Pt(111)	~210, ~300, ~500	0.52 (210 K), 0.73 (300 K), 1.22 (500 K)	TDS	02Wei1
Fe ₂ O ₃ (0001)/Pt(111)	~210, 270-295, ~400	0.52 (210 K), 0.76 (270-295 K), 0.98 (400 K)	TDS	02Wei1

Table 22. Sticking coefficients and coverages of adsorbates on different ordered oxide substrates.

Substrate	Sticking coefficient	Saturation coverage	Notes (methods etc.)	Ref.
Adsorbate: CO				
rutile TiO ₂ (110)	0.84±0.05 (E_{kin} = 0.05 eV), 0.1±0.05 (E_{kin} = 0.57 eV)		molecular beam	03Kun1
Adsorbate: D₂O				
CeO ₂ (001)/SrTiO ₃ (001)		0.9 monolayers (OH groups)	XPS, OH formation	99Her1
Adsorbate: H₂O				
α-Al ₂ O ₃ (0001)	~0.1 (at 300 K)	5×10 ¹⁴ OH groups/cm ²	LITD, OH formation	98Ela1
CaO(100)	~0.9 (at RT, $\theta_{OH} \leq 0.8$), ~3×10 ⁻⁵ at higher coverage		XPS, OH formation	98Liu3
rutile TiO ₂ (110)		5.2×10 ¹⁴ H ₂ O molecules/cm ² (monolayer)	TDS	98Bri2
rutile TiO ₂ (110)		3×10 ¹³ OH groups/ cm ²	HREELS, TDS	96Hen2
α-Cr ₂ O ₃ (0001)/ α-Al ₂ O ₃ (0001)		3-7×10 ¹⁴ OH groups/cm ² , 1.2×10 ¹⁵ OH groups + chem. H ₂ O molecules/cm ²	TDS	00Hen1
NiO(111)/Ni(111)		0. 85±0.1 monolayers (OH groups)	XPS	98Kit1
Adsorbate: HCOOH				
ZnO(000 $\bar{1}$)-O	0.3 monolayers (subst. ann. at 1070 K), 0.1 monolayers (subst. ann. at 1370 K)	XPS, HCOO+ OH	02Lin1	

Table 23. Vibrational energies of adsorbates.

Substrate	Vibrational Energy [cm ⁻¹]	Notes (method, etc)	References
Adsorbate: CO			
a-Al ₂ O ₃ /NiAl(100)	2074 (dose 1 L), 2065 and 2117 (dose 1.5 L)	IRAS	98Hsi1
θ-Al ₂ O ₃ /NiAl(100)	2047 and 2027 (dose 1 L), 2047 and 2033 (dose 3 L)	IRAS	98Hsi1
α-Al ₂ O ₃ /NiAl(100)	1994 (dose 0.5 L), 2003 and 2030 (dose 2 L)	IRAS	98Hsi1
α-Cr ₂ O ₃ (0001)/Cr(110)	2132-2136, 2170-2178	IRAS	01Pyk1
CoO(100)/Co(11 $\bar{2}$ 0)←	~2142	HREELS	96Sch1
CoO(111)/Co(0001)←	~2168	HREELS	96Sch1
MgO(100)	2152.2, 2137.2, 2132.2 [c(4×2) phase], 2150.5 [(1×1)phase]	IRAS	95Hei1
NiO(100)/Mo(100)	2156	IRAS	94Ves1
NiO(111)/Ni(111)	2079 (not fully oxidized Ni sites), 2146 (fully ox. Ni sites)	IRAS, SFG	98Mat1, 97Ban1, 99Ban1
reduced RuO ₂ (110)/Ru(0001)	53.5 (CO-Ru), 234.5 (symmetric CO-Ru _{bridge}), 248.5 (asym. CO-Ru _{bridge})	HREELS, see Fig. 14	01Wan2, 02Sei1, 03Kim1
RuO ₂ (110)/Ru(0001)	39 (CO-Ru), 262 (CO on Ru _{cus})	HREELS, see Fig. 14	01Wan2, 02Sei1, 03Kim1
Adsorbate: CO₂			
α-Cr ₂ O ₃ (0001)/Cr(110)	2346- 2353 (<i>T_{des}</i> =180 K), 2375 (<i>T_{des}</i> =120 K), 1277-1289 (CO ₂ ^{δ-})	IRAS, Cr term. surf.	99Sei1
MgO(100)	2334, 2308, 2306	IRAS [(2√2×2√2)R45° phase]	96Hei1, 93Hei1
NiO(111)/Ni(111)	1263 (dehydrox. surf.), (910: carbonate), 1267 (OD covered surf.)	IRAS	99Mat1
Adsorbate: D₂O			
α-Cr ₂ O ₃ (0001)/α-Al ₂ O ₃ (0001)	2645 (terminal OD), 2120 (bridging OD)	HREELS	00Hen1
Adsorbate: H₂O			
α-Al ₂ O ₃ (0001)	3720 (OH groups)	HREELS	97Cou1
α-Cr ₂ O ₃ (0001)/α-Al ₂ O ₃ (0001)	3600 (terminal OH), 2885 (bridging OH)	HREELS	00Hen1
CoO(111)/Co(0001)	~3670 (hydroxyl groups)	HREELS	95Has1
MgO(100)	3050-3500 (broad band)	IRAS [c(4×2) phase]	95Hei2
NiO(111)/Ni(100)	3710 (hydroxyl groups)	HREELS	78And1, 95Cap1
rutile TiO ₂ (110)	3690 (hydroxyl groups), 1625 and 3420- 3505 (molec. water)	HREELS	96Hen2
Adsorbate: HCOOH			
NiO(111)/Ni(111), NiO(100)/Mo(100)	see Table 13	IRAS, HREELS	96Ban1, 92Tru1

Substrate	Vibrational Energy [cm^{-1}]	Notes (method, etc)	References
rutile $\text{TiO}_2(110)$	(1566 [$\nu_{\text{asym}}(\text{OCO})$], 1363 [$\nu_{\text{sym}}(\text{OCO})$], molec. plane par. [001]), (1535 [$\nu_{\text{asym}}(\text{OCO})$], 1393 [$\nu_{\text{sym}}(\text{OCO})$], molec. plane par. [$1\bar{1}0$])	IRAS, adsorbed formate	99Hay1
$\text{ZnO}(000\bar{1})\text{-O}$	~ 750 [$\delta(\text{OCO})$], 1080 [$\pi(\text{CH})$], 1371 [$\nu(\text{OCO})$], 1605 [$\nu_{\text{a}}(\text{OCO})$], 2928 [$\nu(\text{CH})$]	HREELS, adsorbed formate	97Cro1, 98Tho1
$\text{ZnO}(10\bar{1}0)$	1040 [$\pi(\text{CH})$], 1363 [$\nu_{\text{s}}(\text{OCO})$], 1573 [$\nu_{\text{a}}(\text{OCO})$], 2895 [$\nu(\text{CH})$]	HREELS, adsorbed formate	97Cro1
Adsorbate: NO			
$\alpha\text{-Cr}_2\text{O}_3(0001)/\text{Cr}(110)$	1759-1794 ($T_{\text{des}}=340$ K), 1847- 1857 (NO dimers)	IRAS, Cr term. surf.	99Wil1
$\text{CoO}(100)/\text{Co}(11\bar{2}0)\leftarrow$	~ 1813	HREELS	96Sch1
$\text{CoO}(111)/\text{Co}(0001)\leftarrow$	~ 1789 , (~ 1650 , interacting with OH groups; ~ 1621 , interacting with OD groups)	HREELS	96Sch1, 95Has1
$\text{NiO}(111)/\text{Ni}(111)$	1772 (hydrox. surf.), 1805 (dehydrox. surf.)	HREELS	96Sch1
$\text{NiO}(111)/\text{Ni}(111)$	1800 (dehydrox. surf) 1805 (dehydrox. surf)	SFG IRAS	97Ban1
$\text{NiO}(100)/\text{Ni}(100)$	1797	HREELS	91Kuh1, 92Bau1, 93Kuh1, 96Sch1
Adsorbate: O₂			
$\alpha\text{-Cr}_2\text{O}_3(0001)/\text{Cr}(110)$	1005-1012 (chromyl), 990 (O_2^-)	IRAS, Cr term. surf.	96Dil1

Table 24. XPS binding energies and NEXAFS excitation energies.

Substrate	Energy [eV]	Notes(method, etc)	Ref.
Adsorbate: CO			
$\text{CeO}_2(111)/\text{Ru}(0001)$	C1s: 290.5	XPS, possibly carbonate or carboxylate	99Mul1
$\text{NiO}(111)/\text{Ni}(100)$	C1s $\rightarrow 2\pi$: ~ 287.8	NEXAFS	96Sch1
$\text{NiO}(100)/\text{Ni}(100)$	C1s $\rightarrow 2\pi$: 287.4	NEXAFS	95Cap2
$\text{ZnO}(0001)\text{-Zn}$	C1s: 291.8, O1s: 537.9	XPS	00Bec3
$\text{ZnO}(000\bar{1})\text{-O}$	C1s $\rightarrow 2\pi$: 287.7 ± 0.2	NEXAFS	99Lin2
$\text{ZnO}(000\bar{1})\text{-O}$	C1s: 288.6	XPS	88Au2
$\alpha\text{-Cr}_2\text{O}_3(0001)\text{Cr}(110)$	C1s: 290.8 (center, broad peak)	XPS	92Kuh2
$\alpha\text{-Cr}_2\text{O}_3(0001)\text{Cr}(110)$	C1s $\rightarrow 2\pi$: 286.0, C1s $\rightarrow 6\sigma$: 305	NEXAFS	92Kuh2
Adsorbate: CO₂			
$\text{MgO}(100)$	C1s $\rightarrow \pi$: 290.2	NEXAFS	99Car1
Adsorbate: carbonate			
$\text{ZnO}(000\bar{1})\text{-O}$	C1s $\rightarrow 2\pi$: 290.4 ± 0.2	NEXAFS	99Lin2
$\text{ZnO}(000\bar{1})\text{-O}$	C1s: 290, O1s: 532.5	XPS	88Au2

Substrate	Energy [eV]	Notes(method, etc)	Ref.
Adsorbate: D₂O			
CeO ₂ (001)/SrTiO ₃ (001)	O1s: 531.6 (OH)	XPS	99Her1
Adsorbate: H₂O			
α -Al ₂ O ₃ (0001)	O1s: 533.1±0.2 (hydroxyl groups)	XPS	97Cou1
CeO ₂ (111)/Ru(0001)	O1s: 531.8	XPS, fully hydroxylated surface	00Kun1
CeO ₂ (111)/Ru(0001)	O1s: 532.4 (chem. H ₂ O), 533.1 (OH)	XPS, reduced surface	00Kun1
NiO(111)/Ni(111)	O1s: 531.4±0.1 (hydroxyl groups)	XPS	98Kit1
Adsorbate: CH₃OH			
ZnO(0001)-Zn, ZnO(10 $\bar{1}$ 0)	C1s: 290.2, C1s → σ : 295.5	XPS, NEXAFS, methoxide	98Jon1
Cu ₂ O(111)	C1s: 289.5 (methoxide), C1s: 290.7 (multilayer), C1s → σ : 294.8±0.2	XPS, NEXAFS, methoxide	98Jon1
Adsorbate: HCOOH			
rutile TiO ₂ (110)	C1s resonances: 288.7 (2b ₂), 292 (7a ₁), ~300 (8a ₁ + 5b ₁)	NEXAFS, HCOO+ OH	01Gut3
ZnO(000 $\bar{1}$)-O	C1s: 289.6±0.3	XPS, HCOO+OH	02Lin1
ZnO(000 $\bar{1}$)-O	C1s resonances: 288.3 (2b ₂), 291.8 (7a ₁), 297.8 (8a ₁), 301.4 (5b ₁)	NEXAFS, HCOO+OH	01Gut2
ZnO(10 $\bar{1}$ 0)	C1s: 289.9	XPS, HCOO+OH	88Au1
Adsorbate: CH₃COOH			
rutile TiO ₂ (110)	288.8, ~300	NEXAFS, CH ₃ COO+OH	01Gut3
rutile TiO ₂ (110)	289.4±0.2, 285.5±0.2	XPS, CH ₃ COO+OH	01Gut3
Adsorbate: C₂H₅COOH			
rutile TiO ₂ (110)	289, ~300	NEXAFS, CH ₃ CH ₂ COO+OH	01Gut3
rutile TiO ₂ (110)	289.4±0.2, 285.5±0.2	XPS, CH ₃ CH ₂ COO+OH	01Gut3
Adsorbate: NO			
NiO(100)	N1s: 402.8, 407.2	XPS	91Kuh1
NiO(100)/Ni(100)	N1s: 403.1, 407.5	XPS	91Kuh1
NiO(111)/Ni(111)	N1s → 2 π : ~406.5, N1s → σ : ~421	NEXAFS	96Sch1

3.9.19 References for 3.9

- 62Red1 Redhead, P.A.: Vacuum **12** (1962) 203.
 65Kle1 Klein, A.: Z. Phys. **188** (1965) 352.
 65Wyc1 Wyckoff, R.W.G.: Crystal structures, 2nd edition, New York: Wiley Interscience, 1965.
 67Kat1 Katsura, T., Iwasaki, B., Kimura, S., Akimoto, S.-I.: J. Chem. Phys. **47** (1967) 4559.
 69McW1 McWhan, D.B., Rice, T.M., Remeika, J.P.: Phys. Rev. Lett. **23** (1969) 1384.
 70McW1 McWhan, D.B., Remeika, J.P.: Phys. Rev. B **2** (1970) 3734.
 73Liu1 Liu, L.-G., Bassett, W.A.: J. Appl. Phys. **44** (1973) 1475.
 76Gop1 Göpel, W.: Ber. Bunsenges. Phys. Chem. **80** (1976) 481.
 76Hop1 Hopkins, B.J., Taylor, P.A.: J. Phys. C **9** (1976) 571.
 77Dem1 Demuth, J.E.: Surf. Sci. **69** (1977) 365.
 77Gop1 Göpel, W.: Surf. Sci. **62** (1977) 165.
 77Hen1 Henrich, V.E., Dresselhaus, G., Zeiger, H.J.: Solid State Commun. **24** (1977) 623.
 78And1 Andersson, S., Davenport, J.W.: Solid State Commun. **28** (1978) 667.
 78Gop1 Göpel, W.: J. Vac. Sci. Technol. **15** (1978) 1298.
 78Ste1 Steinbrunn, A., Dumas, P., Colson, J.C.: Surf. Sci. **74** (1978) 201 in french..
 79Fie1 Fiermans, L., Vandenbroucke, L., Berghe, R.V., Vennik, J.: J. Microsc. Spectrosc. Electron. **4** (1979) 543 in french..
 79Hot1 Hotan, W., Göpel, W., Haul, R.: Surf. Sci. **83** (1979) 162.
 79Tas1 Tasker, P.W.: J. Phys. C **12** (1979) 4977.
 80DAm1 D'Amico, K.L., McClellan, M.R., Sayers, M.J., Gay, R.R., McFeely, F.R., Solomon, E.I.: J. Vac. Sci. Technol. **17** (1980) 1080.
 80Gop1 Göpel, W., in: Advances in solid state physics, Wiesbaden, Germany: Friedrich Vieweg & Sohn, 1980, p. 177 - 227.
 80Gop2 Göpel, W., Bauer, R.S., Hansson, G.: Surf. Sci. **99** (1980) 138.
 80Say1 Sayers, M.J., McClellan, M.R., Gay, R.R., Solomon, E.I., McFeely, F.R.: Chem. Phys. Lett. **75** (1980) 575.
 80Wep1 Wepfer, G.G., Surratt, G.T., Weidman, R.S., Kunz, A.B.: Phys. Rev. B **21** (1980) 2596.
 81McC1 McClellan, M.R., Trenary, M., Shinn, N.D., Sayers, M.J., D'Amico, K.L., Solomon, E.L., McFeely, F.R.: J. Chem. Phys. **74** (1981) 4726.
 81Pos1 Pöss, D., Ranke, W., Jacobi, K.: Surf. Sci. **105** (1981) 77.
 82Fir1 Firment, L.E.: Surf. Sci. **116** (1982) 205.
 82Gop1 Göpel, W., Rucker, G.: J. Vac. Sci. Technol. **21** (1982) 389.
 83Kur1 Kurtz, R.L., Henrich, V.E.: Phys. Rev. B **28** (1983) 6699.
 83Sti1 Stinespring, C.D., Cook, J.M.: J. Electron Spectrosc. Relat. Phenom. **32** (1983) 113.
 83Zwi1 Zwicker, G., Jacobi, K.: Surf. Sci. **131** (1983) 179.
 84Cla1 Clark, F.T., Drickamer, H.G.: J. Chem. Phys. **81** (1984) 1024.
 84Gut1 Gutmann, A., Zwicker, G., Schmeisser, D., Jacobi, K.: Surf. Sci. **137** (1984) 211.
 84Lee1 Lee, Y.C., Montano, P.A., Cook, J.M.: Surf. Sci. **143** (1984) 423.
 84Zwi1 Zwicker, G., Ranke, W., Jacobi, K., Pöss, D.: Ber. Bunsenges. Phys. Chem. **88** (1984) 364.
 85Fur1 Furstenau, R.P., Langell, H.A.: Surf. Sci. **159** (1985) 108.
 85Fur2 Furstenau, R.P., McDougall, G., Langell, M.A.: Surf. Sci. **150** (1985) 55.
 85Gop1 Göpel, W.: Prog. Surf. Sci. **20** (1985) 9.
 85McK1 McKay, J.M., Henrich, V.E.: Phys. Rev. B **32** (1985) 6764.
 86Fool Foord, J.S., Lambert, R.M.: Surf. Sci. **169** (1986) 327.
 86Hen1 Hendewerk, M., Salmeron, M., Somorjai, G.A.: Surf. Sci. **172** (1986) 544.
 86Lan1 Langell, M.A., Furstenau, R.P.: Appl. Surf. Sci. **26** (1986) 445.
 87Eri1 Erickson, J.W., Semancik, S.: Surf. Sci. **187** (1987) L658.
 87Kur1 Kurtz, R.L., Henrich, V.E.: Phys. Rev. B **36** (1987) 3413.
 87Oni1 Onishi, H., Egawa, C., Aruga, T., Iwasawa, Y.: Surf. Sci. **191** (1987) 479.
 87Rod1 Rodriguez, J.A., Campbell, C.T.: J. Phys. Chem. **91** (1987) 6648.
 87Sem1 Semancik, S., Cox, D.F.: Sens. Actuators **12** (1987) 101.
 88Au1 Au, C.T., Hirsch, W., Hirschwald, W.: Surf. Sci. **199** (1988) 507.
 88Au2 Au, C.T., Hirsch, W., Hirschwald, W.: Surf. Sci. **197** (1988) 391.

- 88Rod1 Rodriguez, J.A., Campbell, C.T.: *Surf. Sci.* **194** (1988) 475.
 88Rod2 Rodriguez, J.A., Campbell, C.T.: *Surf. Sci.* **197** (1988) 567.
 89Mac1 MacKay, J.L., Henrich, V.E.: *Phys. Rev. B* **39** (1989) 6156.
 89Rod1 Rodriguez, J.A.: *Surf. Sci.* **222** (1989) 383.
 89Smi1 Smith, K.E., Henrich, V.E.: *J. Vac. Sci. Technol. A* **7** (1989) 1967.
 89Tho1 Thornton, G.: *J. Phys. Condens. Matter* **1** (1989) B111.
 90Mull1 Mull, T., Kühlenbeck, H., Odörfer, G., Jaeger, R., Xu, C., Baumeister, B., Menges, M., Illing, G., Freund, H.-J., Weide, D., Andresen, P.: Desorption Induced by Electronic Transitions DIET IV, Proc. 4th Int. Workshop, Gloggnitz, Austria, October 1989, in: Springer Series in Surface Sciences, Vol. 19, Berlin: Springer-Verlag, 1990, p. 169.
 90Voh1 Vohs, J.M., Barteau, M.A.: *J. Phys. Chem.* **94** (1990) 882.
 90Yam1 Yamada, T., Kuroda, Y., Fukuoka, A., Ichikawa, M., Tanaka, K.: *J. Electron Spectrosc. Relat. Phenom.* **54/55** (1990) 845.
 91Bau1 Bäumer, M., Cappus, D., Kühlenbeck, H., Freund, H.-J., Wilhelmi, G., Brodde, A., Neddermeyer, H.: *Surf. Sci.* **253** (1991) 116.
 91Che1 Chen, J.G., Weisel, M.D., Hall, R.B.: *Surf. Sci.* **250** (1991) 159.
 91Cox1 Cox, D.F., Schulz, K.H.: *Surf. Sci.* **249** (1991) 138.
 91Cox2 Cox, D.F., Schulz, K.H.: *Surf. Sci.* **256** (1991) 67.
 91Hay1 Haynes, D.R., Helwig, K.R., Tro, N.J., George, S.M.: *J. Phys. Chem.* **95** (1991) 839.
 91Jae1 Jaeger, R.M., Kühlenbeck, H., Freund, H.-J., Wuttig, M., Hoffmann, W., Franchy, R., Ibach, H.: *Surf. Sci.* **259** (1991) 235.
 91Jen1 Jeng, S.-P., Zhang, Z., Henrich, V.E.: *Phys. Rev. B* **44** (1991) 3266.
 91Kuh1 Kühlenbeck, H., Odörfer, G., Jaeger, R., Illing, G., Menges, M., Mull, T., Freund, H.-J., Pöhlchen, M., Staemmler, V., Witzel, S., Scharfschwerdt, C., Wennemann, K., Liedtke, T., Neumann, M.: *Phys. Rev. B* **43** (1991) 1969.
 91Pac1 Pacchioni, G., Cogliandro, G., Bagus, P.S.: *Surf. Sci.* **255** (1991) 344.
 91Sch1 Schulz, K.H., Cox, D.F.: *Phys. Rev. B* **43** (1991) 1610.
 91Tok1 Tokmakoff, A., Haynes, D.R., George, S.M.: *Chem. Phys. Lett.* **186** (1991) 450.
 91Wu1 Wu, M.-C., Estrada, C.A., Goodman, D.W.: *Phys. Rev. Lett.* **67** (1991) 2910.
 91Xu1 Xu, C., Dillmann, B., Kühlenbeck, H., Freund, H.-J.: *Phys. Rev. Lett.* **67** (1991) 3551.
 91Xu2 Xu, C., Häfel, M., Kühlenbeck, H., Freund, H.-J.: *Surf. Sci.* **258** (1991) 23.
 92Ass1 Asscher, M., Zimmermann, F.M., Springsteen, L.L., Houston, P.L., Ho, W.: *J. Chem. Phys.* **96** (1992) 4808.
 92Bau1 Bäumer, M., Cappus, D., Illing, G., Kühlenbeck, H., Freund, H.-J.: *J. Vac. Sci. Technol. A* **10** (1992) 2407.
 92He1 He, J.-W., Corneille, J.S., Estrada, C.A., Wu, M.-C., Goodman, D.W.: *J. Vac. Sci. Technol. A* **10** (1992) 2248.
 92He2 He, J.-W., Estrada, C.A., Corneille, J.S., Wu, M.-C., Goodman, D.W.: *Surf. Sci.* **261** (1992) 164.
 92Kuh1 Kühlenbeck, H., Freund, H.-J.: Metal-ligand-interactions: From atoms to clusters to surfaces, Cetraro, Italy, June 1992, Salahub, D.R., Russo, N. (eds.), in: Nato Advanced Study Institute Series, Vol. 378, Dordrecht: Kluwer Academic Publishers, 1992, p. 37 - 70.
 92Kuh2 Kühlenbeck, H., Xu, C., Dillmann, B., Häfel, M., Adam, B., Ehrlich, D., Wohlrab, S., Freund, H.-J., Ditzinger, U.A., Neddermeyer, H., Neuber, M., Neumann, M.: *Ber. Bunsenges. Phys. Chem.* **96** (1992) 15.
 92Pac1 Pacchioni, G., Cogliandro, G., Bagus, P.S.: *Int. J. Quantum Chem.* **42** (1992) 1115.
 92Poh1 Pöhlchen, M., Staemmler, V.: *J. Chem. Phys.* **97** (1992) 2583.
 92She1 Shen, G.L., Casanova, R., Thornton, G.: *Vacuum* **43** (1992) 1129.
 92Str1 Strömberg, D.: *Surf. Sci.* **275** (1992) 473.
 92Tru1 Truong, C.M., Wu, M.-C., Goodman, D.W.: *J. Chem. Phys.* **97** (1992) 9447.
 92Vur1 Vurens, G.H., Maurice, V., Salmeron, M., Somorjai, G.A.: *Surf. Sci.* **268** (1992) 170.
 92Wol1 Wolf, D.: *Phys. Rev. Lett.* **68** (1992) 3315.
 92Wu1 Wu, M.-C., Corneille, J.S., He, J.-W., Estrada, C.A., Goodman, D.W.: *J. Vac. Sci. Technol. A* **10** (1992) 1467.
 92Wu2 Wu, M.-C., Estrada, C.A., Corneille, J.S., Goodman, D.W.: *J. Chem. Phys.* **96** (1992) 3892.
 92Wu3 Wu, M.-C., Goodman, D.W.: *Catal. Lett.* **15** (1992) 1.

- 92Wu4 Wu, M.-C., Truong, C.M., Coulter, K., Goodman, D.W.: *J. Catal.* **140** (1992) 344.
- 92Wul1 Wulser, K.W., Hearty, B.P., Langell, M.A.: *Phys. Rev. B* **46** (1992) 9724.
- 92Wul2 Wulser, K.W., Langell, M.A.: *J. Electron Spectrosc. Relat. Phenom.* **59** (1992) 223.
- 93Cap1 Cappus, D., Xu, C., Ehrlich, D., Dillmann, B., Ventrice jr, C.A., Al-Shamery, K., Kuhlenbeck, H., Freund, H.-J.: *Chem. Phys.* **177** (1993) 533.
- 93Fre1 Freitag, A., Staemmler, V., Cappus, D., Ventrice jr, C.A., Al-Shamery, K., Kuhlenbeck, H., Freund, H.-J.: *Chem. Phys. Lett.* **210** (1993) 10.
- 93Fre2 Freund, H.-J., Dillmann, B., Ehrlich, D., Haßel, M., Jaeger, R.M., Kuhlenbeck, H., Ventrice jr, C.A., Winkelmann, F., Wohlrab, S., Xu, C., Bertrams, T., Brodde, A., Neddermeyer, H.: *J. Mol. Catal.* **82** (1993) 143.
- 93Gon1 Goniakowski, J., Bouette-Russo, S., Noguera, C.: *Surf. Sci.* **284** (1993) 315.
- 93Gor1 Gordon, D.E.A., Lambert, R.M.: *Surf. Sci.* **287/288** (1993) 114.
- 93Har1 Hardman, P.J., Prakash, N.S., Muryn, C.A., Raikar, G.N., Thomas, A.G., Prime, A.F., Thornton, G., Blake, R.J.: *Phys. Rev. B* **47** (1993) 16056.
- 93Hei1 Heidberg, J., Meine, D., Redlich, B.: *J. Electron. Spectrosc. Relat. Phenom.* **64/65** (1993) 599.
- 93Jae1 Jaeger, R.M., Homann, K., Kuhlenbeck, H., Freund, H.-J.: *Chem. Phys. Lett.* **203** (1993) 41.
- 93Jae2 Jaeger, R.M., Libuda, J., Bäumer, M., Homann, K., Kuhlenbeck, H., Freund, H.-J.: *J. Electron Spectrosc. Relat. Phenom.* **64/65** (1993) 217.
- 93Kuh1 Kuhlenbeck, H., Freund, H.-J.: Adsorption and reaction of small molecules on oxide surfaces, in: *Springer Proceedings in Physics*, Vol. 73, Berlin: Springer-Verlag, 1993, 227.
- 93Li1 Li, X., Henrich, V.E.: *Phys. Rev. B* **48** (1993) 17486.
- 93Nog1 Noguera, C., Goniakowski, J., Bouette-Russo, S.: *Surf. Sci.* **287/288** (1993) 188.
- 93Pac1 Pacchioni, G.: *Surf. Sci.* **281** (1993) 207.
- 93Pet1 Petrie, W.T., Vohs, J.M.: *J. Vac. Sci. Technol. A* **11** (1993) 2169.
- 93Suz1 Suzanne, J., Panella, V., Ferry, D., Sidoumou, M.: *Surf. Sci.* **293** (1993) L912.
- 93Tru1 Truong, C.M., Wu, M.-C., Goodman, D.W.: *J. Am. Chem. Soc.* **115** (1993) 3647.
- 93Wal1 Walsh, J.F., Davis, R., Muryn, C.A., Thornton, G., Dhanak, V.R., Prince, K.C.: *Phys. Rev. B* **48** (1993) 14749.
- 93Wu1 Wu, M.-C., Truong, C.M., Coulter, K., Goodman, D.W.: *J. Vac. Sci. Technol. A* **11** (1993) 2174.
- 93Wu2 Wu, M.-C., Truong, C.M., Goodman, D.W.: *J. Phys. Chem.* **97** (1993) 9425.
- 93Wu3 Wu, M.-C., Truong, C.M., Goodman, D.W.: *J. Phys. Chem.* **97** (1993) 4182.
- 94AlS1 Al-Shamery, K., Beauport, I., Freund, H.-J., Zacharias, H.: *Chem. Phys. Lett.* **222** (1994) 107.
- 94Cap1 Cappus, D., Menges, M., Xu, C., Ehrlich, D., Dillmann, B., Ventrice jr, C.A., Libuda, J., Bäumer, M., Wohlrab, S., Winkelmann, F., Kuhlenbeck, H., Freund, H.-J.: *J. Electron Spectrosc. Relat. Phenom.* **68** (1994) 347.
- 94Cas1 Casarin, M., Tondello, E., Vittadini, A.: *Surf. Sci.* **307-309** (1994) 1182.
- 94Cou1 Coulomb, J.P., Larher, Y., Trabelsi, M., Mirabeau, I.: *Mol. Phys.* **81** (1994) 1259.
- 94Cou2 Coustet, V., Jupille, J.: *Surf. Sci.* **307-309** (1994) 1161.
- 94Dua1 Duan, Y., Zhang, K., Xie, X.: *Surf. Sci.* **321** (1994) L249.
- 94Elv1 Elvers, B., Hawkins, S., Russey, W.: *Ullmann's Encyclopedia of Industrial Chemistry*, Weinheim: VCH publishers, 1994.
- 94Fer1 Fernandez-Garcia, M., Conesa, J.C., Bagus, P.S., Rubio, J., Illas, F.: *J. Chem. Phys.* **101** (1994) 10134.
- 94Gas1 Gassmann, P., Franchy, R., Ibach, H.: *Surf. Sci.* **319** (1994) 95.
- 94Ge1 Ge, Q., Möller, P.J.: *Surf. Sci.* **82/83** (1994) 305.
- 94Ger1 Gercher, V.A., Cox, D.F.: *Surf. Sci.* **306** (1994) 279.
- 94Hol1 Holbert, V.P., Garrett, S.J., Bruns, J.C., Stair, P.C., Weitz, E.: *Surf. Sci.* **314** (1994) 107.
- 94Hug1 Hugenschmidt, M.B., Gamble, L., Campbell, C.T.: *Surf. Sci.* **302** (1994) 329.
- 94Jen1 Jenks, C.J., Jacobson, J.A., Thiel, P.A.: *J. Vac. Sci. Technol. A* **12** (1994) 2101.
- 94Kuh1 Kuhlenbeck, H.: *Appl. Phys. A* **59** (1994) 469.
- 94Lan1 Langel, W., Parrinello, M.: *Phys. Rev. Lett.* **73** (1994) 504.
- 94Lan2 Langell, M.A., Berrie, C.L., Nassir, M.H., Wulser, K.H.: *Surf. Sci.* **320** (1994) 25.
- 94Lud1 Ludviksson, A., Zhang, R., Campbell, C.T., Griffiths, K.: *Surf. Sci.* **313** (1994) 64.

- 94Mar Martins, J.B.L., Longo, E., Igualda, J.A., Beltran, A.A.: *An. Fis.* **90**(3) (1994) 187-189.
- 94Men1 Menges, M., Baumeister, B., Al-Shamery, K., Freund, H.-J., Fischer, C., Andresen, P.: *J. Chem. Phys.* **101** (1994) 3318.
- 94Men2 Menges, M., Baumeister, B., Al-Shamery, K., Freund, H.-J., Fischer, C., Andresen, P.: *Surf. Sci.* **316** (1994) 103.
- 94Mol1 Møller, P.J., Komolov, S.A., Lazneva, E.F.: *Appl. Surf. Sci.* **82/83** (1994) 569.
- 94Nyg1 Nygren, M.A., Pettersson, L.G.M.: *Chem. Phys. Lett.* **230** (1994) 456.
- 94Oni1 Onishi, H., Aruga, T., Iwasawa, Y.: *J. Catal.* **146** (1994) 557.
- 94Pac1 Pacchioni, G., Ricart, J.M., Illas, F.: *J. Am. Chem. Soc.* **116** (1994) 10152.
- 94Pan1 Panella, V., Suzanne, J., Hoang, P.N.M., Girardet, C.: *J. Phys. I (France)* **4** (1994) 905.
- 94Pet1 Pettersson, L.G.M.: *Theor. Chim. Acta* **87** (1994) 293.
- 94Pug1 Pugh, S., Gillan, M.J.: *Surf. Sci.* **320** (1994) 331.
- 94Roh1 Rohr, F., Wirth, K., Libuda, J., Cappus, D., Bäumer, M., Freund, H.-J.: *Surf. Sci.* **315** (1994) L977.
- 94Sca1 Scamehorn, C.A., Harrison, N.M., McCarthy, M.I.: *J. Chem. Phys.* **101** (1994) 1547.
- 94Szu1 Szuber, J.: *Phys. Status Solidi* **185** (1994) K9.
- 94Ves1 Vesecky, S.M., Xu, X., Goodman, D.W.: *J. Vac. Sci. Technol. A* **12** (1994) 2114.
- 94Wij1 Wijekoon, W.M.K.P., Koenig, E.W., Hetherinton III, W.M., Salzman, W.R.: *Appl. Surf. Sci.* **81** (1994) 347.
- 94Win1 Winkelmann, F., Wohlrab, S., Libuda, J., Bäumer, M., Cappus, D., Menges, M., Al-Shamery, K., Kuhlenbeck, H., Freund, H.-J.: *Surf. Sci.* **307-309** (1994) 1148.
- 94Zha1 Zhang, Z., Henrich, V.E.: *Surf. Sci.* **321** (1994) 133.
- 95All1 Allouche, A., Cora, F., Girardet, C.: *Chem. Phys.* **201** (1995) 59.
- 95Bea1 Beauport, I., Al-Shamery, K.: *SPIE - Int. Soc. Opt. Eng.* **2547** (1995) 176.
- 95Ben1 Bender, M., Ehrlich, D., Yakovkin, I.N., Rohr, F., Bäumer, M., Kuhlenbeck, H., Freund, H.-J.: *J. Phys. Condens. Matter* **7** (1995) 5289.
- 95Bre1 Bredow, T., Jug, K.: *Surf. Sci.* **327** (1995) 398.
- 95Bri1 Briquez, S., Lakhliifi, A., Picaud, S., Girardet, C.: *Chem. Phys.* **194** (1995) 65.
- 95Cap1 Cappus, D., Haßel, M., Neuhaus, E., Heber, M., Rohr, F., Freund, H.-J.: *Surf. Sci.* **337** (1995) 268.
- 95Cap2 Cappus, D., Klinkmann, J., Kuhlenbeck, H., Freund, H.-J.: *Surf. Sci.* **325** (1995) L421.
- 95Cas1 Casarin, M., Maccato, C., Tondello, E., Vittadini, A.: *Surf. Sci.* **343** (1995) 115.
- 95Cas2 Casarin, M., Tondello, E., Vittadini, A.: *Inorg. Chim. Acta* **235** (1995) 151.
- 95Con1 Condon, N.G., Leibsle, F.M., Lennie, A.R., Murray, P.W., Vaughan, D.J., Thornton, G.: *Phys. Rev. Lett.* **75** (1995) 1961.
- 95Fah1 Fahmi, A., Minot, C., Fourre, P., Nortier, P.: *Surf. Sci.* **343** (1995) 261.
- 95Fai1 Fairbrother, D.H., Briggman, K.A., Stair, P.C., Weitz, E.: *J. Chem. Phys.* **102** (1995) 7267.
- 95Fan1 Fang, J.-Y., Guo, H.: *Chem. Phys. Lett.* **235** (1995) 341.
- 95Fer1 Ferro, Y., Allouche, A., Cora, F., Pisani, C., Girardet, C.: *Surf. Sci.* **325** (1995) 139.
- 95Ger1 Gercher, V.A., Cox, D.F.: *Surf. Sci.* **322** (1995) 177.
- 95Ger2 Gerlach, R., Glebov, A., Lange, G., Toennies, J.P., Weiss, H.: *Surf. Sci.* **331-333** (1995) 1490.
- 95Gon1 Goniakowski, J., Noguera, C.: *Surf. Sci.* **330** (1995) 337.
- 95Has1 Hassel, M., Freund, H.-J.: *Surf. Sci.* **325** (1995) 163.
- 95Has2 Haßel, M., Kuhlenbeck, H., Freund, H.-J., Shi, S., Freitag, A., Staemmler, V., Lütkehoff, S., Neumann, M.: *Chem. Phys. Lett.* **240** (1995) 205.
- 95Hei1 Heidberg, J., Kandel, M., Meine, D., Wildt, U.: *Surf. Sci.* **331-333** (1995) 1467.
- 95Hei2 Heidberg, J., Redlich, B., Wetter, D.: *Ber. Bunsenges. Phys. Chem.* **99** (1995) 1333.
- 95Hin1 Hintenender, M., Rebentrost, F., Kosloff, R., Gerber, R.B.: *Surf. Sci.* **331-333** (1995) 1486.
- 95Lak1 Lakhliifi, A., Picaud, S., Girardet, C., Allouche, A.: *Chem. Phys.* **201** (1995) 73.
- 95Lan1 Langel, W., Parrinello, M.: *J. Phys. Chem.* **102** (1995) 3240.
- 95Lin1 Linsebigler, A., Lu, G., Yates jr, J.T.: *J. Chem. Phys.* **103** (1995) 9438.
- 95Mar1 Martins, J.B.L., Longo, E., Andres, J., Taft, C.A.: *J. Mol. Struct.* **335** (1995) 167.
- 95Mej1 Mejias, J.A., Marquez, A.M., Sanz, J.F., Fernandez-Garcia, M., Ricart, J.M., Sousa, C., Illas, F.: *Surf. Sci.* **327** (1995) 59.
- 95Mol1 Møller, P.J., Komolov, S.A., Lazneva, E.F., Pedersen, E.H.: *Surf. Sci.* **323** (1995) 102.

- 95Nak1 Nakatsuji, H., Yoshimoto, M., Hada, M., Domen, K., Hirose, C.: *Surf. Sci.* **336** (1995) 232.
95Ney1 Neyman, K.M., Ruzankin, S.P., Rösch, N.: *Chem. Phys. Lett.* **246** (1995) 546.
95Pic1 Picaud, S., Briquez, S., Lakhli, A., Girardet, C.: *J. Chem. Phys.* **102** (1995) 7229.
95Pie1 Pierce, K.G., Barteau, M.A.: *Surf. Sci.* **326** (1995) L473.
95Ran1 Rantala, T.S., Golovanov, V., Lantto, V.: *Sens. Actuators B* **24-25** (1995) 532.
95Ref1 Refson, K., Wogelius, R.A., Fraser, D.G., Payne, M.C., Lee, M.H., Milman, V.: *Phys. Rev. B* **52** (1995) 10823.
95Sei1 Seideman, T., Guo, H.: *J. Chem. Phys.* **103** (1995) 2745.
95Set1 Setzler, J.V., Huang, Z.-H., Guo, H.: *J. Chem. Phys.* **103** (1995) 4300.
95Shu1 Shultz, A.N., Jang, W., Hetherington III, W.M., Baer, D.R., Wang, L.-Q., Engelhard, M.H.: *Surf. Sci.* **339** (1995) 114.
95Sni1 Snis, A., Panas, I.: *J. Chem. Phys.* **103** (1995) 7926.
95Ste1 Stefanovich, E.V., Truong, T.N.: *J. Chem. Phys.* **102** (1995) 5071.
95Tor1 Torquemada, M.C., de Segovia, J.L., Roman, E.: *Surf. Sci.* **337** (1995) 31.
95Wai1 Wainhaus, S.B., Burroughs, J.A., Hanley, L.: *Surf. Sci.* **344** (1995) 122.
95Wal1 Walsh, J.F., Dhariwal, H.S., Gutierrez-Sosa, A., Lindsay, R., Thornton, G., Oldman, R.J.: *Nucl. Instrum. Methods Phys. Res. Sect. B* **97** (1995) 392.
95Wan1 Wang, L.-Q., Baer, D.R., Engelhard, M.H., Shultz, A.N.: *Surf. Sci.* **344** (1995) 237.
95Xu1 Xu, C., Goodman, D.W.: *J. Chem. Soc. Faraday Trans.* **91** (1995) 3709.
95Xu2 Xu, C., Koel, B.E.: *J. Chem. Phys.* **102** (1995) 8158.
95Xu3 Xu, X., Lü, X., Wang, N.Q., Zhang, Q.E.: *Chem. Phys. Lett.* **235** (1995) 541.
96All1 Allouche, A.: *J. Phys. Chem.* **100** (1996) 1820.
96AlS1 Al-Shamery, K.: *Appl. Phys. A* **63** (1996) 509.
96Anc1 Anchell, J.L., Hess, A.C.: *J. Phys. Chem.* **100** (1996) 18317.
96Ban1 Bandara, A., Kubota, J., Wada, A., Domen, K., Hirose, C.: *Surf. Sci.* **364** (1996) L580.
96Ban2 Bandara, A., Kubota, J., Wada, A., Domen, K., Hirose, C.: *J. Phys. Chem. B* **100** (1996) 14962.
96Bea1 Beauport, I., Al-Shamery, K., Freund, H.-J.: *Surf. Sci.* **363** (1996) 252.
96Bea2 Beauport, I., Al-Shamery, K., Freund, H.-J.: *Chem. Phys. Lett.* **256** (1996) 641.
96Ber1 Bertrams, T., Neddermeyer, H.: *J. Vac. Sci. Technol. B* **14** (1996) 1141.
96Bul1 Bullock, E.L., Patthey, L., Steinemann, S.G.: *Surf. Sci.* **352-354** (1996) 504.
96Cas1 Casarin, M., Maccato, C., Tabacchi, G., Vittadini, A.: *Surf. Sci.* **352-354** (1996) 341.
96Cor1 Cornell, R.M., Schwertmann, U.: *The iron oxides-structure, properties, reaction, occurrences and uses*, Weinheim: VCH Publishers, 1996.
96Dil1 Dillmann, B., Rohr, F., Seiferth, O., Klivenyi, G., Bender, M., Homann, K., Yakovkin, I.N., Ehrlich, D., Bäumer, M., Kühlenbeck, H., Freund, H.-J.: *Faraday Discuss. Chem. Soc.* **105** (1996) 295.
96Eic1 Eichhorn, G., Richter, M., Al-Shamery, K., Zacharias, H.: *Surf. Sci.* **368** (1996) 67.
96Fah1 Fahmi, A., Ahdjoudj, J., Minot, C.: *Surf. Sci.* **352-354** (1996) 529.
96Fer1 Fernandez-Garcia, M., Conesa, J.C., Illas, F.: *Surf. Sci.* **349** (1996) 207.
96Fer2 Ferry, D., Glebov, A., Senz, V., Suzanne, J., Toennies, J.P., Weiss, H.: *J. Chem. Phys.* **105** (1996) 1697.
96Fer3 Ferry, D., Suzanne, J.: *Surf. Sci.* **345** (1996) L19.
96Fre1 Freund, H.-J., Dillmann, B., Seiferth, O., Klivenyi, G., Bender, M., Ehrlich, D., Hemmerich, I., Cappus, D.: *Catal. Today* **32** (1996) 1.
96Fre2 Freund, H.-J., Kühlenbeck, H., Staemmler, V.: *Rep. Prog. Phys.* **59** (1996) 283.
96Gam1 Gamble, L., Jung, L.S., Campbell, C.T.: *Surf. Sci.* **348** (1996) 1.
96Gir1 Girardet, C., Hoang, P.N.M., Picaud, S.: *Phys. Rev. B* **53** (1996) 16615.
96Gon1 Goniakowski, J., Gillan, M.J.: *Surf. Sci.* **350** (1996) 145.
96Goo1 Goodman, D.W.: *J. Vac. Sci. Technol. A* **14** (1996) 1526.
96Gut1 Gutierrez-Sosa, A., Crook, S., Haq, S., Lindsay, R., Ludviksson, A., Parker, S., Campbell, C.T., Thornton, G.: *Faraday Discuss. Chem. Soc.* **105** (1996) 355.
96Hav1 Havighorst, M., Prager, M., Coddens, G.: *Chem. Phys. Lett.* **259** (1996) 1.
96Hei1 Heidberg, J., Redlich, B.: *Surf. Sci.* **368** (1996) 140.
96Hen1 Henderson, M.A.: *Langmuir* **12** (1996) 5093.
96Hen2 Henderson, M.A.: *Surf. Sci.* **355** (1996) 151.

- 96Hin1 Hintenender, M., Rebentrost, F., Kosloff, R., Gerber, R.B.: J. Chem. Phys. **105** (1996) 11347.
- 96Hoa1 Hoang, P.N.M., Picaud, S., Girardet, C.: Surf. Sci. **360** (1996) 261.
- 96Hol1 Holbert, V.P., Garrett, S.J., Stair, P.C., Weitz, E.: Surf. Sci. **346** (1996) 189.
- 96Idr1 Idriss, H., Lusvardi, V.S., Barteau, M.A.: Surf. Sci. **348** (1996) 39.
- 96Irw1 Irwin, J.S.G., Prime, A.F., Hardman, P.J., Wincott, P.L., Thornton, G.: Surf. Sci. **352-354** (1996) 480.
- 96Jug1 Jug, K., Geudtner, G.: J. Chem. Phys. **105** (1996) 5285.
- 96Kli1 Klinkmann, J., Cappus, D., Homann, K., Risse, T., Sandell, A., Porwol, T., Freund, H.-J., Fink, K., Fink, R., Staemmler, V.: J. Electron Spectrosc. Relat. Phenom. **77** (1996) 155.
- 96Klu1 Klüner, T., Freund, H.-J., Freitag, J., Staemmler, V.: J. Chem. Phys. **104** (1996) 10030.
- 96Kub1 Kubota, J., Bandara, A., Wada, A., Domen, K., Hirose, C.: Surf. Sci. **368** (1996) 361.
- 96Lak1 Lakhlifi, A., Girardet, C.: J. Chem. Phys. **105** (1996) 2471.
- 96Lan1 Langel, W.: Chem. Phys. Lett. **259** (1996) 7.
- 96Lin1 Lindan, P. J.D., Harrison, N.M., Holender, J.M., Gillan, M.J.: Chem. Phys. Lett. **261** (1996) 246.
- 96Lin2 Linsebiegler, A., Lu, G., Yates jr., J.T.: J. Phys. Chem. **100** (1996) 6631.
- 96Mar1 Markovits, A., Ahdjoudj, J., Minot, C.: Surf. Sci. **365** (1996) 649.
- 96Mar2 Marre, K., Neddermeyer, H., Chasse, A., Rennert, P.: Surf. Sci. **357-358** (1996) 233.
- 96Mar3 Martins, J.B.L., Longo, E., Andres, J., Taft, C.A.: J. Mol. Struct. **363** (1996) 249.
- 96McC1 McCarthy, M.I., Schenter, G.K., Scamehorn, C.A., Nicholas, J.B.: J. Phys. Chem. **100** (1996) 16989.
- 96Min1 Minot, C., Van Hove, M.A., Biberian, J.-P.: Surf. Sci. **346** (1996) 283.
- 96Nak1 Nakajima, Y., Doren, D.J.: J. Chem. Phys. **105** (1996) 7753.
- 96Nybl1 Nyberg, M., Nygren, M.A., Pettersson, L.G.M., Gay, D.H., Rohl, A.L.: J. Phys. Chem. **100** (1996) 9054.
- 96Nyg1 Nygren, M.A., Pettersson, L.G.M.: J. Phys. Chem. **100** (1996) 1874.
- 96Nyg2 Nygren, M.A., Pettersson, L.G.M.: J. Chem. Phys. **105** (1996) 9339.
- 96Nyg3 Nygren, M.A., Pettersson, L.G.M., Freitag, A., Staemmler, V., Gay, D.H., Rohl, A.L.: J. Phys. Chem. **100** (1996) 294.
- 96Oni1 Onishi, H., Iwasawa, Y.: Surf. Sci. **357-358** (1996) 773.
- 96Oni2 Onishi, H., Iwasawa, Y.: Phys. Rev. Lett. **76** (1996) 791.
- 96Oni3 Onishi, H., Yamaguchi, Y., Fukui, K.-I., Iwasawa, Y.: J. Phys. Chem. **100** (1996) 9582.
- 96Pac1 Pacchioni, G., Ferrari, A.M., Bagus, P.S.: Surf. Sci. **350** (1996) 159.
- 96Pac2 Pacchioni, G., Ferrari, A.M., Giamello, E.: Chem. Phys. Lett. **255** (1996) 58.
- 96Pan1 Panella, V., Suzanne, J., Coulomb, J.-P.: Surf. Sci. **350** (1996) L211.
- 96Put1 Putna, E.S., Vohs, J.M., Gorte, R.J.: J. Phys. Chem. **100** (1996) 17862.
- 96Raz1 Raza, H., Harte, S.P., Muryn, C.A., Wincott, P.L., Thornton, G., Casanova, R., Rodriguez, A.: Surf. Sci. **366** (1996) 519.
- 96Rei1 Reinhardt, P., Causa, M., Marian, C.M., Heß, B.A.: Phys. Rev. B **54** (1996) 14812.
- 96Sch1 Schönnenbeck, M., Cappus, D., Klinkmann, J., Freund, H.-J., Pettersson, L.G.M., Bagus, P.S.: Surf. Sci. **347** (1996) 337.
- 96Spe1 Speedy, R.J., Debenedetti, P.G., Smith, R.S., Huang, C., Kay, B.D.: J. Chem. Phys. **105** (1996) 240.
- 96Sti1 Stirniman, M.J., Huang, C., Smith, R.S., Joyce, S.A., Kay, B.D.: J. Chem. Phys. **105** (1996) 1295.
- 96Str1 Street, S.C., Guo, Q., Goodman, D.W.: J. Phys. Chem. **100** (1996) 17599.
- 96Szy1 Szymanski, M.A., Gillan, M.J.: Surf. Sci. **367** (1996) 135.
- 96Wit1 Witko, M.: Catal. Today **32** (1996) 89.
- 96Xu1 Xu, C., Goodman, D.W.: Catal. Today **28** (1996) 297.
- 96Xu2 Xu, C., Oh, W.S., Goodman, D.W.: J. Vac. Sci. Technol. A **14** (1996) 1395.
- 97And1 Andrews, S.B., Burton, N.A., Hillier, I.H.: Chem. Phys. Lett. **269** (1997) 475.
- 97Ban1 Bandara, A., Dobashi, S., Kubota, J., Onda, K., Wada, A., Domen, K., Hirose, C., Kano, S.S.: Surf. Sci. **387** (1997) 312.
- 97Ban2 Bandara, A., Kubota, J., Wada, A., Domen, K., Hirose, C.: J. Phys. Chem. B **101** (1997) 361.
- 97Bre1 Bredow, T., Pacchioni, G.: Surf. Sci. **373** (1997) 21.
- 97Cas1 Casarin, M., Maccato, C., Vittadini, A.: Chem. Phys. Lett. **280** (1997) 53.

- 97Cas2 Casarin, M., Maccato, C., Vittadini, A.: *Surf. Sci.* **377-379** (1997) 587.
- 97Cas3 Casarin, M., Vittadini, A.: *Surf. Sci.* **387** (1997) L1079.
- 97Cha1 Chambers, S.A., Thevuthasan, S., Kim, Y.J., Herman, G.S., Wang, Z., Tober, E., Ynzunza, R., Morais, J., Peden, C.H.F., Ferris, K., Fadley, C.S.: *Chem. Phys. Lett.* **267** (1997) 51.
- 97Cha2 Chaturvedi, S., Rodriguez, J.A., Hrbek, J.: *J. Phys. Chem. B* **101** (1997) 10860.
- 97Coc1 Cocks, I.D., Guo, Q., Williams, E.M., Roman, E., de Segovia, J.L.: *Surf. Sci.* **377-379** (1997) 135.
- 97Con1 Condon, N.G., Leibsle, F.M., Parker, T., Lennie, A.R., Vaughan, D.J., Thornton, G.: *Phys. Rev. B* **55** (1997) 15885.
- 97Cou1 Coustet, V., Jupille, J.: *Nuovo Cimento* **19** (1997) 1657.
- 97Cro1 Crook, S., Dhariwal, H., Thornton, G.: *Surf. Sci.* **382** (1997) 19.
- 97deS1 de Sainte Claire, P., Hass, K.C., Schneider, W.F., Hase, W.L.: *J. Phys. Chem.* **106** (1997) 7331.
- 97Fer1 Fernandez-Garcia, M., Conesa, J.C., Illas, F.: *J. Mol. Catal. A* **119** (1997) 87.
- 97Fer2 Ferrari, A.M., Pacchioni, G.: *J. Chem. Phys.* **107** (1997) 2066.
- 97Fer3 Ferry, D., Glebov, A., Senz, V., Suzanne, J., Toenies, J.P., Weiss, H.: *Surf. Sci.* **377-379** (1997) 634.
- 97Fer4 Ferry, D., Hoang, P.N.M., Suzanne, J., Biberian, J.-P., Van Hove, M.A.: *Phys. Rev. Lett.* **78** (1997) 4237.
- 97Fer5 Ferry, D., Suzanne, J., Hoang, P.N.M., Girardet, C.: *Surf. Sci.* **375** (1997) 315.
- 97Gar1 Garrett, S.J., Heyd, D.V., Polanyi, J.C.: *J. Chem. Phys.* **106** (1997) 7847.
- 97Guo1 Guo, Q., Cocks, I., Williams, E.M.: *J. Chem. Phys.* **106** (1997) 2924.
- 97Guo2 Guo, Q., Cocks, I., Williams, E.M.: *Surf. Sci.* **393** (1997) 1.
- 97Guo3 Guo, Q., Möller, P.J.: *Appl. Surf. Sci.* **115** (1997) 39.
- 97Hem1 Hemmerich, I., Rohr, F., Seiferth, O., Dillmann, B., Freund, H.-J.: *Z. Phys. Chem.* **202** (1997) 31.
- 97Hen1 Henderson, M.A.: *J. Phys. Chem. B* **101** (1997) 221.
- 97Jug1 Jug, K., Geudtner, G.: *J. Mol. Catal. A* **119** (1997) 143.
- 97Kan1 Kantorovich, L.N., Gillan, M.J.: *Surf. Sci.* **376** (1997) 169.
- 97Kan2 Kantorovich, L.N., Gillan, M.J.: *Mater. Sci. Forum* **239-241** (1997) 637.
- 97Kan3 Kantorovich, L.N., Gillan, M.J.: *Surf. Sci.* **374** (1997) 373.
- 97Kat1 Katter, U.K., Risse, T., Schliez, H., Beckendorf, M., Klüner, T., Hamann, H., Freund, H.-J.: *J. Magn. Reson.* **126** (1997) 242.
- 97Klu1 Klüner, T., Freund, H.-J., Freitag, J., Staemmler, V.: *J. Mol. Catal. A* **119** (1997) 155.
- 97Kuh1 Kuhlenbeck, H., Freund, H.-J.: Structure and electronic properties of ultrathin oxide films on metallic substrates, in: *Growth and properties of ultrathin epitaxial layers*, Vol. 8, The chemical physics of solid surfaces, King, D.A., Woodruff, D.P. (eds.), Amsterdam: Elsevier, 1997, 340 - 371.
- 97Lib1 Libuda, J., Frank, M., Sandell, A., Andersson, S., Brühwiler, P.A., Bäumer, M., Martensson, N., Freund, H.-J.: *Surf. Sci.* **384** (1997) 106.
- 97Lin1 Lindan, P.J.D., Muscat, J., Bates, S., Harrison, N.M., Gillan, M.: *Faraday Discuss. Chem. Soc.* **106** (1997) 135.
- 97Nyg1 Nygren, M.A., Gay, D.H., Richard, C., Catlow, A.: *Surf. Sci.* **380** (1997) 113.
- 97Ove1 Overbury, S.H., Huntley, D.R., Mullins, D.R., Alley, K.S., Radulovic, P.V.: *J. Vac. Sci. Technol. A* **15** (1997) 1647.
- 97Pra1 Prager, M., Havighorst, M., Coddens, G., Büttner, H.: *Physica B* **234** (1997) 170.
- 97Pra2 Prager, M., Havighorst, M., Coddens, G., Büttner, H.: *J. Phys. Condens. Matter* **9** (1997) 43.
- 97Raz1 Raza, H., Wincott, P.L., Thornton, G., Casanova, R., Rodriguez, A.: *Surf. Sci.* **390** (1997) 256.
- 97Rod1 Rodriguez, J.A., Chaturvedi, S., Kuhn, M., van Ek, J., Diebold, U., Robbert, P.S., Geisler, H., Ventrice jr, C.A.: *J. Chem. Phys.* **107** (1997) 9146.
- 97Roh1 Rohr, F., Bäumer, M., Freund, H.-J., Mejias, J.A., Staemmler, V., Müller, S., Hammer, L., Heinz, K.: *Surf. Sci.* **389** (1997) 391.
- 97Roh2 Rohr, F., Bäumer, M., Freund, H.-J., Mejias, J.A., Staemmler, V., Müller, S., Hammer, L., Heinz, K.: *Surf. Sci.* **372** (1997) L291.

- 97Rom1 Roman, E., de Segovia, J.L., Martin-Gago, J.A., Comtet, G., Hellner, L.: *Vacuum* **48** (1997) 597.
- 97Sam1 Sambeth, J., Juan, A., Gambaro, L., Thomas, H.: *J. Mol. Catal. A* **118** (1997) 283.
- 97Shu1 Shultz, A.N., Hetherington III, W.M., Baer, D.R., Wang, L.-Q., Engelhard, M.H.: *Surf. Sci.* **392** (1997) 1.
- 97Sor1 Soria, E., de Segovia, J.L., Colera, I., Gonzalez, R.: *Surf. Sci.* **390** (1997) 140.
- 97Szu1 Szuber, J., Czempik, G.: *Vacuum* **48** (1997) 289.
- 97Tik1 Tikhomirov, V.A., Geudtner, G., Jug, K.: *J. Phys. Chem. B* **101** (1997) 10398.
- 97Tra1 Trabelsi, M., Coulomb, J.P., Degenhardt, D., Lauter, H.: *Surf. Sci.* **377-379** (1997) 38.
- 97Van1 Vanolli, F., Heiz, U., Schneider, W.-D.: *Surf. Sci.* **377-379** (1997) 780.
- 97Wan1 Wang, L.-Q., Ferris, K.F., Shultz, A.N., Baer, D.R., Engelhard, M.H.: *Surf. Sci.* **380** (1997) 352.
- 97Was1 Wasserman, E., Rustad, J.R., Felmy, A.R., Hay, B.P., Halley, J.W.: *Surf. Sci.* **385** (1997) 217.
- 97Wol1 Wolter, K., Seiferth, O., Libuda, J., Kühlenbeck, H., Bäumer, M., Freund, H.-J.: *Chem. Phys. Lett.* **277** (1997) 513.
- 97Xu1 Xu, C., Goodman, D.W.: *Chem. Phys. Lett.* **265** (1997) 341.
- 97Yam1 Yamamoto, H., Watanabe, N., Wada, A., Domen, K., Hirose, C.: *J. Chem. Phys.* **106** (1997) 4734.
- 97Zsc1 Zscherpel, D., Weiss, W., Schlögl, R.: *Surf. Sci.* **382** (1997) 326.
- 98Ahd1 Ahdjoudj, J., Minot, C.: *Surf. Sci.* **402-404** (1998) 104.
- 98Ala1 Alam, M., Henderson, M.A., Kaviranta, P.D., Herman, G.S., Peden, C.H.F.: *J. Phys. Chem. B* **102** (1998) 111.
- 98Bar1 Barbier, A., Renaud, G., Stierle, A.: *Surf. Sci.* **402-404** (1998) 757.
- 98Bat1 Bates, S.P., Gillan, M.J., Kresse, G.: *J. Phys. Chem. B* **102** (1998) 2017.
- 98Bat2 Bates, S.P., Kresse, G., Gillan, M.J.: *Surf. Sci.* **409** (1998) 336.
- 98Bre1 Bredow, T.: *Surf. Sci.* **401** (1998) 82.
- 98Bri1 Brinkley, D., Casarin, T.E., Maccato, C., Vittadini, A.: *J. Phys. Chem. B* **102** (1998) 7596.
- 98Bri2 Brinkley, D., Dietrich, M., Engel, T., Farall, P., Gantner, G., Schäfer, A., Szuchmacher, A.: *Surf. Sci.* **395** (1998) 292.
- 98Bri3 Brinkley, D., Engel, T.: *Surf. Sci.* **415** (1998) L1001.
- 98Bur1 Burns, T.E., Dennison, J.R.: *Surf. Sci.* **395** (1998) 46.
- 98Cas1 Casarin, M., Maccato, C., Vittadini, A.: *Inorg. Chem.* **37** (1998) 5482.
- 98Cas2 Casarin, M., Maccato, C., Vittadini, A.: *J. Phys. Chem. B* **102** (1998) 10745.
- 98Cha1 Chambers, S.A., Henderson, M.A., Kim, Y.J., Thevuthasan, S.: *Surf. Rev. Lett.* **5** (1998) 381.
- 98Che1 Chen, L., Wu, R., an Q.Zhang, N.K.: *Chem. Phys. Lett.* **290** (1998) 255.
- 98deL1 de Leeuw, N.H., Parker, S.C.: *Phys. Rev. B* **58** (1998) 13901.
- 98Dic1 Dickens, K.A., Stair, P.C.: *Langmuir* **14** (1998) 1444.
- 98Die1 Diebold, U., Hebenstreit, W.: *Phys. Rev. Lett.* **81** (1998) 405.
- 98Die2 Diebold, U., Lehman, J., Mahmoud, T., Kuhn, M., Leonardelli, G., Hebenstreit, W., Schmid, M., Varga, P.: *Surf. Sci.* **411** (1998) 137.
- 98Egd1 Egdell, R.G., Jones, F.H.: *J. Mater. Chem.* **8** (1998) 469.
- 98Eic1 Eichhorn, G., Richter, M., Al-Shamery, K., Zacharias, H.: *Chem. Phys. Lett.* **289** (1998) 367.
- 98Ela1 Elam, J.W., Nelson, C.E., Cameron, M.A., Tolbert, M.A., George, S.M.: *J. Phys. Chem. B* **102** (1998) 7008.
- 98Epl1 Epling, W.S., Peden, C.H.F., Henderson, M.A., Diebold, U.: *Surf. Sci.* **412/413** (1998) 333.
- 98Fer1 Ferry, D., Picaud, S., Hoang, P.N.M., Girardet, C., Giordano, L., Demirdjian, B., Suzanne, J.: *Surf. Sci.* **409** (1998) 101.
- 98Gam1 Gamble, L., Henderson, M.A., Campbell, C.T.: *J. Phys. Chem. B* **102** (1998) 4536.
- 98Gio1 Giordano, L., Goniakowski, J., Suzanne, J.: *Phys. Rev. Lett.* **81** (1998) 1271.
- 98Gir1 Girardet, C., Hoang, P.N.M., Marmier, A., Picaud, S.: *Phys. Rev. B* **57** (1998) 11931.
- 98Gir2 Girardet, C., Humbert, J., Hoang, P.N.M.: *Chem. Phys.* **230** (1998) 67.
- 98Gun1 Günster, J., Liu, G., Kempter, V., Goodman, D.W.: *Surf. Sci.* **415** (1998) 303.
- 98Gun2 Günster, J., Liu, G., Kempter, V., Goodman, D.W.: *J. Vac. Sci. Technol. A* **16** (1998) 996.
- 98Has1 Hass, K.C., Schneider, W.F., Curioni, A., Andreoni, W.: *Science (Washington)* **282** (1998) 265.

- 98Hay1 Hayden, B.E., King, A., Newton, M.A.: Surf. Sci. **397** (1998) 306.
- 98Hen1 Henderson, M.A.: Surf. Sci. **400** (1998) 203.
- 98Hen2 Henderson, M.A., Joyce, S.A., Rustad, J.A.: Surf. Sci. **417** (1998) 66.
- 98Hen3 Henderson, M.A., Otero-Tapia, S., Castro, M.E.: Surf. Sci. **412/413** (1998) 252.
- 98Her1 Hermansson, K., Baudin, M., Ensing, B., Alfredsson, M., Wojcik, M.: J. Chem. Phys. **109** (1998) 7515.
- 98Hsi1 Hsiao, G.S., Erley, W., Ibach, H.: Surf. Sci. **405** (1998) L465.
- 98Iwa1 Iwasawa, Y.: Surf. Sci. **402-404** (1998) 8.
- 98Joh1 Johnson, M.A., Stefanovich, E.V., Truong, T.N.: J. Phys. Chem. B **102** (1998) 6391.
- 98Jon1 Jones, P.M., May, J.A., Reitz, J.B., Solomon, E.I.: J. Am. Chem. Soc. **120** (1998) 1506.
- 98Jon2 Jones, P.M., May, J.A., Solomon, E.I.: Inorg. Chim. Acta **275-276** (1998) 327.
- 98Kim1 Kim, S.H., Stair, P., E.Weitz: J. Chem. Phys. **108** (1998) 5080.
- 98Kit1 Kitakatsu, N., Maurice, V., Hinnen, C., Marcus, P.: Surf. Sci. **407** (1998) 36.
- 98Kit2 Kitakatsu, N., Maurice, V., Marcus, P.: Surf. Sci. **411** (1998) 215.
- 98Klu1 Klüner, T., Freund, H.-J., Staemmler, V., Kosloff, R.: Phys. Rev. Lett. **80** (1998) 5208.
- 98Klu2 Klüner, T., Thiel, S., Freund, H.-J., Staemmler, V.: Chem. Phys. Lett. **294** (1998) 413.
- 98Lar1 Larese, J.Z.: Physica B **248** (1998) 297.
- 98Laz1 Lazneva, E.F., Komolov, S.A., Möller, P.J.: Phys. Low-Dim. Struct **7/8** (1998) 147.
- 98Lin1 Lindan, P.J.D., Harrison, N.M.: Phys. Rev. Lett. **80** (1998) 762.
- 98Liu1 Liu, P., Kendelewicz, T., Brown jr., G.E., Nelson, E.J., Chambers, S.A.: Surf. Sci. **417** (1998) 53.
- 98Liu2 Liu, P., Kendelewicz, T., Brown jr., G.E., Parks, G.A.: Surf. Sci. **412/413** (1998) 287.
- 98Liu3 Liu, P., Kendelewicz, T., Brown jr., G.E., Parks, G.A., Pianetta, P.: Surf. Sci. **416** (1998) 326.
- 98Liu4 Liu, P., Kendelewicz, T., Gordon jr, G.E.: Surf. Sci. **412/413** (1998) 315.
- 98Liu5 Liu, P., Kendelewicz, T., Nelson, E.J., Brown jr., G.E.: Surf. Sci. **415** (1998) 156.
- 98Mar1 Marmier, A., Hoang, P.N.M., Picaud, S., Girardet, C., Lynden-Bell, R.M.: J. Chem. Phys. **109** (1998) 3245.
- 98Mat1 Matsumoto, T., Bandara, A., Kubota, J., Hirose, C., Domen, K.: J. Phys. Chem. B **102** (1998) 2979.
- 98Nel1 Nelson, C.E., Elam, J.W., Cameron, M.A., Tolbert, M.A., George, S.M.: Surf. Sci. **416** (1998) 341.
- 98Nis1 Nishimura, S.Y., Gibbons, R.F., Tro, N.J.: J. Phys. Chem. B **102** (1998) 6831.
- 98Ovi1 Oviedo, J., Calzado, C.J., Sanz, J.F.: J. Chem. Phys. **108** (1998) 4219.
- 98Ovi2 Oviedo, J., Sanz, J.F.: Surf. Sci. **397** (1998) 23.
- 98Pou1 Pouthier, V., Ramseyer, C., Girardet, C.: J. Chem. Phys. **108** (1998) 6502.
- 98Pra1 Prager, M., Havighorst, M., Büttner, H., Langel, W.: Physica B **241-253** (1998) 262.
- 98Ran1 Ranke, W., Weiss, W.: Surf. Sci. **414** (1998) 236.
- 98Raz1 Raza, H., Wincott, P.L., Thornton, G., Casanova, R., Rodriguez, A.: Surf. Sci. **402-404** (1998) 710.
- 98Rei1 Reissner, R., Radke, U., Schulze, M., Umbach, E.: Surf. Sci. **402-404** (1998) 71.
- 98Rit1 Rittner, F., Fink, R., Boddenberg, B., Staemmler, V.: Phys. Rev. B **57** (1998) 4160.
- 98Sel1 Selloni, A., Vittadini, A., Grätzel, M.: Surf. Sci. **402-404** (1998) 219.
- 98Slo1 Sloan, D., Sun, Y.-M., White, J.M.: J. Phys. Chem. B **102** (1998) 6825.
- 98Sni1 Snis, A., Miettinen, H.: J. Phys. Chem. B **102** (1998) 2555.
- 98Sni2 Snis, A., Panas, I.: Surf. Sci. **412/413** (1998) 477.
- 98Soe1 Soetens, J.C., Millot, C., Hoang, P.N.M., Girardet, C.: Surf. Sci. **419** (1998) 48.
- 98Sor1 Sorescu, D.C., Yates jr, J.T.: J. Phys. Chem. B **102** (1998) 4556.
- 98The1 Thevuthasan, S., Herman, G.S., Kim, Y.J., Chambers, S.A., Peden, C.H.F., Wang, Z., Ynzunza, R.X., Tober, E.D., Morais, J., Fadley, C.S.: Surf. Sci. **401** (1998) 261.
- 98Thi1 Thiel, S., Klüner, T., Wilde, M., Al-Shamery, K., Freund, H.-J.: Chem. Phys. **228** (1998) 185.
- 98Tho1 Thornton, G., Crook, S., Chang, Z.: Surf. Sci. **415** (1998) 122.
- 98Tol1 Toledano, D.S., Dufresne, E.R., Henrich, V.E.: J. Vac. Sci. Technol. A **16** (1998) 1050.
- 98Van1 Van Hove, M.A., Somorjai, G.A.: J. Mol. Catal. A **131** (1998) 243.
- 98Van2 Vanolli, F., Heiz, U., Schneider, W.-D.: Surf. Sci. **414** (1998) 261.
- 98Vit1 Vittadini, A., Selloni, A., Rotzinger, F.P., Grätzel, M.: Phys. Rev. Lett. **81** (1998) 2954.
- 98Vogl Vogtenhuber, D., Podloucky, R., Redinger, J.: Surf. Sci. **402-404** (1998) 798.

- 98Wei1 Weiss, W., Zscherpel, D., Schlögl, R.: *Catal. Lett.* **52** (1998) 215.
- 98Wil1 Wilde, M., Al-Shamery, K., Freund, H.-J.: *SPIE - Int. Soc. Opt. Eng.* **3272** (1998) 152.
- 98Yos1 Yoshihara, J., Campbell, C.T.: *Surf. Sci.* **407** (1998) 256.
- 98Yuz1 Yuzawa, T., Shioda, T., Kubota, J., Onda, K., Wada, A., Domen, K., Hirose, C.: *Surf. Sci.* **416** (1998) L1090.
- 98Zsc1 Zscherpel, D., Ranke, W., Weiss, W., Schlögl, R.: *J. Chem. Phys.* **108** (1998) 9506.
- 99Abr1 Abriou, D., Jupille, J.: *Surf. Sci.* **430** (1999) L527.
- 99Ahd1 Ahdjoudj, J., Markovits, A., Minot, C.: *Catal. Today* **50** (1999) 541.
- 99Ban1 Bandara, A., Kubota, J., Onda, K., Wada, A., Kano, S.S., Domen, K., Hirose, C.: *Surf. Sci.* **427-428** (1999) 331.
- 99Bol1 Bolton, K., Bosio, S.B.M., Hase, W.L., Schneider, W.F., Hass, K.C.: *J. Phys. Chem. B* **103** (1999) 3885.
- 99Bre1 Bredow, T., Marquez, A.M., Pacchioni, G.: *Surf. Sci.* **430** (1999) 137.
- 99Bro1 Brown jr., G.E., Henrich, V.E., Casey, W.H., Clark, D.L., Eggleston, C., Felmy, A., Goodman, D.W., Grätzel, M., Maciel, G., McCarthy, M.I., Nealson, K.H., Sverjenski, D.A., Toney, M.F., Zachara, J.M.: *Chem. Rev.* **99** (1999) 77.
- 99Cal1 Calatayud, M., Andres, J., Beltran, A.: *Surf. Sci.* **430** (1999) 213.
- 99Car1 Carrier, X., Doyle, C.S., Kendelewicz, T., Brown jr, G.E.: *Surf. Rev. Lett* **6** (1999) 1237.
- 99Cas1 Casarin, M., Maccato, C., Vigato, N., Vittadini, A.: *Appl. Surf. Sci.* **142** (1999) 164.
- 99Cas2 Casarin, M., Maccato, C., Vittadini, A.: *Chem. Phys. Lett.* **300** (1999) 403.
- 99Cas3 Casarin, M., Maccato, C., Vittadini, A.: *Appl. Surf. Sci.* **142** (1999) 192.
- 99Cas4 Casarin, M., Maccato, C., Vittadini, A.: *Appl. Surf. Sci.* **142** (1999) 196.
- 99Che1 Cheng, H., Reiser, D.B., Dean jr., S.: *Catal. Today* **50** (1999) 579.
- 99DiF1 Di Felice, R., Northrup, J.E.: *Phys. Rev. B* **60** (1999) R16287.
- 99Dom1 Domen, K., Bandara, A., Kubota, J., Onda, K., Wada, A., Kano, S.S., Hirose, C.: *Surf. Sci.* **427-428** (1999) 349.
- 99Doy1 Doyle, C.S., Kendelewicz, T., Carrier, X., Brown jr, G.E.: *Surf. Rev. Lett* **6** (1999) 1247.
- 99Eic1 Eichhorn, G., Richter, M., Al-Shamery, K., Zacharias, H.: *J. Chem. Phys.* **111** (1999) 386.
- 99Eng1 Engkvist, O., Stone, A.J.: *Surf. Sci.* **437** (1999) 239.
- 99Fuk1 Fukui, K.-I., Onishi, H., Iwasawa, Y.: *Appl. Surf. Sci.* **140** (1999) 259.
- 99Gun1 Günster, J., Liu, G., Stultz, J., Goodman, D.W.: *J. Chem. Phys.* **110** (1999) 2558.
- 99Guo1 Guo, Q., McBreen, P.H., Møller, P.J.: *Surf. Sci.* **423** (1999) 19.
- 99Guo2 Guo, Q., Williams, E.M.: *Surf. Sci.* **433-435** (1999) 322.
- 99Hay1 Hayden, B.E., King, A., Newton, M.A.: *J. Phys. Chem. B* **103** (1999) 203.
- 99Hen1 Henderson, M.A., Epling, W.S., Perkins, C.L., Peden, C.H.F., Diebold, U.: *J. Phys. Chem. B* **103** (1999) 5328.
- 99Hen2 Henderson, M.A., Otero-Tapia, S., Castro, M.E.: *Faraday Discuss. Chem. Soc.* **114** (1999) 313.
- 99Her1 Herman, G.S., Kim, Y.J., Chambers, S.A., Peden, C.H.F.: *Langmuir* **15** (1999) 3993.
- 99Her2 Herman, G.S., McDaniel, E.P., Joyce, S.A.: *J. Electron Spectrosc. Relat. Phenom.* **101-103** (1999) 433.
- 99Her3 Hermann, K., Witko, M., Druzinic, R., Chakrabarti, A., Tepper, B., Elsner, M., Gorschlüter, A., Kühlenbeck, H., Freund, H.-J.: *J. Electron Spectrosc. Relat. Phenom.* **98-99** (1999) 245.
- 99Joh1 Johnson, D.E., Larese, J.Z.: *Phys. Rev. B* **59** (1999) 8247.
- 99Joh2 Johnson, M.A., Stefanovich, E.V., Truong, T.N., Günster, J., Goodman, D.W.: *J. Phys. Chem.* **103** (1999) 3391.
- 99Jos1 Joseph, Y., Kuhrs, C., Ranke, W., Ritter, M., Weiss, W.: *Chem. Phys. Lett.* **314** (1999) 195.
- 99Jos2 Joseph, Y., Kuhrs, C., Ranke, W., Weiss, W.: *Surf. Sci.* **433-435** (1999) 114.
- 99Lin1 Lindsay, R., Baumgärtel, P., Terborg, R., Schaff, O., Bradshaw, A.M., Woodruff, D.P.: *Surf. Sci.* **425** (1999) L401.
- 99Lin2 Lindsay, R., Gutierrez-Sosa, A., Thornton, G., Ludviksson, A., Parker, S., Campbell, C.T.: *Surf. Sci.* **439** (1999) 131.
- 99Lu1 Lu, X., Xu, X., Wang, N., Zhang, Q.: *J. Phys. Chem. B* **103** (1999) 3373.
- 99Lu2 Lu, X., Xu, X., Wang, N., Zhang, Q.: *J. Phys. Chem. B* **103** (1999) 5657.
- 99Mat1 Matsumoto, T., Kubota, J., Kondo, J.N., Hirose, C., Domen, K.: *Langmuir* **15** (1999) 2158.
- 99Mul1 Mullins, D.R., Overbury, S.H.: *J. Catal.* **188** (1999) 340.

- 99Nis1 Nishimura, S.Y., Aldrich, D.N., Hoerth, M.T., Ralston, C.J., Tro, N.J.: *J. Phys. Chem. B* **103** (1999) 9717.
- 99Ode1 Odelius, M.: *Phys. Rev. Lett.* **82** (1999) 3919.
- 99Ove1 Overbury, S.H., Mullins, D.R., Huntley, D.R., Kundakovic, L.: *J. Phys. Chem. B* **103** (1999) 11308.
- 99Pac1 Pacchioni, G., Ferrari, A.M.: *Catal. Today* **50** (1999) 533.
- 99Pat1 Patthey, L., Rensmo, H., Persson, P., Westermark, K., Vayssieres, L., Stashans, A., Peterson, A., Brüwiler, P.A., Siegbahn, H., Lunell, S., Martensson, N.: *J. Chem. Phys.* **110** (1999) 5913.
- 99Ped1 Peden, C.H.F., Herman, G.S., Ismagilov, I.Z., Kay, B.D., Henderson, M.A., Kim, Y.-J., Chambers, S.A.: *Catal. Today* **51** (1999) 513.
- 99Pic1 Picaud, S., Girardet, C., Duhoo, T., Lemoine, D.: *Phys. Rev. B* **60** (1999) 8333.
- 99Pol1 Polcik, M., Lindsay, R., Baumgärtel, P., Terborg, R., Schaff, O., Kulkarni, S., Bradshaw, A.M., Toomes, R.L., Woodruff, D.P.: *Faraday Discuss. Chem. Soc.* **114** (1999) 141.
- 99Ran1 Ranea, V.A., Vicente, J.L., Mola, E.E., Mananu, R.U.: *Surf. Sci.* **442** (1999) 498.
- 99Rit1 Ritter, M., Weiss, W.: *Surf. Sci.* **432** (1999) 81.
- 99Rit2 Rittner, F., Boddenberg, B., Bojan, M.J., Steele, W.A.: *Langmuir* **15** (1999) 1456.
- 99Rit3 Rittner, F., Boddenberg, B., Fink, R.F., Staemmler, V.: *Langmuir* **15** (1999) 1449.
- 99Rod1 Rodriguez, J.A., Jirsak, T., Chaturvedi, S.: *J. Chem. Phys.* **111** (1999) 8077.
- 99Rod2 Rodriguez, J.A., Jirsak, T., Chaturvedi, S., Kuhn, M.: *Surf. Sci.* **442** (1999) 400.
- 99Sam1 Sambeth, J., Gambaro, L., Thomas, H.: *J. Mol. Catal. A* **139** (1999) 25.
- 99Saw1 Sawunyama, P., Fujishima, A., Hashimoto, K.: *Langmuir* **15** (1999) 3551.
- 99Seb1 Sebastian, I., Bertrams, T., Meinel, K., Neddermeyer, H.: *Faraday Discuss. Chem. Soc.* **114** (1999) 129.
- 99Sei1 Seiferth, O., Wolter, K., Dillmann, B., Klivenyi, G., Freund, H.-J., Scarano, D., Zecchina, A.: *Surf. Sci.* **421** (1999) 176.
- 99Shal Shaikhutdinov, S.K., Joseph, Y., Ranke, W., Weiss, W.: *Faraday Discuss. Chem. Soc.* **114** (1999) 363.
- 99Shul Shu, C., Sukumar, N., Ursenbach, C.P.: *J. Chem. Phys.* **110** (1999) 10539.
- 99Sor1 Soria, E., Roman, E., Milliams, E.M., de Segovia, J.L.: *Surf. Sci.* **433-435** (1999) 543.
- 99Ste1 Stefanovich, E.V., Truong, T.N.: *Chem. Phys. Lett.* **299** (1999) 623.
- 99Suz1 Suzuki, S., Fukui, K.-I., Onishi, H., Iwasawa, Y.: *Surf. Interface Anal.* **28** (1999) 135.
- 99Tod1 Todnem, K., Børve, K.J., Nygren, M.: *Surf. Sci.* **421** (1999) 296.
- 99Toul Toubin, C., Picaud, S., Girardet, C.: *Chem. Phys.* **244** (1999) 227.
- 99Wan1 Wang, L.-Q., Ferris, K.F., Skiba, P.X., Shultz, A.N., Baer, D.R., Engelhard, M.H.: *Surf. Sci.* **440** (1999) 60.
- 99Wic1 Wichtendahl, R., Rodriguez-Rodrigo, M., Härtel, U., Kuhlenbeck, H., Freund, H.-J.: *Surf. Sci.* **423** (1999) 90.
- 99Wic2 Wichtendahl, R., Rodriguez-Rodrigo, M., Härtel, U., Kuhlenbeck, H., Freund, H.-J.: *Phys. Status Solidi (a)* **173** (1999) 93.
- 99Will Wilde, M., Seiferth, O., Al-Shamery, K., Freund, H.-J.: *J. Chem. Phys.* **111** (1999) 1158.
- 99Wit1 Witko, M., Hermann, K., Tokarz, R.: *Catal. Today* **50** (1999) 553.
- 99Wool Woodhead, A.P., Harte, S.P., Haycock, S.A., Muryn, C.A., Wincott, P.L., Dhanak, V.R., Thornton, G.: *Surf. Sci.* **420** (1999) L138.
- 99Woo2 Woods, G.A., Haq, S., Richardson, N.V., Shaw, S., Digby, R., Raval, R.: *Surf. Sci.* **433-435** (1999) 199.
- 99Yor1 York, S.C., Abee, M.W., Cox, D.F.: *Surf. Sci.* **437** (1999) 386.
- 99Zac1 Zacharias, H., Eichhorn, G., Schliesing, R., Al-Shamery, K.: *Appl. Phys. B* **68** (1999) 605.
- 99Zap1 Zapol, P., Jaffe, J.B., Hess, A.C.: *Surf. Sci.* **422** (1999) 1.
- 00Ahl1 Ahlswede, B., Homann, T., Jug, K.: *Surf. Sci.* **445** (2000) 49.
- 00Ahm1 Ahmed, S.I.-U., Perry, S.S., El-Bjeirami, O.: *J. Phys. Chem. B* **104** (2000) 3343.
- 00Bar1 Barbier, A., Mocuta, C., Kuhlenbeck, H., Peters, K.F., Richter, B., Renaud, G.: *Phys. Rev. Lett.* **84** (2000) 2897.
- 00Bar2 Barbier, A., Mocuta, C., Renaud, G.: *Phys. Rev. B* **62** (2000) 16056.
- 00Bec1 Becker, T., Boas, C., Burghaus, U., Wöll, C.: *J. Vac. Sci. Technol. A* **18** (2000) 1089.
- 00Bec2 Becker, T., Boas, C., Burghaus, U., Wöll, C.: *Phys. Rev. B* **61** (2000) 4538.

- 00Bec3 Becker, T., Kunat, M., Boas, C., Burghaus, U., Wöll, C.: *J. Chem. Phys.* **113** (2000) 6334.
00Ben1 Bennett, R.A., Stone, P., Smith, R.D., Browker, M.: *Surf. Sci.* **454-456** (2000) 390.
00Bri1 Brinkley, D., Engel, T.: *J. Phys. Chem. B* **104** (2000) 9836.
00Cas1 Casarin, M., Maccato, C., Vittadini, A.: *Inorg. Chem.* **39** (2000) 5232.
00Cha1 Chang, Z., G.Thornton: *Surf. Sci.* **462** (2000) 68.
00deL1 de Leeuw, N.H., Purton, J.A., Parker, S.C., Watson, G.W., Kresse, G.: *Surf. Sci.* **452** (2000) 9.
00Die1 Diebold, U., Li, M., Dulub, O., Hebenstreit, E.L.D., Hebenstreit, W.: *Surf. Rev. Lett.* **7** (2000) 613.
00Eval1 Evans, J., Hayden, B.E., Newton, M.A.: *Surf. Sci.* **462** (2000) 169.
00Fuk1 Fukui, K.-I., Iwasawa, Y.: *Surf. Sci.* **464** (2000) L719.
00Gra1 Grant, A.W., Jamieson, A., Campbell, C.T.: *Surf. Sci.* **458** (2000) 71.
00Gun1 Günster, J., Liu, G., Stultz, J., Krischok, S., Goodman, D.W.: *J. Phys. Chem. B* **104** (2000) 5738.
00Has1 Hass, K.C., Schneider, W.F., Curioni, A., Andreoni, W.: *J. Phys. Chem. B* **104** (2000) 5527.
00Hen1 Henderson, M.A., Chambers, S.A.: *Surf. Sci.* **449** (2000) 135.
00Hov1 Hövel, S., Kolczewski, C., Wühn, M., Albers, J., Weiss, K., Staemmler, V., Wöll, C.: *J. Chem. Phys.* **112** (2000) 3909.
00Jin1 Jin, R.Y., Song, K., Hase, W.L.: *J. Phys. Chem. B* **104** (2000) 2692.
00Jon1 Jones, F., Rohl, A., Farrow, J.B., van Bronswijk, W.: *Phys. Chem. Chem. Phys.* **2** (2000) 3209.
00Jos1 Joseph, Y., Ranke, W., Weiss, W.: *J. Phys. Chem. B* **104** (2000) 3224.
00Jos2 Joseph, Y., Wün, M., Niklewski, A., Ranke, W., Weiss, W., Wolf, C., Schlögl, R.: *Phys. Chem. Chem. Phys.* **2** (2000) 5314.
00Kac1 Käckell, P., Terakura, K.: *Appl. Surf. Sci.* **166** (2000) 370.
00Kac2 Käckell, P., Terakura, K.: *Surf. Sci.* **461** (2000) 191.
00Kam1 Kämper, A., Auroux, A., Baerns, M.: *Phys. Chem. Chem. Phys.* **2** (2000) 1069.
00Kam2 Kämper, A., Hahndorf, I., Baerns, M.: *Top. Catal.* **11/12** (2000) 77.
00Kaw1 Kawabe, T., Tabata, K., Suzuki, E., Nagasawa, Y.: *Surf. Sci.* **454-456** (2000) 374.
00Ken1 Kendelewicz, T., Liu, P., Doyle, C.S., Brown jr, G.E., Nelson, E.J., Chambers, S.A.: *Surf. Sci.* **453** (2000) 32.
00Kim1 Kim, S.H., Stair, P.C., Weitz, E.: *Surf. Sci.* **445** (2000) 177.
00Kor1 Korolik, M., Suchan, M.M., Johnson, M.J., Arnold, D.W., Reisler, H., Wittig, C.: *Chem. Phys. Lett.* **326** (2000) 11.
00Kun1 Kundakovic, L.J., Mullins, D.R., Overbury, S.H.: *Surf. Sci.* **457** (2000) 51.
00Lin1 Lindan, P.J.D.: *Chem. Phys. Lett.* **328** (2000) 325.
00Mell1 Melle-Franco, M., Pacchioni, G.: *Surf. Sci.* **461** (2000) 54.
00Moc1 Mocuta, C., Barbier, A., Renaud, G.: *Appl. Surf. Sci.* **162-163** (2000) 56.
00Ove1 Over, H., Kim, Y.D., Seitsonen, A.P., Wendt, S., Lundgren, E., Schmid, M., Varga, P., Morgante, A., Ertl, G.: *Science (Washington)* **287** (2000) 1474.
00Pac1 Pacchioni, G.: *Surf. Rev. Lett.* **7** (2000) 277.
00Per1 Persson, P., Lunell, S., Brühwiler, P.A., Schnadt, J., Södergren, S., O'Shea, J.N., Karis, O., Siegbahn, H., Martensson, N., Bässler, M., Patthey, L.: *J. Chem. Phys.* **112** (2000) 3945.
00Ran1 Ranea, V.A., Vicente, J.L., Mola, E.E., Arnal, P., Thomas, H., Gambaro, L.: *Surf. Sci.* **463** (2000) 115.
00Rei1 Reissner, R., Schulze, M.: *Surf. Sci.* **454-456** (2000) 183.
00Rus1 Rusu, C.N., Yates jr., J.T.: *J. Phys. Chem. B* **104** (2000) 1729.
00Sall1 Sallabi, A.K., Jack, D.B.: *J. Chem. Phys.* **112** (2000) 5133.
00Shal1 Shaikhutdinov, S., Weiss, W.: *J. Mol. Catal.* **158** (2000) 129.
00Shel1 Sherrill, A.B., Lusvardi, V.S., Eng jr, J., Chen, J.G., Barteau, M.A.: *Catal. Today* **63** (2000) 43.
00Siu1 Siu, W.K., Bartynski, R.A., Hulbert, S.L.: *J. Chem. Phys.* **113** (2000) 10697.
00Sny1 Snyder, J.A., Alfonso, D.R., Jaffe, J.E., Lin, Z., Hess, A.C., Gutowski, M.: *J. Phys. Chem. B* **104** (2000) 4717.
00Sor1 Sorescu, D.C., Rusu, C.N., Yates jr., J.T.: *J. Phys. Chem. B* **104** (2000) 4408.
00Sor2 Soria, E., Colera, I., Roman, E., Williams, E.M., de Segovia, J.L.: *Surf. Sci.* **451** (2000) 188.

- 00Sti1 Stierle, A., Formoso, V., Comin, F., Franchy, R.: *Surf. Sci.* **467** (2000) 85.
- 00Sti2 Stierle, A., Formoso, V., Comin, F., Schmitz, G., Franchy, R.: *Physica B* **283** (2000) 208.
- 00Vit1 Vittadini, A., Selloni, A., Rotzinger, F.P., Grätzel, M.: *J. Phys. Chem. B* **104** (2000) 1300.
- 00Wil1 Wilson, J.N., Titheridge, D.J., Kieu, L., Idriss, H.: *J. Vac. Sci. Technol. A* **18** (2000) 1887.
- 00Wol1 Wolter, K., Scarano, D., Fritsch, J., Kuhlenbeck, H., Zecchina, A., Freund, H.-J.: *Chem. Phys. Lett.* **320** (2000) 206.
- 00Wuh1 Wühn, M., Joseph, Y., Bagus, P.S., Niklewski, A., Püttner, R., Reiss, S., Weiss, W., Martins, M., Kaindl, G., Wöll, C.: *J. Phys. Chem. B* **104** (2000) 7694.
- 00Xu1 Xu, C., Oh, W.S., Goodman, D.W.: *J. Phys. Chem. B* **104** (2000) 10310.
- 00Yam1 Yamaguchi, Y., Nagasawa, Y., Shimomura, S., Tabata, K., Suzuki, E.: *Chem. Phys. Lett.* **316** (2000) 477.
- 00Yin1 Yin, X., Han, H., Miyamoto, A.: *Phys. Chem. Chem. Phys.* **2** (2000) 4243.
- 00Zhu1 Zhuang, F., Tang, J.C., He, J.P., Wang, L.: *Phys. Chem. Chem. Phys.* **2** (2000) 3571.
- 01Bec1 Becker, T., Hövel, S., Kunat, M., Boas, C., Burghaus, U., Wöll, C.: *Surf. Sci.* **486** (2001) L502.
- 01Ben1 Bennett, R.A., Newton, M.A., Smith, R.D., Bowker, M., Evans, J.: *Surf. Sci.* **487** (2001) 223.
- 01Bra1 Brause, M., Kempter, V.: *Surf. Sci.* **476** (2001) 78.
- 01Bur1 Burghaus, U.: *Surf. Rev. Lett.* **8** (2001) 353.
- 01Cai1 Cai, S., Neyman, K.M., Knözinger, H., Rösch, N.: *Surf. Sci.* **479** (2001) 169.
- 01Dam1 Damin, A., Dovesi, R., Zecchina, A., Ugliengo, P.: *Surf. Sci.* **479** (2001) 255.
- 01Doh1 Dohnalek, Z., Kimmel, G.A., Joyce, S.A., Ayotte, P., Smith, R.S., Kay, B.D.: *J. Phys. Chem. B* **105** (2001) 3747.
- 01Fan1 Fan, C.Y., Wang, J., Jacobi, K., Ertl, G.: *J. Chem. Phys.* **114** (2001) 10058.
- 01Fin1 Finocchi, F., Goniakowski, J.: *Phys. Rev. B* **64** (2001) 125426.
- 01Fuj1 Fujino, T., Katayama, M., Inudzuka, K., Okuno, T., Oura, K., Hirao, T.: *Appl. Phys. Lett.* **79** (2001) 2716.
- 01Gut1 Gutierrez Sosa, A., Evans, T.M., Parker, S.C., Campbell, C.T., Thornton, G.: *J. Phys. Chem. B* **105** (2001) 3783.
- 01Gut2 Gutierrez-Sosa, A., Evans, T.M., Woodhead, A.P., Lindsay, R., Muryn, C.A., Thornton, G., Yoshihara, J., Parker, S.C., Campbell, C.T., Oldman, R.J.: *Surf. Sci.* **477** (2001) 1.
- 01Gut3 Gutierrez-Sosa, A., Martinez-Escolano, P., Raza, H., Lindsay, L., Wincott, P.L., Thornton, G.: *Surf. Sci.* **471** (2001) 163.
- 01Hoe1 Hoefl, J.-T., Kittel, M., Polcik, M., Bao, S., Toomes, R.L., Kang, J.-H., Woodruff, D.P., Pascal, M., Lamont, C.L.A.: *Phys. Rev. Lett.* **87** (2001) 086101.
- 01Iwa1 Iwasawa, Y., Onishi, H., Fukui, K.-I.: *Top. Catal.* **14** (2001) 163.
- 01Ket1 Ketteler, G., Weiss, W., Ranke, W., Schlögl, R.: *Phys. Chem. Chem. Phys.* **3** (2001) 1114.
- 01Kim1 Kim, Y.D., Seitsonen, A.P., Over, H.: *Phys. Rev. B* **63** (2001) 115419.
- 01Kim2 Kim, Y.D., Seitsonen, A.P., Wendt, S., Wang, J., Fan, C., Jacobi, K., Over, H., Ertl, G.: *J. Phys. Chem. B* **105** (2001) 3752.
- 01Kuh1 Kuhrs, C., Arita, Y., Weiss, W., Ranke, W., Schlögl, R.: *Top. Catal.* **14** (2001) 111.
- 01Li1 Li, J., Wu, L., Zhang, Y.: *Chem. Phys. Lett.* **342** (2001) 249.
- 01Mad1 Madhavaram, H., Idriss, H., Wendt, S., Kim, Y.D., Knapp, M., Over, H., Aßmann, J., Löffler, E., Muhler, M.: *J. Catal.* **202** (2001) 296.
- 01Mel1 Melle-Franco, M., Pacchioni, G., Chadwick, A.V.: *Surf. Sci.* **478** (2001) 25.
- 01Miu1 Miura, T., Kobayashi, H., Domen, K.: *J. Phys. Chem. B* **105** (2001) 10001.
- 01Nel1 Nelson, C.E., Elam, J.W., Tolbert, M.A., George, S.M.: *Appl. Surf. Sci.* **171** (2001) 21.
- 01Ovi1 Oviedo, J., Gillan, M.J.: *Surf. Sci.* **490** (2001) 221.
- 01Per1 Perkins, C.L., Henderson, M.A.: *J. Phys. Chem. B* **105** (2001) 3856.
- 01Pyk1 Pykavy, M., Staemmler, V., Seifert, O., Freund, H.-J.: *Surf. Sci.* **479** (2001) 11.
- 01Rod1 Rodriguez, J.A., Jirsak, T., Chaturvedi, S., Dvorak, J.: *J. Mol. Catal.* **167** (2001) 47.
- 01Rod2 Rodriguez, J.A., Jirsak, T., Liu, G., Hrbek, J., Dvorak, J., Maiti, A.: *J. Am. Chem. Soc.* **123** (2001) 9597.
- 01Rod3 Rodriguez, J.A., Jirsak, T., Perez, M., Gonzalez, L., Maiti, A.: *J. Chem. Phys.* **114** (2001) 4186.
- 01Rod4 Rodriguez, J.A., Perez, M., Jirsak, T., Gonzalez, L., Maiti, M.: *Surf. Sci.* **477** (2001) L279.

- 01Rod5 Rodriguez, J.A., Perez, M., Jirsak, T., Gonzalez, L., Maiti, M., Larese, J.Z.: *J. Phys. Chem. B* **105** (2001) 5497.
- 01Sas1 Sasahara, A., Uetsuka, H., Onishi, H.: *J. Phys. Chem. B* **105** (2001) 1.
- 01Sas2 Sasahara, A., Uetsuka, H., Onishi, H.: *Phys. Rev. B* **64** (2001) 121406.
- 01Say1 Sayago, D.I., Serrano, P., Böhme, O., Goldoni, A., Paolucci, G., Roman, E., Martin-Gago, J.A.: *Surf. Sci.* **482-485** (2001) 9.
- 01Sch1 Schneider, W.F., Li, J., Hass, K.C.: *J. Phys. Chem. B* **105** (2001) 6972.
- 01Sch2 Schulze, M., Reissner, R.: *Surf. Sci.* **482-485** (2001) 285.
- 01She1 Sherrill, A.B., Medlin, J.W., Chen, J.G., Barteau, M.A.: *Surf. Sci.* **492** (2001) 203.
- 01Thi1 Thiel, S., Pykavy, M., Klüner, T., Freund, H.-J., Kosloff, R., Staemmler, V.: *J. Am. Chem. Soc.* **123** (2001) 9597.
- 01Tit1 Titheridge, D.J., Barteau, M.A., Idriss, H.: *Langmuir* **17** (2001) 2120.
- 01Tol1 Toledano, D.S., Henrich, V.E.: *J. Phys. Chem. B* **105** (2001) 3872.
- 01Tol2 Toledano, D.S., Metcalf, P., Henrich, V.E.: *Surf. Sci.* **472** (2001) 21-32.
- 01Wan1 Wander, A., Harrison, N.M.: *J. Chem. Phys.* **115** (2001) 2312.
- 01Wan2 Wang, J., Fan, C.Y., Jacobi, K., Ertl, G.: *Surf. Sci.* **481** (2001) 113.
- 01Yan1 Yang, Z., Wu, R., Zhang, Q., Goodman, D.W.: *Phys. Rev. B* **63** (2001) 045419.
- 02Bat1 Bates, S.P.: *Surf. Sci.* **512** (2002) 29.
- 02Bow1 Bowker, M., Stone, P., Bennett, R., Perkins, N.: *Surf. Sci.* **511** (2002) 435.
- 02Bre1 Bredow, T.: *J. Phys. Chem. B* **106** (2002) 7053.
- 02Cam1 Camillone III, N., Adib, K., Fitts, J.P., Rim, K.T., Flynn, G.W., Joyce, S.A., Osgood, R.M.: *Surf. Sci.* **511** (2002) 267.
- 02Cha1 Chang, Z., Li, Z., Udby, L., He, J., Nielsen, T.V., Møller, P.J.: *Surf. Sci.* **505** (2002) 71.
- 02DiM1 Di Matteo, S., Perkins, N.B., Natoli, C.R.: *J. Phys. Condens. Matter* **44** (2002) L37.
- 02DiV1 Di Valentin, C., Pacchioni, G., Bredow, T., Dominguez-Ariza, D., Illas, F.: *J. Chem. Phys.* **117** (2002) 2299.
- 02Dul1 Dulub, O., Boatner, L.A., Diebold, U.: *Surf. Sci.* **519** (2002) 201.
- 02Hau1 Haukka, M., Hirva, P.: *Surf. Sci.* **511** (2002) 373.
- 02Kit1 Kittel, M., Hoeft, J.T., Bao, S., Polcik, M., Toomes, R.L., Kang, J.-H., Woodruff, D.P., Pascal, M., Lamont, C. L.A.: *Surf. Sci.* **499** (2002) 1.
- 02Kun1 Kunat, M., Gil Girol, S., Becker, T., Burghaus, U., Wöll, C.: *Phys. Rev. B* **66** (2002) 081402.
- 02Laf1 Lafosse, A., Wang, Y., Jacobi, K.: *J. Chem. Phys.* **117** (2002) 2823.
- 02Lin1 Lindsay, R., Michelangeli, E., Daniels, B.G., Ashworth, T.V., Limb, A.J., Thornton, G., Gutierrez-Sosa, A., Baraldi, A., Larciprete, R., Lizzit, S.: *J. Am. Chem. Soc.* **124** (2002) 7117.
- 02Mat1 Matsuura, A.Y., Obayashi, T., Kondoh, H., Ohta, T., Oji, H., Kosugi, N., Sayama, K., Arakawa, H.: *Chem. Phys. Lett.* **360** (2002) 133.
- 02Ove1 Over, H.: *Appl. Phys. A* **75** (2002) 37.
- 02Ran1 Ranke, W., Joseph, Y.: *Phys. Chem. Chem. Phys.* **4** (2002) 2483.
- 02Rei1 Reiß, S., Krumm, H., Niklewski, A., Staemmler, V., Wöll, C.: *J. Chem. Phys.* **116** (2002) 7704.
- 02Rod1 Rodriguez, J.A., Hanson, J.C., Frenkel, A.I., Kim, J.Y., Perez, M.: *J. Am. Chem. Soc.* **124** (2002) 346.
- 02Sei1 Seitsonen, A.P., Kim, Y.D., Knapp, M., Wendt, S., Over, H.: *Phys. Rev. B* **65** (2002) 035413.
- 02Sha1 Shapovalov, V., Stefanovich, E.V., Truong, T.N.: *Surf. Sci.* **498** (2002) L103.
- 02She1 Sherrill, A.B., Barteau, M.A.: *J. Mol. Catal. A* **184** (2002) 301.
- 02Tan1 Tanner, R.E., Liang, Y., Altman, E.I.: *Surf. Sci.* **506** (2002) 251.
- 02Tan2 Tanner, R.E., Sasahara, A., Liang, Y., Altman, E.I., Onishi, H.: *J. Phys. Chem. B* **106** (2002) 8211.
- 02Tep1 Tepper, B., Richter, B., Dupuis, A.-C., Kühlenbeck, H., Hucho, C., Schilbe, P., bin Yarmo, M.A., Freund, H.-J.: *Surf. Sci.* **496** (2002) 64.
- 02Wan1 Wang, Y., Lafosse, A., Jacobi, K.: *J. Phys. Chem. B* **106** (2002) 5476.
- 02Wei1 Weiss, W., Ranke, W.: *Prog. Surf. Sci.* **70** (2002) 1.
- 02Wen1 Wendt, S., Seitsonen, A.P., Kim, Y.D., Knapp, M., Idriss, H., Over, H.: *Surf. Sci.* **505** (2002) 137.

- 03Adi1 Adib, K., Mullins, D.R., Totir, G., Camillone III, N., Fitts, J.P., Rim, K.T., Flynn, G.W., Osgood jr., R.M.: *Surf. Sci.* **524** (2003) 113.
- 03Bac1 Bach, C., Klüner, T., Groß, A.: *Chem. Phys. Lett.* **376** (2003) 424.
- 03Die1 Diebold, U.: *Surf. Sci. Rep.* **48** (2003) 53.
- 03Dul1 Dulub, O., Diebold, U., Kresse, G.: *Phys. Rev. Lett.* **90** (2003) 016102.
- 03Dup1 Dupuis, A.-C., Haija, M.A., Richter, B., Kühlenbeck, H., Freund, H.-J.: *Surf. Sci.* **539** (2003) 99.
- 03Far1 Farfan-Arribas, E., Madix, R.J.: *J. Phys. Chem. B* **107** (2003) 3225.
- 03Far2 Farfan-Arribas, E., Madix, R.J.: *Surf. Sci.* **544** (2003) 241.
- 03Hen1 Henderson, M.A.: *Geochim. Cosmochim. Acta* **67** (2003) 1055.
- 03Her1 Herman, G.S., Dohnalek, Z., Ruzycki, N., Diebold, U.: *J. Phys. Chem. B* **107** (2003) 3225.
- 03Kim1 Kim, S.H., Paulus, U.A., Wang, Y., Winterlin, J., Jacobi, K., Ertl, G.: *J. Chem. Phys.* **119** (2003) 9729.
- 03Kul1 Kulawik, M., Nilius, N., Rust, H.-P., Freund, H.-J.: *Phys. Rev. Lett.* **91** (2003) 256101.
- 03Kun1 Kunat, M., Burghaus, U.: *Surf. Sci.* **544** (2003) 170.
- 03Kun2 Kunat, M., Burghaus, U., Wöll, C.: *Phys. Chem. Chem. Phys.* **5** (2003) 4962.
- 03Lei1 Leist, U., Ranke, W., Al-Shamery, K.: *Phys. Chem. Chem. Phys.* **5** (2003) 2435.
- 03Liu1 Liu, G., Rodriguez, J.A., Hrbek, J., Long, B.T., Chen, D.A.: *J. Mol. Catal. A* **202** (2003) 215.
- 03Lob1 Lobo, A., Conrad, H.: *Surf. Sci.* **523** (2003) 279.
- 03Mey1 Meyer, R., Bäumer, M., Shaikhutdinov, S.K., Freund, H.-J.: *Surf. Sci.* **546** (2003) L813.
- 03Ode1 Odelius, M., Persson, P., Lunell, S.: *Surf. Sci.* **529** (2003) 47.
- 03Ove1 Over, H., Muhler, M.: *Prog. Surf. Sci.* **72** (2003) 3.
- 03Paul1 Paulus, U.A., Wang, Y., Jacobi, K., Ertl, G.: *Surf. Sci.* **547** (2003) 349.
- 03Reu1 Reuter, K., Scheffler, M.: *Phys. Rev. B* **68** (2003) 045407.
- 03Rim1 Rim, K.T., Fitts, J.P., Müller, T., Adib, K., Camillone III, N., Osgood, R.M., Joyce, S.A., Flynn, G.W.: *Surf. Sci.* **541** (2003) 59.
- 03Sai1 Saidi, S., Trabelsi, M., Chefi, C., Coulomb, J.P.: *Surf. Sci.* **532-535** (2003) 431.
- 03Sch1 Schnadt, J., O'Shea, J.N., Patthey, L., Schiessling, J., Krempasky, J., Shi, M., Martensson, N., Brühwiler, P.A.: *Surf. Sci.* **544** (2003) 74.
- 03Sch2 Schnadt, J., Schiessling, J., O'Shea, J.N., Gray, S.M., Patthey, L., Johansson, M.K.-J., Shi, M., Krempasky, J., Ahlund, J., Karlsson, P.G., Persson, P., Martensson, N., Brühwiler, P.A.: *Surf. Sci.* **540** (2003) 39.
- 03Sha1 Shapovalov, V., Wang, Y., Truong, T.N.: *Chem. Phys. Lett.* **375** (2003) 321.
- 03Stal1 Staemmler, V., Fink, K., Meyer, B., Marx, D., Kunat, M., Gil Girol, S., Burghaus, U., Wöll, C.: *Phys. Rev. Lett.* **90** (2003) 106102.
- 03Ter1 Tero, R., Fukui, K.-I., Iwasawa, Y.: *J. Phys. Chem. B* **107** (2003) 3207.
- 03Tho1 Thompson, T.L., Diwald, O., Yates, J.T.: *J. Phys. Chem. B* **107** (2003) 11700.
- 03Til1 Tilocca, A., Selloni, A.: *J. Chem. Phys.* **119** (2003) 7445.
- 03Wan1 Wang, Q., Biener, J., Guo, X.-C., Farfan-Arribas, E., Madix, R.J.: *J. Phys. Chem. B* **107** (2003) 11709.
- 03Wan2 Wang, Y., Jacobi, K., Ertl, G.: *J. Phys. Chem. B* **107** (2003) 13918.
- 03Will1 Wilson, J.N., Idriss, H.: *J. Catal.* **214** (2003) 46.
- 03Yu1 Yu, Y., Guo, Q., Liu, S., Wang, E., Möller, P.J.: *Phys. Rev. B* **68** (2003) 115414.
- 03Zha1 Zhang, C., Lindan, P.J.D.: *Chem. Phys. Lett.* **373** (2003) 15.
- 03Zha2 Zhang, C., Lindan, P. J.D.: *J. Chem. Phys.* **119** (2003) 9183.
- 04Fos1 Foster, M., Passno, D., Rudberg, J.: *J. Vac. Sci. Technol. A* **22** (2004) 1640.
- 04Paul1 Paulus, U.A., Bonzel, H.P., Jacobi, K., Ertl, G.: *Surf. Sci.* **566-568** (2004) 989.
- 04Sch1 Schoiswohl, J., Sock, M., Surnev, S., Ramsey, M.G., Netzer, F.P., Kresse, G., Andersen, J.N.: *Surf. Sci.* **555** (2004) 101.
- 04Sti1 Stierle, A., Renner, F., Streitl, R., Dosch, H., Drube, W., Cowie, B.C.: *Science (Washington)* **303** (2004) 1652.
- 05Haw1 Hawkins, S., Kumi, G., Malyk, S., Reisler, H., Wittig, C.: *Chem. Phys. Lett.* **404** (2005) 19.
- 05Wad1 Waddill, G.D., Ozturk, O.: *Surf. Sci.* **575** (2005) 35.
- 06Abu1 Haija, M.A., Guimond, S., Uhl, A., Kühlenbeck, H., Freund, H.-J.: *Surf.Sci.* **600** (2006) 1040.